



Norwegian University of
Science and Technology

Restoration and Testing of the Hydra Research Engine

Åsmund Kyrkjeide Karlsen

Marine Technology

Submission date: June 2017

Supervisor: Sergey Ushakov, IMT

Norwegian University of Science and Technology
Department of Marine Technology

ACKNOWLEDGEMENTS

This report is the result of my master thesis. The report has been written for the Department of Marin Technologies, in the specialization of Marine Engineering.

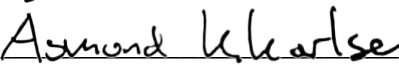
The objective of the report is to be a part of the restoration of the Hydra research-engine, where special attention will be shown to operability of the engine.

First, I want to thank my supervisor, professor Sergey Ushakov for impeccable guidance, support, and advice during my thesis writing. Without him this thesis would contain worse quality.

Secondly, I want to thank Head Engineer Frode Gran for his work on the control and measuring system. Furthermore, my gratitude is directed to Engineer Gunnar Bremset for his mechanical expertise during the restoration process of the Hydra Engine.

Lastly but not least I want to thank my wonderful girlfriend, Kay Sarah Rott for support during this hectic semester, and for her effort in proofreading this thesis. Without her, I would be lost.

Åsmund Kyrkjeeide Karlsen



June 2017, Trondheim, Norway

SUMMARY

This thesis has aimed to be a driving factor in the restoration process of the Hydra research engine. During the semester, several changes and improvements has been done to restore the engine to its former glory. These changes and the overall state of the engine is covered in detail. The thesis is concluded with an experimental study of the engine, where daily operation and experimental stability was in focus.

Regrettably these studies needed to be shortened due to an injector failure and a bad pressure transducer. It was found that the engine performs in a stabile way at engine speeds between 20 and 50 RPS, from 50 to 75 RPS flow restrictions in the exhaust system causes the volumetric efficiency to drop to unacceptable levels. If the injector and the pressure transducer is exchanged the engine will be operational in the range 20 to 50 RPS. If the exhaust system is improved the engine will ascertain its original operating range. The engine was found to have a very stable engine speed and common rail pressure.

SAMMENDRAG

Denne oppgaven sikter på å være en drivende faktor i restorasjonsprosessen av forskningsmotoren kalt Hydra. I løpet av dette semester er det gjort en rekke endringer og forbedringer for å gjennomrette motoren til sin tidligere stand. Disse endringene og den nåværende standen til motoren er vist på et detaljnivå. Oppgaven er avsluttet med en eksperimentell studie av motoren, hvor den daglige bruken og stabiliteten til motoren er i sentrum.

Dessverre ble de eksperimentelle studien avbrutt på grunn av en ødelagt injektor, i tillegg til en dårlig trykkføler. Gjennom de studiene som ble utført ble det funnet at motoren kjørte på en stabil måte med hastigheter mellom 20 og 50 RPS. Derimot ble de oppdaget restriksjoner i eksossystemet som gjorde at volumetrisk effektivitet falt til uakseptable nivåer ved hastigheter mellom 50 og 75 RPS. Om injektoren og trykkføleren blir byttet ut, eller reparerte vil motoren være operasjonell ved hastigheter mellom 20 og 50 RPS. Om i tillegg eksosystemet blir utbedret vil motoren kunne opereres innenfor dens originale operasjonsområde mellom 20 og 75 RPS. I tillegg til dette ble det avdekket at motoren opererer ved svært stabile hastigheter og drivstofftrykk.

CONTENTS

ACKNOWLEDGEMENTS	I
SUMMARY	III
SAMMENDRAG	IV
CONTENTS	V
FIGURE LIST	VIII
ABBREVIATIONS	X
1 INTRODUCTION	1
1.1 BACKGROUND	1
1.2 SCOPE AND LIMITATIONS.....	1
1.3 STRUCTURE OF THESIS	3
2 COMPRESSION IGNITION ENGINES	4
2.1 GENERAL PRINCIPLE	7
2.1.1 <i>Engine Geometry</i>	7
2.1.2 <i>Parameters and Definitions</i>	9
2.3 DIESEL FUEL.....	12
2.3.1 <i>Properties of Diesel Fuel</i>	12
2.4 FUEL INJECTION	15
2.4.1 <i>General Principle of Injectors</i>	15
2.4.2 <i>Variables and Limitations of Injectors</i>	17
2.5 HEAT RELEASE RATE ANALYSIS	19
2.6 FORMATION OF POLLUTANTS	22
2.6.1 <i>Particulate Matter</i>	22
2.6.2 <i>Nitrogen Oxides</i>	26
2.6.3 <i>Sulphur Oxides</i>	27
2.6.4 <i>Hydrocarbons</i>	27
3 RICARDO HYDRA RESEARCH ENGINE	29
3.1 STATUS QUO	29
3.1.1 <i>Mechanical and Fluid Containment Problems</i>	29
3.1.2 <i>Control, Safety, and Data Acquisition</i>	30
4 TEST-BED REVIEW	31
4.1 LAYOUT OF ENGINE ROOM	31
4.2 HYDRA ENGINE OVERVIEW	32

4.2.1	<i>Cooling and Lubrication</i>	33
4.2.2	<i>Air Intake</i>	35
4.2.3	<i>Exhaust and Emission Measurement Ports</i>	36
4.3	DYNAMOMETER.....	36
4.4	FUEL SYSTEM.....	37
4.4.1	<i>Fuel Tank and Fuel Consumption</i>	38
4.4.2	<i>Fuel-Pump</i>	39
4.4.3	<i>Fuel Injector</i>	41
4.5	ENGINE CONTROL.....	42
4.5.1	<i>Sensor Overview</i>	43
5	PRINCIPLES OF MEASUREMENT EQUIPMENT	44
5.1	CRANK ANGLE AND CYLINDER PRESSURE.....	44
5.1.1	<i>Locating Top Dead Center</i>	44
5.1.2	<i>Optical Angle Encoder</i>	45
5.1.3	<i>Piezoelectric Transducers</i>	46
5.1.4	<i>Dynamic Measurements of Pressure and Crank Angle</i>	48
5.2	TEMPERATURE.....	48
5.2.1	<i>Thermistors</i>	48
5.2.2	<i>Thermocouples</i>	49
5.3	HORIBA GAS ANALYZER.....	50
5.3.1	<i>Nitrogen Oxides</i>	50
5.3.2	<i>Oxygen</i>	51
5.3.3	<i>Carbon Oxides</i>	52
5.4	TOTAL HYDROCARBON ANALYZER.....	53
5.5	AVL SMOKE METER.....	53
6	ENGINE MAPPING	55
6.1	PROCESS OF ENGINE MAPPING.....	56
6.1.1	<i>Choosing Load-Points</i>	57
6.2	CURVE-FITTING.....	58
6.2.1	<i>Models of Fitting</i>	58
6.2.2	<i>Evaluating Goodness of Fit</i>	59
7	METHODOLOGY	62
7.1	TEST SETUP.....	62
7.2	FUEL.....	63
7.3	TESTING METHODS.....	63
7.3.1	<i>Function Check</i>	64

7.3.2	<i>Motored Test</i>	65
7.3.3	<i>Time until Stability Evaluation</i>	65
7.3.4	<i>Finding Operational Limits</i>	65
7.3.5	<i>Engine Mapping using Gridded Test-points</i>	66
7.4	PREPARATION AND CALIBRATION	66
7.5	DATA PROCESSING	67
8	RESULTS AND DISCUSSION	68
8.1	PERFORMED MODIFICATIONS.....	68
8.2	MODIFICATIONS NOT PERFORMED.....	71
8.3	FUNCTION CHECK	72
8.4	MOTORED TEST.....	73
8.4.1	<i>Volumetric Efficiency and Flow Restrictions</i>	73
8.4.2	<i>Mechanical Efficiency and Pressure Measurements</i>	75
8.5	STABILITY TEST	76
8.5.1	<i>Stability of NOx and Speed</i>	78
8.6	INVESTIGATION OF OPERATIONAL LIMITS	80
8.6.1	<i>Volumetric Efficiency and Fuel Flow</i>	81
8.7	RECOMMENDATION FOR TEST-BED IMPROVEMENT	83
8.8	TIPS AND TRICKS LEARNED FROM EXPERIMENTS.....	84
9	CONCLUSION	85
9.1	FURTHER WORK	86
10	REFERENCES	87
	APPENDIX	90
	APPENDIX A – PLANED AND CONDUCTED TESTS	90
	APPENDIX B – OPERATION MANUAL	91
	APPENDIX C – MATLAB SCRIPT - READING DATA	92
	APPENDIX D – MATLAB SCRIPT – MOTORED TEST	93
	APPENDIX E – MATLAB SCRIPT – STABILITY TEST	94
	APPENDIX F – MATLAB SCRIPT – LIMIT TEST	95
	APPENDIX G – REVIEW OF PREVIOUS INTAKE SYSTEM.....	96
	APPENDIX H – FUEL PROPERTIES	97

FIGURE LIST

FIGURE 2-1 ILLUSTRATION OF FOUR-STROKE CYCLE [10]	7
FIGURE 2-2 CRANK ASSEMBLY OF INTERNAL COMBUSTION ENGINE [1]	8
FIGURE 2-3 DIESEL FUEL SPECIFICATIONS ACCORDING TO EN590:2013	13
FIGURE 2-4 DRAWING OF TYPICAL INNER WORKINGS OF FUEL INJECTOR. SOLENOID TYPE LEFT, PIEZO TYPE RIGHT [15]	16
FIGURE 2-5 OVERVIEW OF DIFFERENT VARIABLES IN RELATION TO FUEL INJECTION [15]	17
FIGURE 2-6 EXAMPLE OF INJECTION TIMING [18]	18
FIGURE 2-7 RATE OF HEAT RELEASE FOR CI-ENGINE [7]	21
FIGURE 2-8 PARTICULATE COMPOSITION [20]	23
FIGURE 2-9 SOURCES OF DIFFERENT FRACTION OF PARTICULATES [20]	24
FIGURE 2-10 LOCATION OF PRODUCTION OF NO _x AND PM [1]	24
FIGURE 2-11 SOOT FORMATION [21]	24
FIGURE 2-12 FORMATION OF SUBSTANCES DURING COMBUSTION [22]	25
FIGURE 2-13 SCHEMATIC OF VARIABLE EQUIVALENCE RATIO IN DIESEL ENGINES [7]	28
FIGURE 4-1 TEST-BED LAYOUT	31
FIGURE 4-2 ILLUSTRATION OF INSTALLED PISTON	33
FIGURE 4-3 CAMSHAFT ASSEMBLY	33
FIGURE 4-4 CAD DRAWING OF OIL AND COOLANT DELIVERY SYSTEM	34
FIGURE 4-5 TEMPORARY FLOW METER MOUNTING ON TOP OF CABLE BRIDGE	35
FIGURE 4-8 EXHAUST PIPING	36
FIGURE 4-9 COMPLETE SCHEMATIC OF GENERIC COMMON RAIL SYSTEM [29]	38
FIGURE 4-10 FUEL TANK SETUP	39
FIGURE 4-11 DENSO HP3 FUEL SUPPLY PUMP [29]	40
FIGURE 4-12 DENSO HP3 ILLUSTRATION [29]	41
FIGURE 4-13 INJECTOR AND FUEL PRESSURE CONTROL INTERFACE	42
FIGURE 5-1 DEFINITION OF LOSS ANGLE [31]	45
FIGURE 5-2 PRINCIPLE OF OPTICAL ANGLE ENCODER [31]	46
FIGURE 5-3 SCHEMATIC OF PIEZOELECTRIC TRANSDUCER [31]	47
FIGURE 5-4 DYNAMIC MEASUREMENT SETUP	48
FIGURE 5-5 THERMISTOR	49
FIGURE 5-6 REPRESENTATION OF THERMOCOUPLE [39]	49
FIGURE 5-7 LAMBDA SENSOR [42]	51
FIGURE 5-8 PRINCIPLE OF WIDE BAND ZIRCONIUM SENSOR [43]	52
FIGURE 5-9 NDIR SENSOR [43]	53
FIGURE 5-10 FILTER REFLECTION MEASUREMENT	54
FIGURE 6-1 MAP OF OUTPUT TORQUE AS FUNCTION OF ENGINE SPEED AND THROTTLE OPENING [44]	55
FIGURE 6-2 GENERAL MODEL OF ENGINE/PROCESS/SYSTEM [45]	56
FIGURE 6-3 ENGINE INPUTS AND OUTPUTS WITH FIXED SPEED AND LOAD [47]	56

FIGURE 7-1 ILLUSTRATION OF TEST SETUP62

FIGURE 7-2 FAULT DIAGNOSTICS PROCESS.....64

FIGURE 8-1 SEALED HOLE BEHIND EXHAUST MANIFOLD.....69

FIGURE 8-2 PERFORMED EXPERIMENTS, MOTORED TEST73

FIGURE 8-3 VOLUMETRIC EFFICIENCY, MOTORED TEST.....74

FIGURE 8-4 PERFORMED EXPERIMENTS, STABILITY TEST.....76

FIGURE 8-5 OIL TEMPERATURE, STABILITY TEST.....77

FIGURE 8-6 ENGINE SPEED, STABILITY TEST78

FIGURE 8-7 NO_x, STABILITY TEST79

FIGURE 8-8 OPERATIONAL LIMITS80

FIGURE 8-9 VOLUMETRIC EFFICIENCY, LIMIT TEST.....81

FIGURE 8-10 FUEL FLOW MEASUREMENT, LIMIT TEST82

FIGURE 8-11 LOCATION OF IMPROVEMENT NR.2 AND 4. YELLOW LINE IS PROPOSED ROUTE FOR FUEL RETURN.....83

FIGURE 8-12 LOCATION OF IMPROVEMENT NR.183

ABBREVIATIONS

Abbreviation	Explanation
ABDC	After Bottom Dead Center
ATDC	After Top Dead Center
BBDC	Before Bottom Dead Center
BDC	Before Dead Center
BDC	Bottom Dead Center
bmep	Break mean effective pressure
BTDC	Before Top Dead Center
CAD	Crank Angle Degrees
CI	Compression Ignition
CLD	Chemiluminescence Detection
CN	Cetane Number
DI	Direct Injection
ECU	Engine Control Unit
FAME	Fatty methyl esters
FID	Flame Ionization Detection
FSN	Filter Smoke Number
HC	Hydrocarbons
HRR	Heat Release Rate
imep	Indicated mean effective pressure
LHV	Lower heating value
LoLO	Lift-on Lift-off
mep	Mean effective pressure
MGO	Marine Gas Oil
NDIR	Non-Dispersive Infrared
PAH	Polycyclic Aromatic Hydrocarbons
PM	Particulate Matter
RMSE	Root Mean Square Error
ROHR	Rate of Heat Release
SCV	Suction Control Valve
SSE	Sum of Square due to Error
SSR	Sum of Square of the Regression
SST	Total Sum of Squares
TDC	Top Dead Center
THC	Total Hydrocarbons

1 INTRODUCTION

1.1 BACKGROUND

Internal combustion engine research has for many years been centered around efficiency and performance improvement. However, the last decades, new challenges related to pollutant emissions has arisen. For diesel engines, the main pollutants are nitrogen oxides and particulate matter, these are rather strictly controlled nowadays. As an educational institution, NTNU is interested in being able to provide students not only with theoretical knowledge, but also with a certain practical experience, as for example engines that the students can operate with little supervision and that can be used to perform emission measurements. NTNU has a suitable engine for such purposes, but unfortunately, it has been out of operation for a long period due to various technical issues.

The Ricardo Hydra diesel engine is a custom made one cylinder research-engine with a common rail injection system. This engine is very flexible in terms of operating parameters that, together with controllable injection pressure, injection timing and duration, makes it an ideal engine for educational and research purposes. The Hydra engine is however still out of operation, needing some alterations before it can be used for testing/student work.

1.2 SCOPE AND LIMITATIONS

This thesis aims to be a driving factor in the restoration of the Hydra engine, where a key goal is to make the engine ready for student-experiments. The restoration of the engine is something that has been a topic for many years, but has not been conducted due to lack of a firm plan with a time schedule. During the process of making this thesis a plan for finishing the modifications to the engine will be provided. All needed modification should be performed before May to allow for sufficient time to conduct needed experiments. The experiments will be used to give a detailed insight in the operation and capabilities of the engine, which will create a basis for the production of an engine guide. The engine guide will be designed to help students with understanding the engine operation and all systems connected to the engine.

The scope and limitations of this thesis is summarized in the following list.

1. Make a detailed description of key components of the Hydra engine
2. Describe data that can be collected (logged) from the engine
3. Describe measurement principles used for emission measurements

4. Become familiarized with the engine operation
5. Perform the necessary alterations to the engine in collaboration with the lab staff
6. Check that every aspect of the engine is working as expected and perform engine mapping
7. Perform control experiments where all relevant emissions are measured together with necessary engine parameters
- ~~8. If particle measurement equipment is available, perform measurements of particle size distribution characteristics of Hydra engine~~
9. Develop an engine guide that can be used to ensure that the engine is ready to be operated in a safe manner
10. Recommend additional changes to the test-bed that will ensure easier data acquisition and more accurate/repeatable results

1.3 STRUCTURE OF THESIS

Chapter 2 gives a general overview of the principles of a compression ignition engine, encompassing both engine operational principles and formation of pollutants.

Chapter 3 outlines the current state of the Hydra research engine, and suggests possible solutions to the discovered problems.

Chapter 4 portrays a review of the Hydra engine, and all connected systems. This chapter provides the background for the engine guide.

Chapter 5 describes the principle of measurement equipment typically used in engine experiments.

Chapter 6 presents the theory behind engine mapping, with a special focus on options related to curve fitting.

Chapter 7 contains the methodology and test setup of the experiments conducted in this thesis. If exact test-plans are of interest the appendix A should be consulted.

Chapter 8 summarizes and discusses the results from the experiments outlined in chapter 7. In addition, it provides an evaluation and an overview of the successfulness of modifications done to the test-bed.

Chapter 9 concludes the thesis with an evaluation of the overall state of the test-bed, and suggests possible improvements for the test-bed in the future.

2 COMPRESSION IGNITION ENGINES

In its most basic form an internal combustion engine is a converter of energy, from chemical energy, through thermal energy ending up in mechanical energy. In marine application, the compression ignition engines (or diesel engines) have been the leading engine choice for ship propulsion for decades. The diesel engine was invented by Rudolf Diesel in 1892 [2]. The engine's relatively high efficiency, robustness and simplicity made it a perfect replacement for the early steam engines that dominated as propulsion power source for marine vessels in the past. There is no agreement among the literature sources regarding which ship was the first to have a diesel engine installed. Gardiner and Greenway [3] suggests that the Russian river tanker "Vandal" was the first diesel-powered ship. Thomas [4], on the other hand, suggests that the French canal barge "Petite-Pierre" was first. Both were built in 1903.

Today the diesel engine is the main power provider for marine vessel, where only a negligible number of vessels are powered by alternative power sources. From Table 1 it can be seen that larger transit vessels, mostly have engines that run on a two-stroke principle, while smaller vessels, with more start and stop operational patterns tend to use the four-stroke principle. Almost all vessels are running on diesel, except for some smaller fishing vessels, that utilize spark ignition engines. Since the Hydra research engine is a four-stroke engine, the theory described in the next chapters will mainly be related to four-stroke engines.

Table 1 Summary of engine types. Adapted from [5]

Ship Types	Installed Main Engines ^a
Bulk carriers, tankers	two-stroke: 91% four-stroke: 6%
Large container vessels (>1500 TEU)	two-stroke: 100%
Small container vessels (<1500 TEU)	two-stroke: 55% four-stroke: 45%
Crude oil carriers	two-stroke: 80% four-stroke: 19%
Lift-on lift-off (LoLo)	two-stroke: 55% four-stroke: 32%
Roll-on roll-off (RoRo)	two-stroke: 11% four-stroke: 77%
Passenger vessels	primarily four-stroke
Fishing vessels ^b	two-stroke: 3% four-stroke: 69%

^aOn the basis of installed power.

^bA number of fishing vessels are not powered by diesel engines, but by Otto cycle, spark-ignited engines.

During the recent years, a strong political “push” towards electrifying the automobile park has been seen, using batteries to store energy, and electrical motors to transfer this energy to motion. The same cannot be said about the marine industry. Marine vessels, in general, are a subject of long distance travels, which means that marine vessels need a huge storage of energy to be able to perform its journey. Today’s battery technology simply does not provide a high enough energy density (approximately 0.875 MJ/kg [6]) to become a candidate in prime movers of marine vessels. This means that the diesel engine will continue to be the most effective power provider for long distance travel, at least in nearest future. However, a shift toward diesel-electric systems has been seen (in certain applications), using the diesel engine as a power supplier to electrical generators. Even so-called hybrid systems have been developed, where the diesel engine is used in cooperation with a battery. The battery can then be used to comply with fast load changes, meaning that the power plant of the vessel can run with less redundancy and give an overall lower fuel consumption. Despite being under increasing pressure due to stricter emission limits, the conventional diesel engines still remain the primary choice for ship propulsion with modern two-stroke engines providing over 50% of thermal efficiency [1]. However, more research is needed to continue to improve not only the performance of the

internal combustion engine, but also to decrease the engine's exhaust emissions. Still there is several possibilities for further development!

The diesel engine has undergone severe research since its invention in 1892, but it still operates on the same principles proposed by Rudolf Diesel¹. The most notable additions to the design during the latest years are forced induction of air and improved injection systems. Forced induction of air (or supercharging) is done to increase the amount of air that can be introduced into the cylinder of the engine. This will subsequently lead to a higher max power output [7]. Forced induction is mostly performed by turbocharging. A turbocharger utilizes excess energy in the exhaust gasses to spin a compressor which increases the inlet pressure, hence giving positive effect on both power and fuel consumption.

As the diesel engine becomes increasingly optimized, the requirements for exact control of the process intensifies. This is the basis for the research conducted on fuel injection systems. The first mass-produced injection system was delivered by Bosch in 1927. It became apparent that direct injection of fuel lead to reduced fuel consumption. However, especially at cold start, the engine became a subject of diesel knocking, leading to a very noisy driving experience [8]. At the time comfort was more important than fuel consumption. Therefore, the system was used only on trucks and heavy applications in the beginning. It was found that much of the noise problem was possible to overcome by adding a pilot injection [8]. However, the technology for performing such a pilot injection was not present at the time, thus leading to much research on the topic. It was not until 1988 that this research payed of for the car manufacturers, when Fiat lunched the first direct injection passenger car. Followed the next year with Audi's first TDI engine [1]. The next big leap in injector technology was the invention of the high pressure fuel pump, and the introduction of the common rail system in 1997, which together with high precision injectors has made the diesel engine an integral part of the automotive industry [9].

Environmental concerns have propelled the last three decades of engine development, especially related to reduction in NO_x, SO_x, and particulate matter. This has led to research both in after treatment systems, fuel alternatives, and engine control.

¹ This is a simplification, in reality the diesel engine was subject to several research projects and prototyping before it was ready for use. However, the principles are very close to what Diesel fist proposed, whit the greatest change being that he first proposed to use pulverized coal as fuel. [1]

2.1 GENERAL PRINCIPLE

A compression ignition (CI) engine, is a reciprocating internal combustion engine, that ignites fuel by compression. This produces a force on a piston, that subsequently rotates a crankshaft, producing rotating motion. Modern compression ignition engines utilize direct injection (DI), where liquid fuel is injected directly into the combustion chamber, creating a homogeneous mix of air and fuel. When the fuel has mixed sufficiently with air, auto-ignition occurs, due to temperatures and pressures above the auto-ignition temperature of the fuel.

Compression ignition engines are typically divided into four-stroke engines and two-stroke engines. For the purpose of this thesis, only four-stroke engines will be covered. A stroke is a piston movement between TDC and bottom dead center (BDC). A four-stroke engine has, as the name suggests, four-strokes, i.e. induction, compression, expansion, and exhaust. These strokes go over two revolutions of the crankshaft, and can be summarized in Figure 2-1. The gas exchange process, or intake and exhaust, is controlled by the valve timing (opening/closing) of corresponding intake and exhaust valve(s), located in the cylinder head.

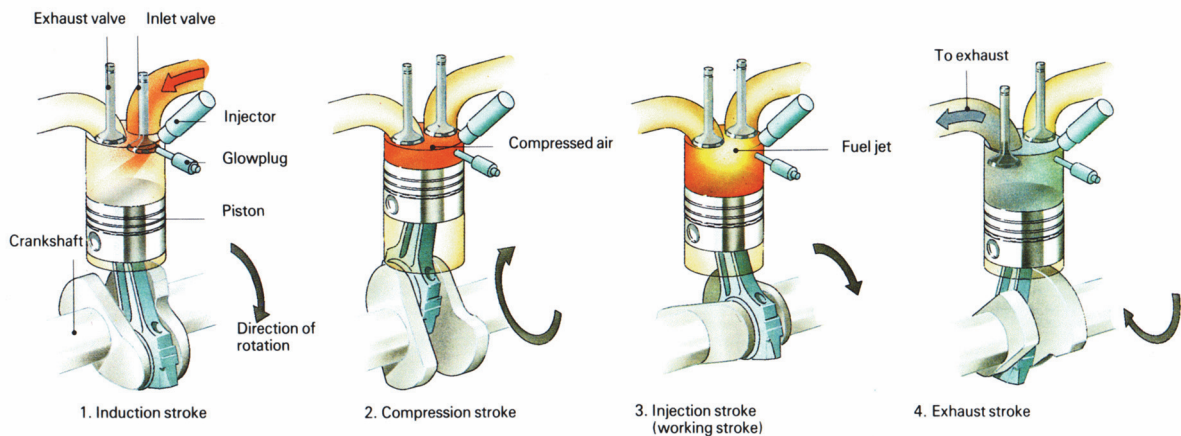


Figure 2-1 Illustration of four-stroke cycle [10]

2.1.1 ENGINE GEOMETRY

Engine control is closely linked to knowing the exact piston position at every given time. This is done by measuring the crankshaft position. The crankshaft is connected to a number of belts or gears, that are responsible for providing the power for additional equipment as for example camshafts, fuel pumps and the alternator, therefore the crankshaft position will also govern the valve lifting (in case of conventional engines). Calculation of the piston position can be made if certain geometrical relations are known. Figure 2-2 depicts commonly known engine geometry. The parameters used are explained in the following list.

D = Bore

S = Stroke

V_d = Displacement volume

TDC = Top Dead Center (Maximum lateral position of piston)

V_c = Combustion volume (Volume between piston at TDC and cylinder top)

BDC = Bottom Dead Center (Minimum lateral position of piston)

l = Length of connecting rod

r = Length of crank arm

Z_k = Distance between center of crankshaft and mass center of piston

φ = Crank angle degrees (CAD)

In addition, it can be beneficial to know the following notations to simplify angle notations.

ABDC = After Bottom Dead Center

BBDC = Before Bottom Dead Center

ATDC = After Top Dead Center

BTDC = Before Top Dead Center

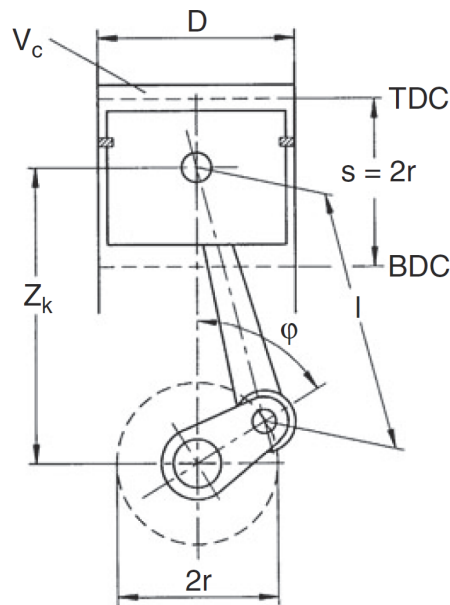


Figure 2-2 Crank Assembly of Internal Combustion Engine [1]

If the parameters above are given, some basic geometrical relations can be calculated, like cylinder position, volume, and piston speeds, depending on crank angle degrees.

$$Z_k = r \cos(\varphi) + \sqrt{l^2 - r^2 \sin^2 \varphi} \quad (1)$$

Knowing the position of the piston gives the opportunity to calculate the volume between the cylinder top and the piston.

$$V = V_c + V_d = V_c + \frac{\pi B^2}{4} (l + r - Z_k) \quad (2)$$

If the rotational speed of the engine ($N=[\text{rev/s}]$) is known, the mean piston speed (c_{mean}) and instantaneous piston speed ($c_{\text{instantaneous}}$) can be calculated.

$$c_{\text{mean}} = 2SN \quad (3)$$

$$c_{\text{instantaneous}} = \frac{\pi}{2} \sin \varphi \left[1 + \frac{\cos \varphi}{\sqrt{R^2 - \sin^2 \varphi}} \right] \quad (4)$$

Where R is the ratio between the length of the connecting rod and the crank arm ($R=l/r$), known as crank arm ratio. According to Heywood [7] the mean piston speed is normally limited to the range 8 to 15m/s due to gas flow resistance and stresses from inertia of moving parts.

2.1.2 PARAMETERS AND DEFINITIONS

Power:

Power is a measure of how much work the engine can exert on the driveshaft per time unit. The power can be directly calculated based on torque and engine speed [7]. Power is defined as follows.

$$P = 2\pi NT \quad (5)$$

Where N is the rotational speed of the engine in revolutions per second, and T is the produced torque of the engine in newton meters. Power is measured in Watts. Note that this is the power directly from the crankshaft. If power delivered to a propeller or to wheels are of interest, the losses between the crankshaft and the power output must be considered.

Mean effective pressure (mep):

Power is a good measurement of the performance of the engine, but does however not give any information about how good the design of the engine is. By definition power is a bad measurement to use for comparison of two differently sized engines. Therefore, mean effective pressure (mep) has been defined. Mean effective pressure is a measurement of the work produced per cycle divided by the volume displaced [7].

$$mep = \frac{Pn_R}{V_d N} \quad (6)$$

Where P is the power, n_R is the number rotations per power stroke (one for 2-stroke, two for 4-stroke). N is the rotational speed in rev/s and V_d is the displacement volume of the engine.

Maximum break mean effective pressure is a good measure of the effectiveness of the engine design in terms of usage of the displacement volume. Through several decades of engine development, it has been established that bmep of a good engine tends to be constant for a wide range of engine sizes [7]. Heywood proposes a bmep for a good naturally aspirated diesel engine to be in the range 700 to 900 kPa with bmep at max rated power of around 700 kPa [7].

Mechanical efficiency:

According to DIN 1940 mechanical efficiency is defined as follows.

$$\eta_m = \frac{W_e}{W_i} \quad (7)$$

Where W_e is the effective work, and W_i is the indicated work produced by the engine. The mechanical efficiency is comprised of the negative contribution from friction produced by pistons, valves, and bearings, as well as the power needed to drive assisting systems like for example, pumps and alternators. Mechanical efficiency tends to be reduced with increasing engine speed, since mechanical efficiency includes the power needed to pump gas into and out of the cylinder [7].

The mechanical efficiency can in practice be measured in two different ways. If it is possible to motor the engine without combustion, the power used to rotate the engine can be measured, and give an estimate of the frictional forces that needs to be overcome. The mechanical efficiency can then be estimated based on the following equation. The biggest source of error in this method is that the pressure on the piston and piston rings are lower than if the engine was fired [7].

$$\eta_m = \frac{P_b}{P_{ig}} = 1 - \frac{P_f}{P_{ig}} \quad (8)$$

Where P_{ig} is the gross indicated power and P_f is the frictional power. P_{ig} can be calculated based on indicated work, which is the integral of the P-V curve of the engine.

$$P_{ig} = \frac{W_i N}{n_R} \quad (9)$$

$$W_i = \oint p dV \quad (10)$$

Mechanical efficiency can also be determined, with reasonable accuracy, based on the ratio between bmep and imep.

$$\eta_m = \frac{bmep}{imep} \quad (11)$$

Where imep is defined as follows.

$$imep = \frac{W_i}{V_d} \quad (12)$$

Volumetric efficiency:

Volumetric efficiency describes how efficiently the engines uses its displacement volume. The volumetric efficiency of a naturally aspirated diesel engine tends to be in the range 80 to 90 % [7] and can be summarized in the equation below.

$$\eta_v = \frac{2\dot{m}_a}{\rho_{a,i} V_d N} \quad (13)$$

Where \dot{m}_a is the mass rate of air introduced through the intake valve, calculated based on ideal gas laws. And $\rho_{a,i}$ is the density of air in the intake manifold and N is the rotational speed of the engine.

2.3 DIESEL FUEL

Petrodiesel is a mixture of hydrocarbons that is distilled from crude oil. Before Rudolf Diesel invented the first compression ignition engine in 1892 [2], diesel fuel or middle distillates were a by-product of gasoline production. Gasoline is extracted in the higher part of the distillation column, having a boiling point between 35 and 200°C. Diesel fuel is extracted in the middle part of the distilling column, extracting hydrocarbons with a boiling point between 200 and 380°C [1]. The middle distillates consist of carbon chains with a length between 11 and 22 carbons. The heavier molecules make diesel fuel more resilient to compression, which means that they are perfect for the principle of compression ignition. Rudolf Diesel understood this in 1892 and started using peanut oil as a compression resistant fuel for his first working engine.

Today diesel fuel is a collective term for all liquid fuels that is used in the compression ignition engine. There are several different types of diesel fuel, depending of the source of raw material and production.

2.3.1 PROPERTIES OF DIESEL FUEL

Diesel fuel is used in a range of different applications. To ensure that the fuel, which can be bought in petrol stations, can be used for all these applications; standard fuel specifications have been developed. Both the American and the European standard organization has standards for fuel specification, ASTM D 975 and EN590 respectively. These specifications are designed to give comparable emission and performance results independent of the manufacturer. To achieve the specification, the refineries need to optimize their production to produce on specification fuels. In Figure 2-3 the European specification for automotive diesel fuel is shown.

Property	Unit	Limits		Test method ^a (See Clause 2)
		minimum	maximum	
Cetane number		51,0	–	EN ISO 5165 ^b EN 15195 EN 16144
Cetane index		46,0	–	EN ISO 4264
Density at 15 °C	kg/m ³	820,0	845,0	EN ISO 3675 ^c EN ISO 12185
Polycyclic aromatic hydrocarbons ^d	% (m/m)	–	8,0	EN 12916
Sulfur content	mg/kg	–	10,0	EN ISO 20846 ^e EN ISO 20884 EN ISO 13032
Manganese content ^f until 2013–12–31 from 2014 to 01–01 onwards	mg/l	- -	6,0 2,0	prEN 16576
Flash point	°C	Above 55,0	–	EN ISO 2719
Carbon residue ^g (on 10 % distillation residue)	% (m/m)	–	0,30	EN ISO 10370
Ash content	% (m/m)	–	0,010	EN ISO 6245
Water content	mg/kg	–	200	EN ISO 12937
Total contamination	mg/kg	–	24	EN 12662 ^h
Copper strip corrosion (3 h at 50 °C)	rating	class 1		EN ISO 2160
Fatty acid methyl ester (FAME) content ⁱ	% (V/V)	-	7,0	EN 14078
Oxidation stability ^j	g/m ³ h	– 20	25 -	EN ISO 12205 EN 15751
Lubricity, corrected wear scar diameter (wsd 1,4) at 60 °C	µm	–	460	EN ISO 12156-1
Viscosity at 40 °C	mm ² /s	2,000	4,500	EN ISO 3104
Distillation ^{k, l} % (V/V) recovered at 250 °C % (V/V) recovered at 350 °C 95 % (V/V) recovered at	% (V/V) % (V/V) °C	85	< 65 360	EN ISO 3405 ^m EN ISO 3924

Figure 2-3 Diesel fuel specifications according to EN590:2013

Some of these specifications are more important than others, especially when it comes to engine research. In the next subsections, a short description of the most important properties connected to fuel behavior are given.

Cetane Number:

Cetane number (CN) describes how easily the fuel will ignite. In other words, it is a measure of how much compression the fuel needs before auto ignition occurs. Higher cetane number will create shorter ignition delay, and therefore reduces the time of combustion. Regarding the CN scale, de Klerk [11] states: “It is defined on an arbitrary scale where n-hexadecane (n-cetane) has a value of 100 and 1-methylnaphthalene has a value of 0. Since 1962, 1-methylnaphthalene has been replaced by 2,2,4,4,6,8,8-heptamethylnonane as a primary reference fuel. The 2,2,4,4,6,8,8-heptamethylnonane has a cetane value of 15 as measured relative to that of the

original definition of CN.” This means that a value of 100 on the scale is a fuel with good auto ignition properties. The scale is not limited to lower and higher bounds, so fuels can also be defined outside of the scale. However, since diesel fuel often is a blend of different substances the CN number tends to be within the scale. Petrodiesel usually has a cetane number between 40 and 55, where the European standard for automotive states that the fuel should have a minimum cetane number of 51.

The process of finding the cetane number is complicated and is described in ASTM D 613. Since the cetane number is costly to derive, by use of the ASTM D613 standard method, empirical methods have been developed. This method is called the cetane index, and is described in ASTM D4737 and ISO4264. It is an alternative scale to the CN and is calculated using a four-variable empirical equation based on density and distillation properties. In practice, this is the more widely used specification for fuel quality.

Density and Viscosity:

CI-engines are dependent on vaporization of the fuel before ignition. This is done by using high-pressure fuel injectors. This secures that all the fuel is vaporized and can be mixed with the air in the combustion chamber. The injectors are highly precise instruments and need a certain fuel specification especially related to density and viscosity of the fuel. Since the fuel injectors operate on a volume basis, the density will influence how much mass will be injected into the combustion chamber. Viscosity on the other hand is a number describing the fuels resistance to flow, high viscosity equal high resistance to flow. According to Song et al. [12] increasing the viscosity will decrease the spray cone angle thus increasing droplet size. This will cause poor atomization, and lead to poor combustion efficiency. Too low viscosity, on the other hand, can lead to decreased lubrication properties, and can induce fuel leakages in for example the fuel pump. This subsequently leads to bad engine durability.

Lower Heating Value:

The lower heating value (LHV) is a measure of the energy density of the fuel. LHV assumes that all exhaust gases (including water) leaves as vapor [13]. The unit of LHV is often given as $\frac{MJ}{kg_{fuel}}$ and is the basis of calculating how much fuel energy that is theoretically possible to exploit.

$$\eta_{combustion} = \frac{\text{Heat Produced}}{\text{Heat available in fuel}} = \frac{H_R(T_A) - H_P(T_A)}{m_f Q_{LHV}} \quad (14)$$

In equation $H_R(T_A)$ is the heat produced by the reactant and $H_P(T_A)$ is the heat produced by the products, while m_f is the mass of fuel and Q_{LHV} is the lower heating value of the fuel. From equation we can see that the theoretical energy available in the fuel is only dependent on mass of fuel and LHV [7]. This means that for a fuel with a low LHV more fuel must be injected, then with for example diesel, if the same available energy shall be produced. The implication, while comparing two different fuels with different LHV, is that we need to inject more of the energy deficient fuel to get comparable results.

The LHV is purely dependent on the composition of the fuel and is not part of the standard specifications. In combination with stoichiometric fuel air ratio it will give a good value of the performance of the fuel, especially connected to fuel economy. Petrodiesel will typically have a LHV of around 43MJ/kg

2.4 FUEL INJECTION

Fuel injection, in compression ignition engines, are typically performed by direct injection. The advantage of this is that the fuel will not occupy space in the cylinder during air induction. This leads to a higher max power output and a lower specific fuel consumption due to more available air in the combustion chamber. As an added benefit, the direct injection makes it possible to control the amount of fuel injected in a very precise manner, giving the possibility of pilot and post injection. There are two types of injectors that have dominated the injector market the latest years, where the piezo-injector has control over the premium market, and the solenoid has control over the volume marked. Innovation in both these injector-types has been central in complying with stricter emission legislations, without resorting to expensive after treatment systems [14].

2.4.1 GENERAL PRINCIPLE OF INJECTORS

An injector is typically composed of three main parts i.e. the injector casing, the needle and the needle actuator. The injector casing is of cylindrical form, and is screw directly into the cylinder header. The end of the casing, which has several nozzle-holes, barely penetrates into the combustion chamber. In closed position the needle will be pressed into its seat by use of a powerful spring, this will cover the nozzle-holes, and restrict all fuel from entering the

combustion chamber. Fuel is let into the combustion chamber by lifting the needle, this is done by hydraulic force, created by opening a valve, using the needle actuator. When a voltage is applied to the actuator, it expands, and lifts a servo valve which opens a gap where fuel can escape to atmospheric pressure. This evacuation of fuel leads to an instantaneous pressure-drop in the control volume above the needle, which creates an upwards acting hydraulic force on the needle [8]. The needle is subsequently lifted from its seat, releasing fuel into the combustion chamber. As can be seen from Figure 2-4, the needle actuator is what separated the solenoid and the piezo type injectors.

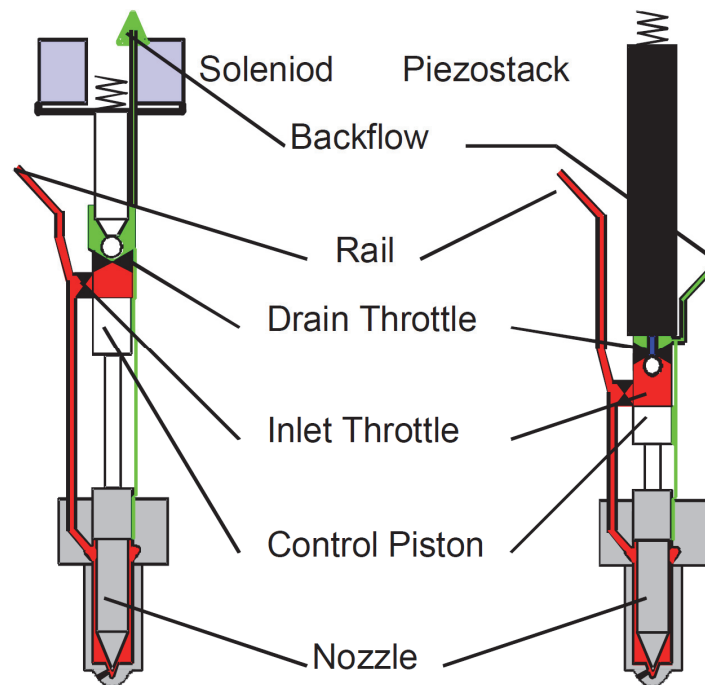


Figure 2-4 Drawing of typical inner workings of fuel injector. Solenoid type left, Piezo type right [15]

There are several advantages and disadvantages between the two main types of injectors. A study by Park et.al [16] shows that the piezo-injector is superior to the solenoid injector, in injection delay (improvement of 0.06ms), atomization and evaporation. However, the piezo-injector is both more expensive and longer than the solenoid-injector due to the relatively large piezo stack used as an actuator.

2.4.2 VARIABLES AND LIMITATIONS OF INJECTORS

Fuel injection is one of the most critical operations for optimizing the conversion of fuel to energy. The process has an enormous set of variables that can be altered to improve the fuel spray characteristics. Some of these variables are fixed in each engine, because of geometrical designs, like for example piston bowl design, number and design of nozzles, injection angle, degree of swirl and needle clearance. Most of the variables are summarized in Figure 2-5.

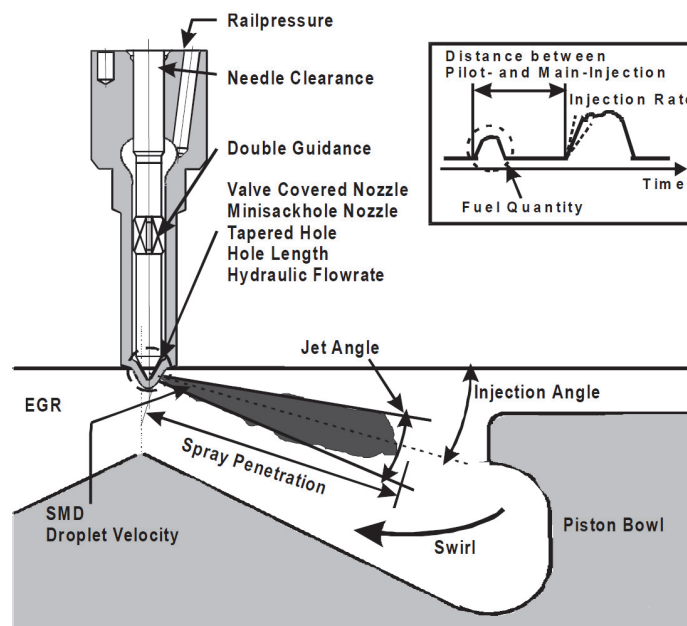


Figure 2-5 Overview of different variables in relation to fuel injection [15]

In an engine control situation, where the engine control unit (ECU) is responsible for altering variables in fuel spray, there is fewer possibilities for alternation. These possibilities are however more applicable to low cost engine research, where no exchange of injectors, piston or cylinder is needed.

The biggest change in injectors, during the latest decade, has been the available rail pressure. The invention of the high pressure fuel pump and the subsequent use of common rail fuel systems has been the driving force for this development [8]. It has been found that increasing the rail pressure has several advantages related to fuel-air mixing and emission characteristics. Increased pressure leads to a longer spray penetration, which can lead to a lower emission of soot [17]. Therefore, injection manufacturers have pushed to increase the maximum pressure

that an injector can achieve. At present the best injectors can achieve a pressure of around 2000 bar [8].

Another parameter that easily can be controlled by the ECU is the injector activation. This makes it possible to control the timing, rate, and quantity of fuel injection, as well as the number of injections per cycle and the time between each injection. The fuel injection control does however, only have two² simple requirements. Fuel must be injected at the right time (timing), and fuel must be injected in the right quantity to meet the power demand [18]. All other variables are controlled to reduce for example noise, emissions, and fuel consumption. In modern diesel engines, it is normal to have several injections during each power stroke. With modern injectors it is possible to have up to 8 separate injections [19], one of these injections are typically a main injection, where the biggest bulk of fuel is delivered. Injections that happen before the main injection is called pre-injections, and injections that happen after the main injection is called post-injections. Pre-injections are often used to condition the combustion chamber for the main injection, this reduces noise (reduces possibility of diesel knocking) and helps with the mixing due to a shorter ignition delay. Post-injections are typically applied to increase the exhaust temperature, which is needed to regenerate particulate filters and NOx traps in the exhaust system. Figure 2-6 shows an example of injection timing that can be used in the ECU.

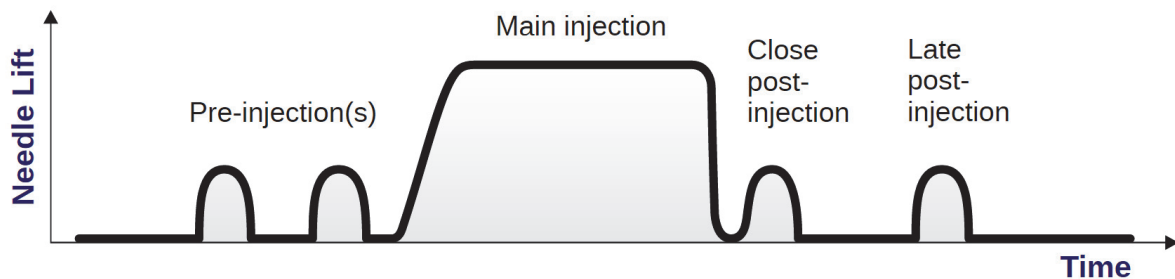


Figure 2-6 Example of injection timing [18]

² Assuming the injection pressure and nozzle configuration helps the fuel to atomize and mix with the air.

2.5 HEAT RELEASE RATE ANALYSIS

Heat release rate (HRR) or rate of heat release (ROHR) is an important tool in engine analysis and engine optimization. The method is based on thermodynamic laws, dynamic cylinder pressure, and cylinder volume. For the purpose of this thesis only the most basic form of ROHR computation will be covered. Several improvements can be done to this model to improve the accuracy, but for most engine analysis the following simple model can be used.

The model starts with the first law of thermodynamics for a quasi-static open system [7].

$$\frac{dQ}{dt} - p \frac{dV}{dt} + \sum_i \dot{m}_f h_f = \frac{dU}{dt} \quad (15)$$

Where $\frac{dQ}{dt}$ is, the heat-transfer rate across the system boundary into the system. The term $p \frac{dV}{dt}$ is the rate of work done due to boundary displacement, \dot{m}_f is the mass flow rate of fuel across the boundary, h_f is the enthalpy of the injected fuel and U is the internal energy of the cylinder [7].

If the content of the cylinder can be assumed to be ideal gas, the following equation can be derived.

$$\frac{dQ}{dt} = p \frac{dV}{dt} + m c_v \frac{dT}{dt} \quad (16)$$

If the gas constant R is assumed constant, T can be omitted from equation 16, and the following equation for ROHR can be written [7]³.

$$\frac{dQ_n}{dt} = \frac{\gamma}{\gamma - 1} p \frac{dV}{dt} + \frac{1}{\gamma - 1} V \frac{dp}{dt} \quad (17)$$

Where γ is ratio of specific heats, i.e. $\frac{c_p}{c_v}$. According to Heywood this value should be in the range from 1.3 to 1.35 [7].

³ Some steps are omitted from this section, see Heywood [7, p.510] for more information.

This method of computing ROHR has several simplifications and assumptions that are strictly not correct, but gives sufficiently correct values. An extensive list of simplifications and assumptions are shown below

- Quasi static process, in reality not the case due to state changes and constantly changing local fuel/air ratio
- Crevice region between piston and cylinder wall not accounted for
- Cooling near cylinder walls not accounted for
- Composition of burned gases are not known
- Does not necessarily follow ideal gas relations
- Not accounted for change of specific heat during the process

If this model was used to compute ROHR for a compression ignition engine, a shape similar to that of Figure 2-7 is to be expected. The combustion process in a compression ignition engine can be divided into the four different phases described below.

Ignition delay:

No combustion occurs, only heating, and mixing of fuel and air. Ignition delay in a modern engine with petrodiesel and high pressure injectors are between 0.3 and 0.8ms [1]. The length of this delay is often a result of the fuel quality. A high cetane number will lead to a shorter delay, and a low cetane number will lead to a longer delay. Nevertheless, the delay can be modified with injector design and pressure, which influence the mixing characteristics, and can change the time until auto-ignition conditions.

Premixed combustion:

After ignition delay premixed fuel and air reaches auto-ignition conditions, which starts a rapid combustion. This is characterized by the high peak in the rate of heat release curve seen in Figure 2-7. It is desired that this peak becomes as low as possible to save energy to the mixing controlled part of combustion. Reducing the ignition delay will reduce the amount of premixed fuel, which again will reduce the peak in the rate of heat release curve. This will subsequently reduce the peak temperature during the combustion process, which reduces the production of thermal NO_x.

Mixing controlled combustion:

This phase is controlled by the rate of which mixture becomes available for combustion. This is where the main part of the combustion energy is released. Figure 2-7 shows that this part produces a smooth rate of heat release which is preferable to the sharp increase in the premixed phase. The rate of heat release curve for mixing controlled combustion is slightly increasing if injection persists. When injection ends, the curve will start decreasing and approaching the next step, which is late combustion.

Late combustion:

This phase happens well into the expansion stroke, and is a product of residual unburned hydrocarbons. Residuals like soot and liquid fractions of fuel can be left after the mixing controlled combustion, and most of them are burned in this phase, resulting in a more complete combustion. As seen from Figure 2-7 the rate of heat release from this combustion phase is quite small in comparison with the other phases.

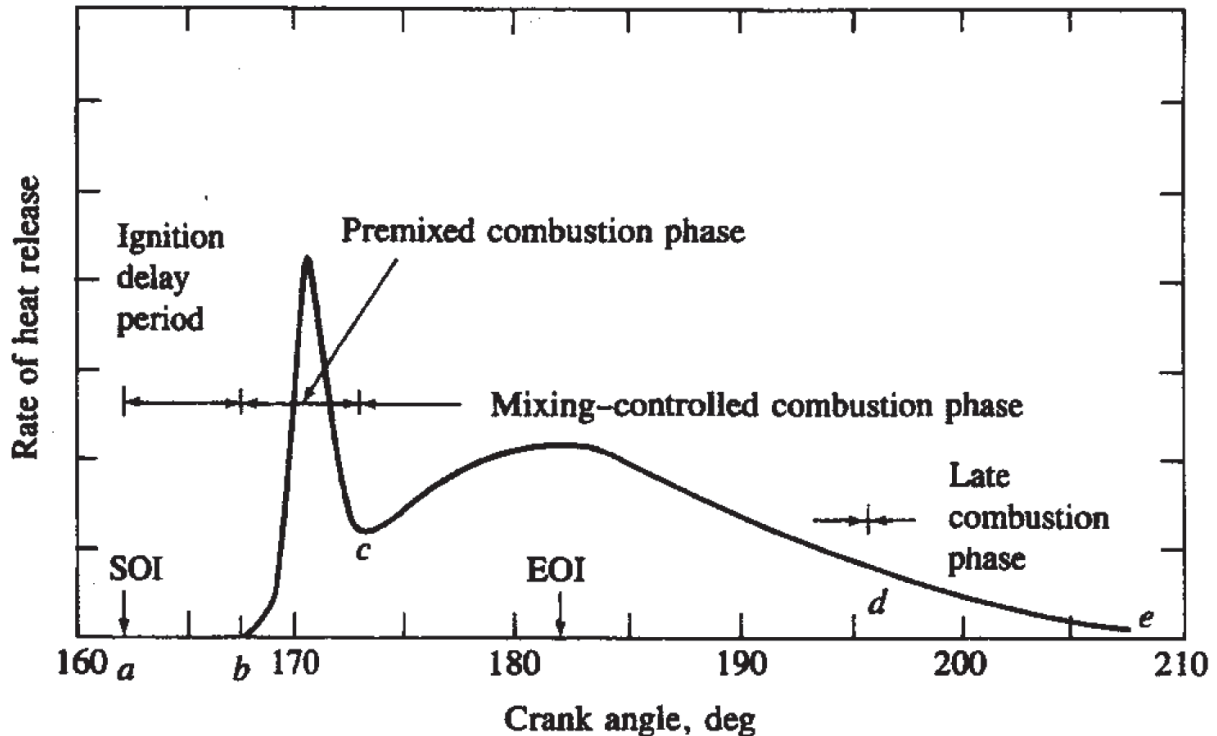


Figure 2-7 Rate of heat release for CI-engine [7]

2.6 FORMATION OF POLLUTANTS

Pollutants from compression ignition engines has been a concern for several decades. The legislations connected to these pollutants are becoming more stringent as time progress. This has led to a shift towards engine optimization in relation to emissions. Today there is two main pollutants that are a concern for the CI-engine, particulate matter, and nitrogen oxides. Both these pollutants have adverse health effects, and are a contributing factor to bad local air quality. Especially NO_x has been a defining factor in ECU tuning the latest years, this has contributed to scandals like the Volkswagens dieselgate scandal, where difficult legislations has led to cheating in engine testing. In addition to particulate matter and nitrogen oxides, there are other emission that also is of interest, but in general is a small problem in modern engines. Emission of sulfur oxides was a problem especially in the 70's, but has in large degree been overcome by introducing low sulfur fuel, while hydrocarbon and carbon monoxide emissions have generally been a small problem for CI-engines. Note that carbon dioxide (CO₂) has not been mentioned as a pollutant. Although it is a contributor to global warming, it is also the purest product that can be produced by combustion of hydrocarbons.

In the next sections the formations of the most relevant pollutants for CI-engines are covered.

2.6.1 PARTICULATE MATTER

Particle matter (PM) is defined as very fine solid or liquid particles that are created during combustion. These particles are normally categorized by size into PM_{2.5} and PM₁₀ which are particles with an equivalent diameter less than 2.5 μ m and 10 μ m respectively. Particle matter has a negative health effect on human respiratory system [20].

Depending on the analysis method used in laboratory the PM can be divided into volatile particles and nonvolatile particles. Volatile particles are composed of Sulfate, Nitrate and Organic fractions while nonvolatile particles come from soot and ash fractions. A representation of the different fractions that particulates can derive from is shown in Figure 2-8.

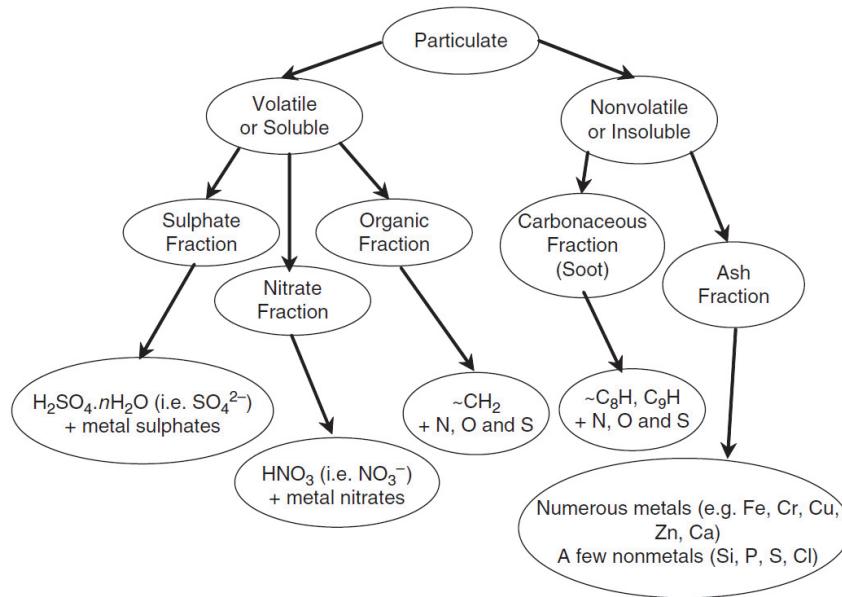


Figure 2-8 Particulate composition [20]

The fractions described above can come from four different sources described in Figure 2-9. The thickness of the arrows in the figure represents the importance of the specific source for production of particulates. The fuel is a major contributor to the production of particulates in a compression ignition engine. This source produces mostly fractions of carbonaceous particulates (or soot) and organic fractions, this is obviously because fuel consists mostly of hydrocarbons. Fuel is evidently a main contributor to all 4 PM fractions simply due to high fuel consumption compared to lube oil. Soot and organics basically form due to incomplete hydrocarbon fuel oxidation, while ash comes from incombustible species (mainly metals) which are used to control certain fuel properties. Sulfates are associated to the level of sulfur in fuel and are linked to the refinery process (also effect the fuel lubricity). Air contains a range of different pollutants that can contribute to the production of particulate matter. The amount of pollutants in the air varies a lot depending on location and time of year. Air is a very small contributor to the overall particulate matter emission, but can become significant if the engine is operated in for example mines. In modern engines exhaust gas recirculation is often applied to reduce the combustion temperatures. This means that contaminated air is induced back into the combustion chamber, which can lead to an increase in production of particulate matter. Engines are always a subject to mechanical wear, this means that the components of the engine are slowly disintegrating, creating the possibility of foreign elements inside the combustion chamber like for example metal particulates, fittings, and ash from cylinder walls and valves. This is however also a very small contributor to the overall particulate formation.

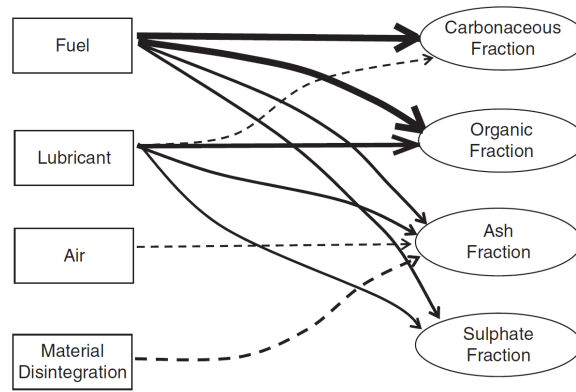


Figure 2-9 Sources of different fraction of particulates [20]

Regarding formation of particulates, a general description will be given, where the focus will be on the particulate formation from fuel.

Combustion in CI-engines is characterized by a changing fuel air ratio throughout the combustion process. Formation of particulates generally happens in fuel rich areas, shown in Figure 2-10 as soot formation. Because of extreme heat, pyrolysis occurs. This is the process of cracking the large hydrocarbon molecules into smaller and more easily ignitable molecules. Some of the molecules are aromatics as shown in Figure 2-11. These aromatics work as precursors to particulate growth, and bind together to form polycyclic aromatic hydrocarbons (PAH). The PAHs

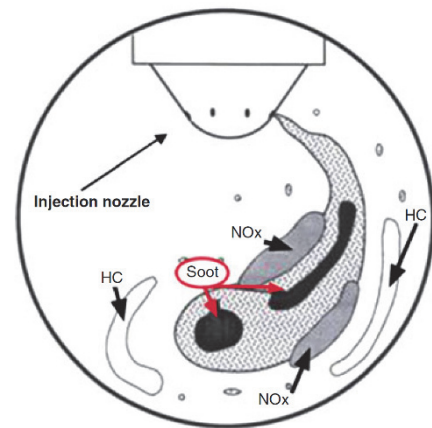


Figure 2-10 Location of production of NOx and PM [1]

then go through a nucleation process where they are connected to create larger particles, called primary particles. These primary particles are very small and are subject to Brownian motion in the turbulent combustion chamber; they clump together and create particle matter.

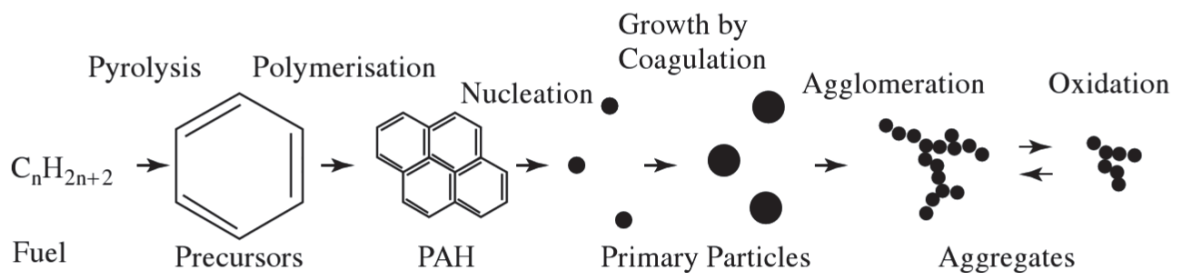


Figure 2-11 Soot formation [21]

Inside the combustion chamber particulates can both be created and combusted. This means that the number of existing particulates will change drastically during the combustion process. In Figure 2-12 measurements done by Aoyagi et al [22] of amounts of different substances during combustion as a function of crank angle is shown. The plot shows that a sharp increase in soot formation happens during the premixed combustion phase, with a peak right after end of injection. Thereafter the combustion enters the mixing controlled combustion phase, and soot formation decreases. The reason for this is that during the premixed phase, combustion happens in an effective manner, which causes a sharp increase in temperature and pressure, this intensifies pyrolysis, which leads to large soot production. During the mixing-controlled phase more soot is consumed, then is produced, due to increased availability of air.

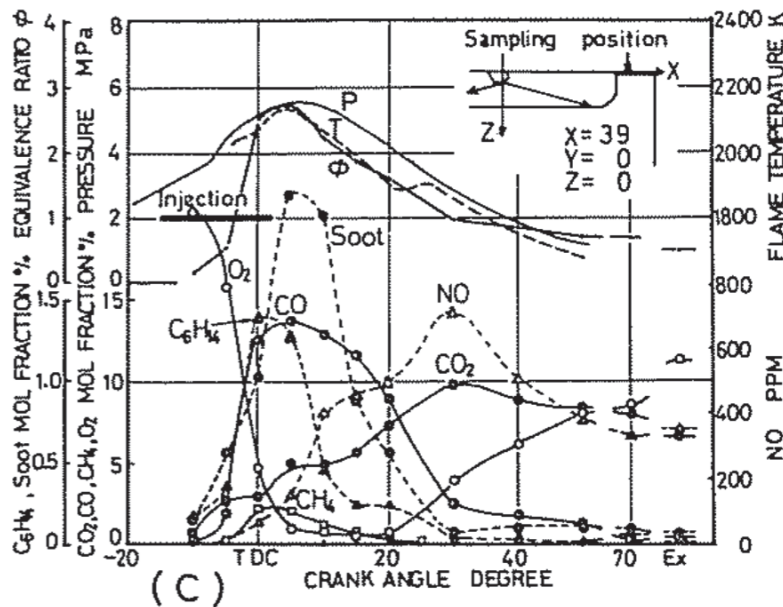


Figure 2-12 Formation of substances during combustion [22]

An indication of how much particle matter is in the exhaust stream, can be derived from the transparency of the exhaust gas. Note that this is not a good way of procuring reliable results in terms of particle count, but is only an indication of how much non-transparent material is present in the exhaust stream. A very large part of these non-transparent materials is particulate matter. Measurement of smoke transparency and general emissions will be discussed in the next chapter.

2.6.2 NITROGEN OXIDES

Nitrogen oxides is a collective term for emissions of NO and NO₂. In emissions from CI-engines NO accounts for around 85% by mass of the total NO_x emission [7]. NO_x is a pollutant that both influence human health and the environment. It can combine with hydrogen and create nitric acid (HNO₃), which can descend from the sky as acid rain. Regarding human health some evidence suggests that long term exposure to NO_x can cause reduced lung function [23]. High concentrations of NO_x are poisonous to humans, and small concentrations can be irritating for the respiratory system.

In combustion, there are two primary mechanisms of NO_x formation; NO_x from the fuel, and thermal NO_x. Prompted NO_x does also exist, but it is a very small part of the total emission.

Thermal NO_x

Air is composed of approximately 21% oxygen and 79% nitrogen. Thermal NO_x is formed when nitrogen and oxygen in the air reacts with each other at high temperatures. Thermal NO formation of near stoichiometric fuel-air mixtures is governed by the so-called extended Zeldovich mechanism shown in the reactions below [7].



Production of thermal NO_x increases exponentially with temperature. Therefore, the production of NO_x will increase drastically with a temperature over 1100°C [24]. This also means that the time at elevated temperatures is an important parameter (often referred to as residence time). Thermal NO_x is a dilemma in terms of efficiency. High combustion efficiency is recognized by high temperatures, while the best way to decrease NO_x emissions is to reduce the combustion temperature. This means that a choice must be made whether low NO_x emissions or low fuel consumption is desired.

Fuel NO_x

NO_x formation from fuel happens when nitrogen in the fuel reacts with oxygen in the fuel or in the air. According to Baukal [24] the conversion efficiency from Nitrogen in fuel to NO_x is

between 15 and 100 % where the highest efficiency is reached in fuels with low Nitrogen content. This mechanism of NO_x formation might be important for certain nitrogen-bearing fuel but can otherwise be neglected for conventional diesel fuel.

2.6.3 SULPHUR OXIDES

Sulfur oxides or SO_x are comprised of SO, S_nO, SO₂ and SO₃. However, most of the SO_x emissions from combustion is SO₂ [24]. SO_x are formed via oxidation of sulfur, meaning that emissions of SO_x are purely dependent on the amount of sulfur in the fuel. Low sulfur content equal low SO_x emissions. Modern automotive diesel fuel has a very low content of sulfur, thus leading to very low SO_x emissions.

Removing sulfur from the fuel has consequences connected to lubricity and oxidation resistance. According to research done by Danping and Spikes [25] sulfur content has a positive effect on wear, implying good lubrication properties. After the introduction of low sulfur content fuel, an increase in failure rate of especially fuel pumps was experienced. To cope with this reduction in lubricity addition of Fatty methyl esters (FAME) has become normal. FAME has proven good lubrication capabilities in blends with petrodiesel [26], and is a good substitute for sulfur in the fuel. However, FAME is an oxygenated fuel which means that reduced oxidation stability is expected.

2.6.4 HYDROCARBONS

During the combustion process, hydrocarbons (HC) are burned to produce power. However, the process is not perfect, and some of the hydrocarbons may escape with the exhaust gas. The mechanisms behind emission of unburned hydrocarbons in diesel engine are many, and relatively complex. Nevertheless, Heywood suggest two primary paths to emission of unburned hydrocarbon; the fuel-air mixture becomes too lean to support auto-ignition, and the fuel-air mixture becomes too rich to support auto-ignition [7].

The combustion process in CI-engines with direct injection are governed by the fuel-air mixing, where, as shown in Figure 2-13, several equivalence ratios can exist at the same time at different locations in the combustion chamber. Auto-ignition occurs at several locations at the same time, and tend to happen, where the equivalence ratio, temperature, and pressure, is closest to ideal conditions. This behavior does however mean that areas of both lean and rich areas exist in the combustion chamber. When operated correctly, diesel engines always operate in lean

conditions. This causes over-lean mixture to be the most important mechanism for production of unburned hydrocarbons [7]. Other mechanisms like quenching near the cylinder walls, and hydrocarbons left in the nozzle sac of the injector can also contribute to emissions of hydrocarbons.

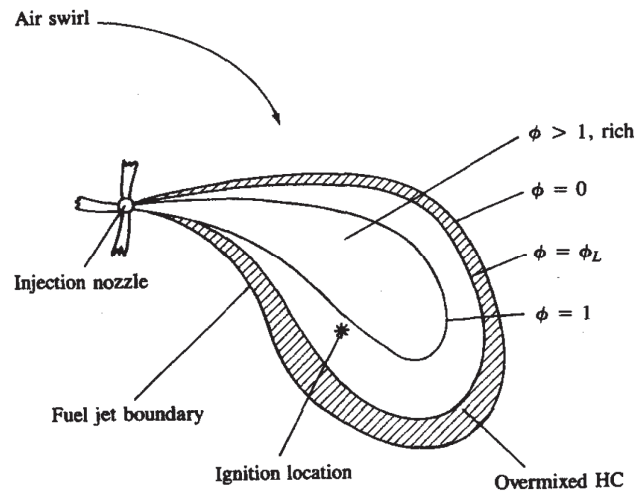


Figure 2-13 Schematic of variable equivalence ratio in diesel engines [7].

Compared to the hydrocarbon emissions from SI-engines, the emission of HC from CI-engines are very low.

3 RICARDO HYDRA RESEARCH ENGINE

3.1 STATUS QUO

The Hydra engine has for several years been out of service. The engine has for a longer time period been used for research purposes by Statoil. The engine has undergone several modifications, including a larger cylinder top modification in 1999. Today (end of January 2017), the engine is at NTNU, but has several problems that must be corrected before it can be used for extensive testing. Below follows a list of problems that needs to be fixed to make the engine fully operational.

3.1.1 MECHANICAL AND FLUID CONTAINMENT PROBLEMS

Below is a list of detected problems denoted by numbers, with possible solutions to the problem denoted by letters.

1. Severe oil leaks.
 - a. Change hoses and fittings that are substandard.
 - b. Change oil and oil filter
2. Fuel system not able to deliver sufficient tolerance of pressure to the common rail, possible oversized fuel pump
 - a. Change the suction control valve
 - b. The combustion rig laboratory has a fuel system that function properly, copying this system may improve the pressure tolerances
 - c. Possible solution is to add a controlled leak to the fuel system, thus increasing the fuel-pump throughput. This may improve consistency of pressure output
 - d. Remove excess pulse dampeners, to decrease the rail pressure response time.
3. The fuel system is overly complicated, with an unpractical setup, utilizing very long fuel lines to deliver fuel to the injectors.
 - a. Relocate fuel system, with simplified piping arrangement
4. The fuel system is slow to react when change in pressure is required
 - a. Remove at least one pulse-dampener
5. No measurement of fuel consumption is possible
 - a. Install fuel flow meter that can measure both fuel flow in, and fuel flow out in the return line.
6. Fuel system has been unused for a long time

- a. Change fuel filter
- 7. No safety cover on fuel pump
 - a. Make transparent safety cover and fit to fuel pump

3.1.2 CONTROL, SAFETY, AND DATA ACQUISITION

1. Dynamic measurements of cylinder pressure are not available
 - a. Install dynamic measurement encoder
2. Startup procedures are not up to date, and not intuitive in use
 - a. Make new procedures
3. No analog emergency-stop on fuel pump
 - a. Install analog emergency-stop
4. Not possible to set a specific common rail pressure. The rail pressure is now controlled by pulse width alteration of input to suction control valve
 - a. Implement controller of rail pressure
5. Not known if the air flow meter performs within specifications
 - a. Disassemble and clean
 - b. Test and calibrate with functioning flow-meter
6. Rate of heat release is not implemented into the logging system
 - a. Reuse the logging system used for the Scania engine
7. Exhaust camera for black smoke limit detection not working
 - a. Reinstall through wireless network

4 TEST-BED REVIEW

This section is a review of all components in the Hydra engine test-bed. The purpose of this section is to give the reader an in-depth understanding of all systems in the engine room. Much of the information portrayed here is collected and interpreted from various service manuals. It is thought that NTNU can use this section as part of an introduction for students that want to use the test-bed. Note that all information collected in this chapter is updated to suite the modifications done to the engine during this project, and does not portray how the engine was at the start of this project.

4.1 LAYOUT OF ENGINE ROOM

In Figure 4-1 the general layout of the engine room is shown. The illustration is highly simplified, but portrays the most important systems of the test-bed. A more detailed description of each component will follow in the next sections.

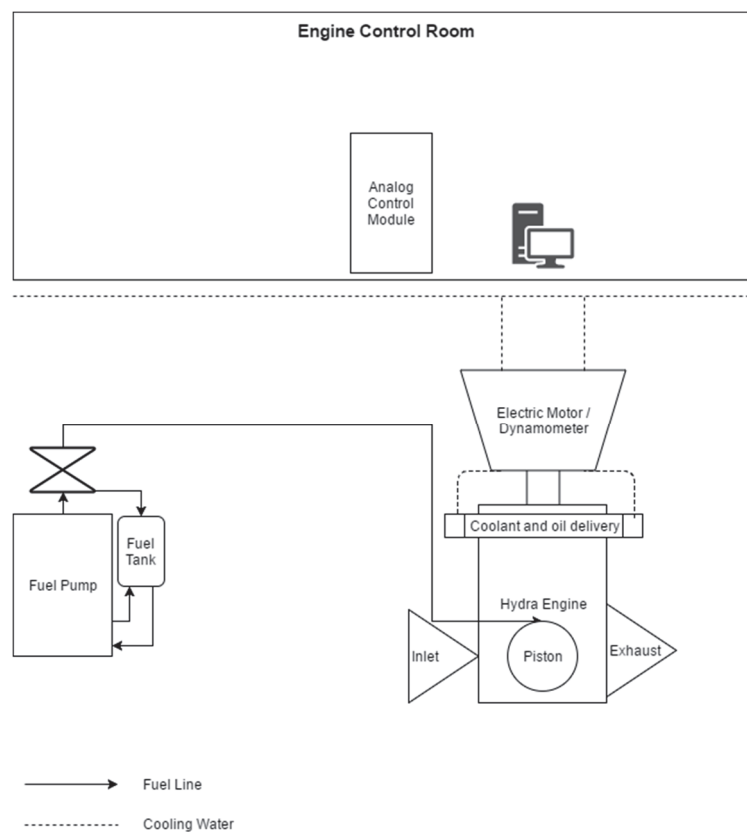


Figure 4-1 Test-bed layout

4.2 HYDRA ENGINE OVERVIEW

The Hydra engine has, as previously mentioned, undergone several modifications, and is not presently in its original form. Many of the modifications are not documented in a good way, therefor only the present state of the engine will be covered. The basic specifications of the engine are shown in Table 2 and are collected from the Ricardo cylinder-head modification documentation from 1999 [27].

Table 2 Basic specifications of Hydra engine

Displacement Volume ^a	0.4286 dm ³
Compression Volume ^a	0.02136 dm ³
Bore	78.35 mm
Stroke	88.9 mm
Compression Ratio ^a	20:1
Number of Valves	4
Valve Timing ^b	12°ATDC, 8°ABDC, 34°BBDC, 12°BTDC

^a Calculated based on original Audi V6 specifications

^b With original Audi V6 camshaft

The engine has structural limitations that must not be exceeded, these limitations are summarized in the table below.

Table 3 Limitations of Hydra engine

Maximum cylinder pressure ^a	120 bar
Maximum rotational speed ^b	4500 rpm or 75 rps
Maximum oil and coolant temperature ^b	90°C

^a Trip system not installed, must be monitored manually in LabVIEW

^b Trip system installed

The cylinder top, piston assembly and injector are modified components from a 1997 Audi A8 2.5 liter V6 engine, the engine code for this engine is AFB, and has since its first appearance in 1997 been used in several of Audi's engines. The piston has a symmetrical bowl configuration with valve indentations as shown in Figure 4-2.



Figure 4-2 Illustration of installed piston

The cylinder head has four valves, two for intake and two for exhaust. These valves are operated by two overhead camshafts, which are belt-driven from the crankshaft with a 2:1 reduction to comply with the four-stroke cycle. The camshaft assembly is shown in Figure 4-3.

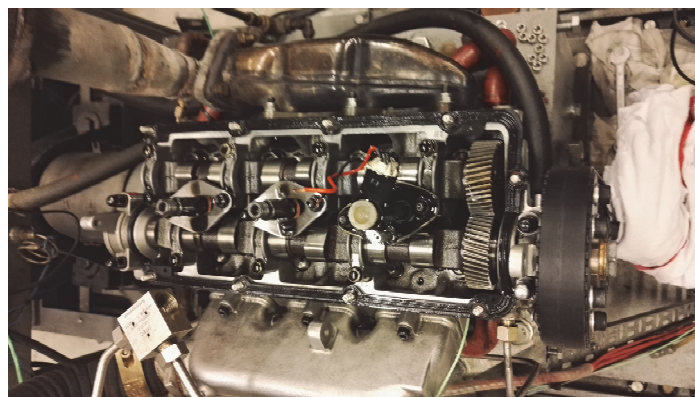


Figure 4-3 Camshaft assembly

The crankcase is originally made by Ricardo. This crankcase was custom made to make it possible to easily change cylinder heads, hence the name Hydra after the many headed-serpent in Greek mythology. As an added bonus, it is possible to separate the crankcase and the cylinder block, hence making it possible to alter bore and stroke [28].

4.2.1 COOLING AND LUBRICATION

Cooling water is supplied to both the engine and the brake from the water mains of the lab. The cooling water is circulated with a water pump located between the engine and the test-bed. This pump should be started and warmed up before any attempt to run the engine is made.

Lubrication oil is supplied to the engine with an oil pump, with a possibility for separate oil heating. This means that it is possible to heat the engine up to operational temperature before it is started. More information regarding precautions related to startup and cooling and lubrication can be found in the startup procedure. A drawing of the delivery system, which connected pumps can be seen in Figure 4-4, the cooling module is mounted between the Hydra engine and the dynamometer.

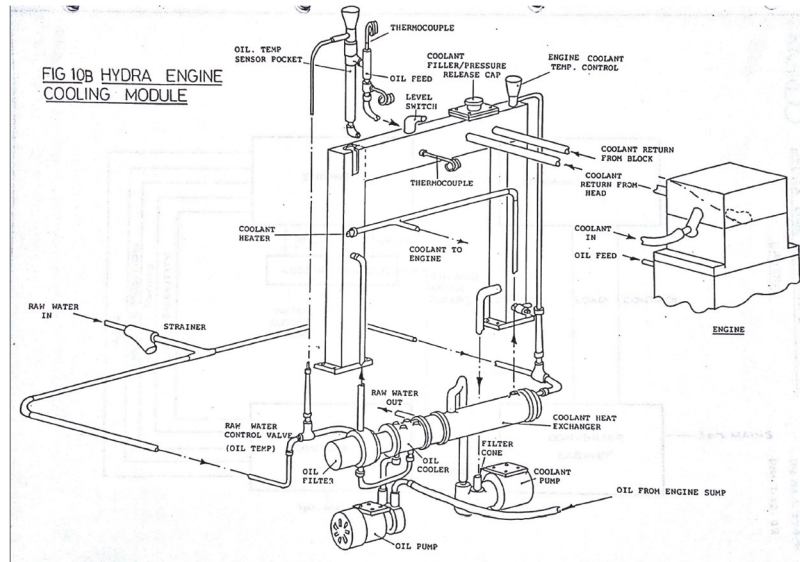


Figure 4-4 Cad drawing of oil and coolant delivery system

4.2.2 AIR INTAKE

The air intake of the Hydra engine is currently mounted in a temporary way, as shown in Figure 4-5. The plastic tube seen on the left side of the figure is connected directly to a standard Audi intake manifold. This install was made to circumvent an unknown flowmeter, more about this problem can be found in chapter 8.7. This solution is in practice a worse solution than the previous air intake, because it lacks the possibility of heated and compressed air. In addition, there is no air filter mounted in this configuration. The previous intake system is covered in appendix G.

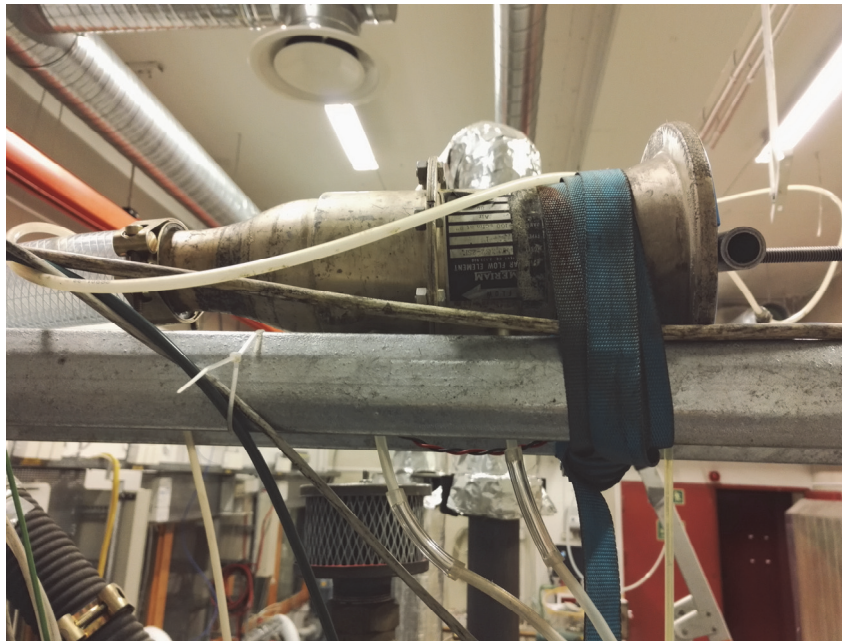


Figure 4-5 Temporary flow meter mounting on top of cable bridge

The air flow meter is of the differential pressure type. Utilizing Bernoulli's law, which states that the pressure drop across a restriction is proportional to the square of the fluid flow velocity. As can be seen from Figure 4-5 three sensors are connected to the flow meter. The two tubes that go down from the flowmeter are differential pressure sensors, taking measurements on both sides of the mesh inside the flowmeter. Additionally, a temperature sensor is mounted in the center of the flowmeter, meant to measure intake temperature. It is important to use this sensor when determining intake temperature, because a fan in the engine room creates large temperature differences between the current intake location and the floor.

4.2.3 EXHAUST AND EMISSION MEASUREMENT PORTS

The exhaust manifold is a production part from an Audi A4 2.5-liter engine, where two of the outlets are plugged. The exhaust is connected to a specialized insulated exhaust system with five ports for exhaust gas collection. As can be seen from Figure 4-6 the exhaust piping goes directly upwards from the engine, where it makes a turn and goes back into the floor. This gives an exhaust system with a long straight pipe (2.3 m), which are perfect for particulate matter measurements.

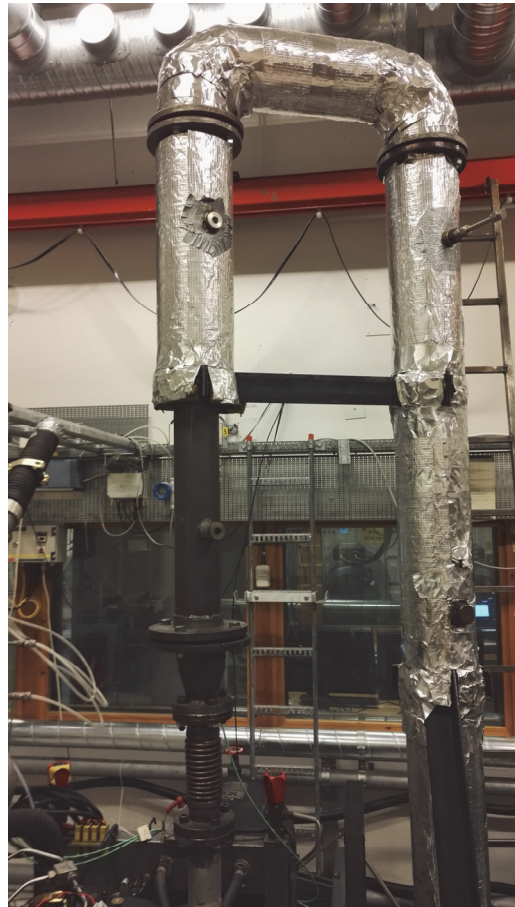


Figure 4-6 Exhaust piping

4.3 DYNAMOMETER

The load on the engine is controlled by an electric dynamometer. The dynamometer is a motor that can both act as a generator (delivering power to the grid and braking the engine) and as a motor (rotating the engine at a specific speed, with no need for combustion). The brake is an DC electrical motor with a shunt-wound stator. It is capable of producing 30 kW of power, at a maximum rotational speed of 6000 rpm. As opposed to an eddy current brake, which can be seen on the Volvo test-bed beside the Hydra test-bed, the brake connected to the Hydra engine can provide power to the engine. Since the Hydra engine is a one cylinder engine, this type of brake is required to make the engine rotate. The biggest advantage of such a brake is that it can deliver a constant rotational speed. This makes it easy to keep the engine on a constant load point, leading to better measurements.

In general dynamometers consist of a rotor and a stator. The rotor dissipates energy as it is rotated, and can provide load. This load can be changed depending on what type of

dynamometer used, for hydraulic dynamometers this is controlled using oil or water level inside the stator, for generators this is done by increasing the magnetic field in the stator. Measurements of torque delivered to the dynamometer is done by extending an arm from the stator to a force sensor. From this torque, can be calculated, and subsequently power using the equations below. The dynamometer can be calibrated by hanging calibration weights on the opposite side of the load cell, creating a known torque.

$$\tau = Fb \quad (21)$$

$$P = \tau N \quad (22)$$

Where τ is torque, F is force measured, b is the arm, N is the rotational speed of the engine and P is power.

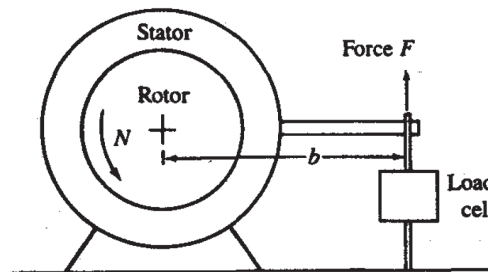


Fig. 1 Principle scratch of dynamometer [7]

4.4 FUEL SYSTEM

The fuel system is responsible for supplying fuel to the cylinder at the right time, right quantity, and pressure. The system consists of a low-pressure soft line assembly, a fuel-pump, a high-pressure hard line assembly and a piezoelectric common rail fuel injector. The low-pressure soft line assembly is responsible for delivering fuel to the fuel-pump, and is connected to the fuel tank with one output line and one return line. The fuel tank is a simple plastic container, where fuel easily can be changed by exchanging the container. The fuel-pump is responsible

for delivering constant pressure to the high-pressure hardline which goes directly into the injector.

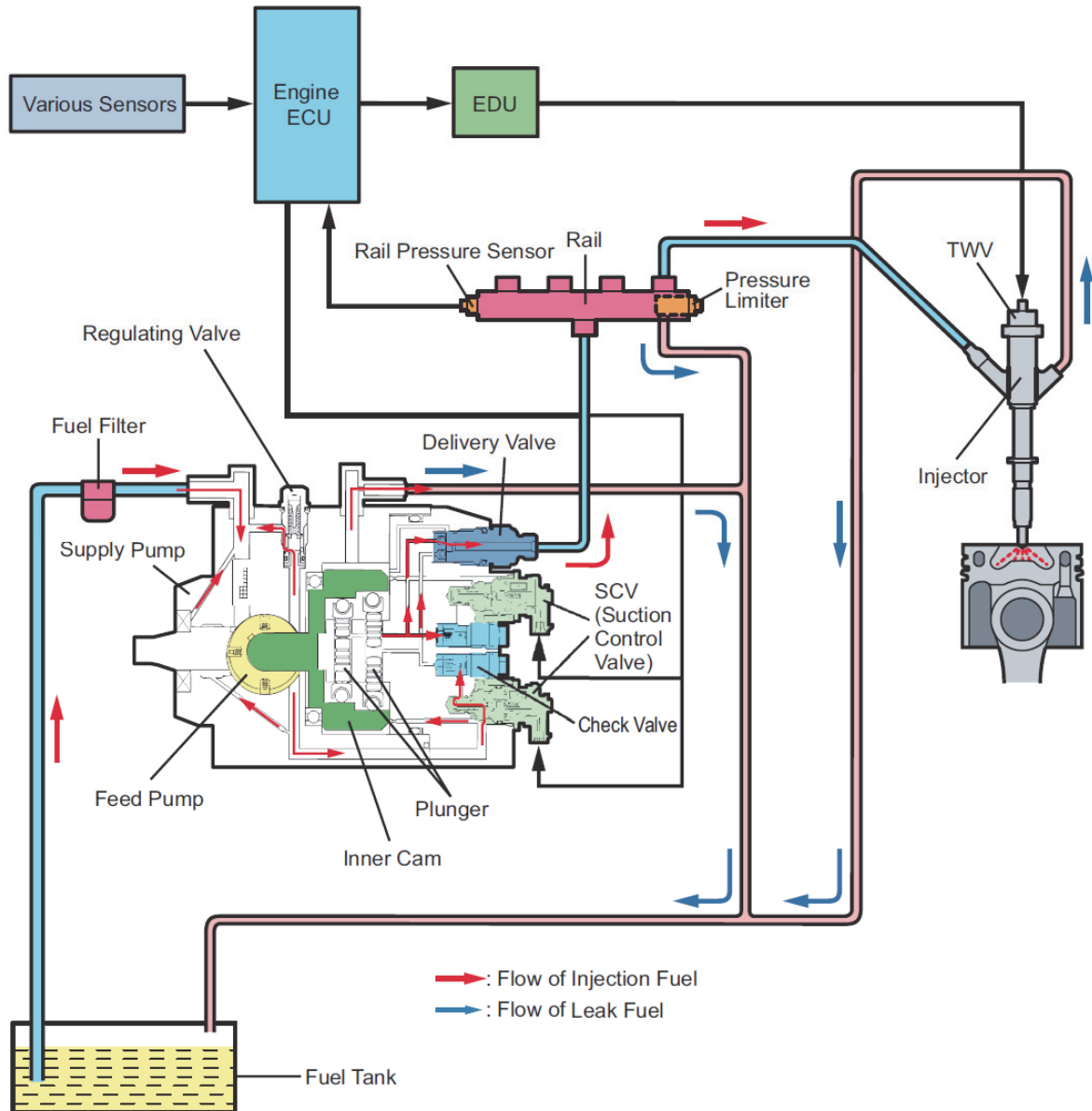


Figure 4-7 Complete schematic of generic common rail system [29]

4.4.1 FUEL TANK AND FUEL CONSUMPTION

Fuel consumption is measured with a gravimetric measurement, where the change of the weight of the fuel tank is measured. Knowing the time between start and end of each experiment will yield an estimate of the fuel consumption in grams per second. The fuel tank is connected to a force cell with a metal band, and has four holes for hoses and sensors. Two of the hoses are

connected to the high-pressure fuel-pump, where one is the supply line, and one is the return line. The third hose is the system leak, which is added to get a more controllable fuel system. The leak rate can be controlled by the micro-metering valve. Since the leakage produces a large amount of heat, the valve is cooled with a CPU cooling rib. In addition, a temperature sensor is located in the fuel tank to give an indication of too high temperatures. The fuel tank, fuel pump and leak valve can be seen in the Figure 4-8.



Figure 4-8 Fuel tank setup

4.4.2 FUEL-PUMP

The fuel-pump is a Denso HP3, which is a standard high-pressure supply pump, used in several different automobiles as part of a common rail system. In the Hydra engine, this pump is connected to an electric motor as opposed to a normal car engine where these pumps often are belt-driven directly from the crankshaft. Denso HP3 has three main parts; the feed pump, the pump chamber, and the suction control valve (SCV). The location of these main components is shown in Figure 4-9. Information about the inner workings of this pump is based on the Denso's service manual on the HP3 fuel pump [29].

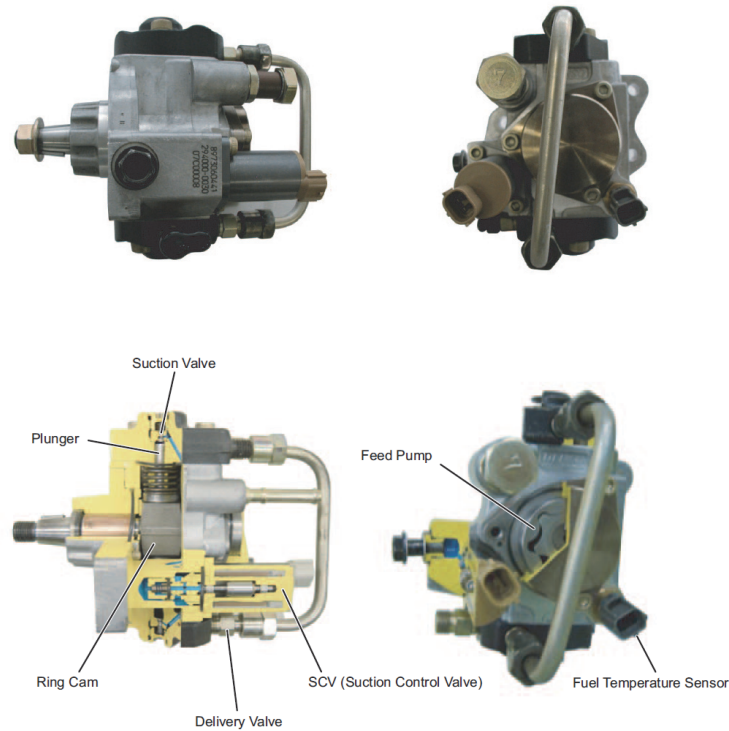


Figure 4-9 Denso HP3 fuel supply pump[29]

The feed pump is a trochoid type volume pump, delivering excess amounts of fuel to the pump chamber. The volume flow supplied by this pump is directly controlled by the speed of the electric motor, which drives the shaft. The feed pump has two inlets and three outlets. The fuel is constantly circulated through a regulating valve, which ensure that the feed pressure does not exceed a preset value. If there is too high pressure in the regulating valve, a spring is compressed, and fuel is diverted back into the fuel tank.

The main stream from the feed pump does however go into the suction control valve (SCV). This valve is a linear solenoid valve, which controls how much fuel that will be directed to the pump chamber, ultimately ensuring that the rail pressure reaches required values. The opening and closing of this valve is controlled in the engine ECU, where the required pressure can be changed depending on experiments needed. Figure 4-10 shows an illustration of the inner workings of the pump.

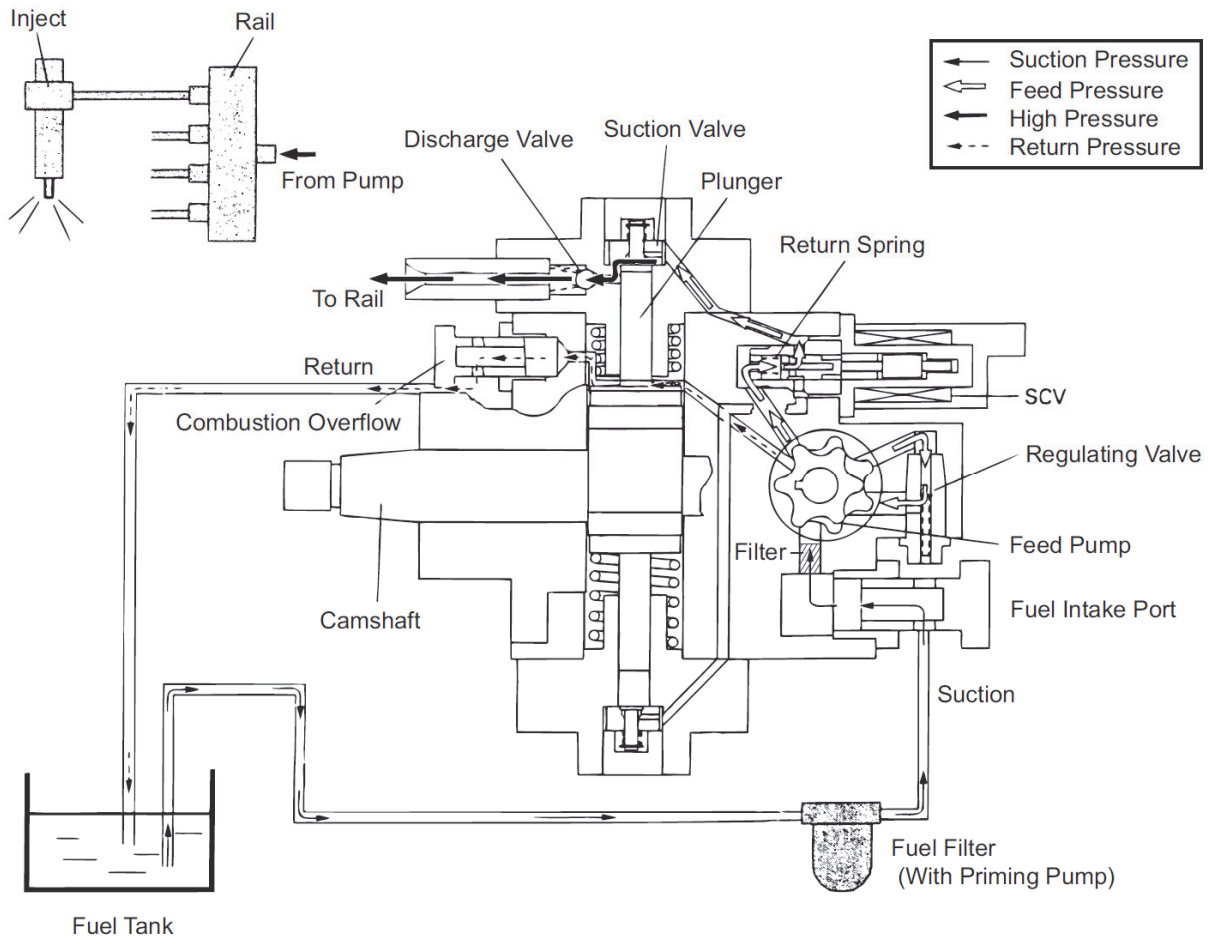


Figure 4-10 Denso HP3 illustration [29]

The pump chamber is composed of an eccentric cam, a ring cam, two plungers. The eccentric cam produces an oscillatory motion on the ring cam, which alternately compresses the plungers, which creates the required rail pressure.

4.4.3 FUEL INJECTOR

The fuel injector mounted to the Hydra engine is of the piezo type and is located in the center of the cylinder-top. The injector is delivered by Bosch and is rated for a maximum pressure of 1800 bar. It is however advised to not exceed a rail pressure of 1400 bar to minimize chances of fuel system failures.

4.5 ENGINE CONTROL

Two separate sources control the Hydra engine. The analog control module is used to start heaters and pumps, furthermore it is used to control the speed of the dynamometer. The speed is controlled through an analog control knob. Where dynamometer is instructed to keep constant speed, independent of the required negative or positive power. The LabVIEW interface is responsible for all other control and monitoring of the engine. The main controllable parameters in the LabVIEW system is related to the injection of fuel. The interface for injector and fuel pressure control is showed in Figure 4-11.

The injection pressure is controlled by pulse width modulation of the signal input to the SCV valve in the high-pressure fuel pump. The signal sent to the SCV valve is controlled by a PID controller. The parameters governing the controller can be altered in the controller interface. The controller has some problems with controlling large changes in rail pressure. Therefore, it is advised to make changes to the rail pressure in 50 bar intervals, and wait for the pressure to become stable before a further increase in pressure is requested. Before any of the parameters can be changed, the injector must be activated. This is done by clicking the button below “Injection Active”. The button can be clicked again to turn of the injector. This will automatically reduce fuel pressure to ambient conditions, and stop any injection of fuel. To increase the durability of the dynamometer it is advised to lower injection duration before the injector is turned off. The injector can be activated even if the engine has no rotational speed. Since the actual injection is determined by the crank angle position of the engine, no fuel will be injected in this state. The injection timing is set to 9° ATDC as standard, and can be changed at any point.

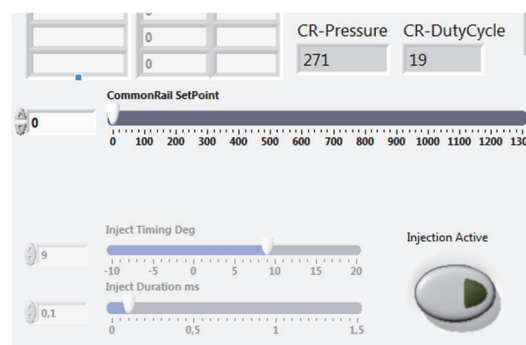


Figure 4-11 Injector and fuel pressure control interface

4.5.1 SENSOR OVERVIEW

Below is an overview of all sensors that are currently read in the control system, shown in two tables, separated as sensors for dynamic and static measurements respectively. The static sensors provide measurements at predefined intervals and give values for engine and engine room parameters. The dynamic sensors provide a total of 1440 measurements each cycle, and include all four strokes of the engine. In addition to these sensors, extra measurements of the exhaust gas composition can be made, these measurements are logged as static measurements. All measurements can be monitored in the LabVIEW interface. A description of the principles behind all sensors and measurement equipment used for engine testing can be found in chapter 5.

Table 4 Static Sensors

Sensor Name	Unit	Location
Speed	RPS	Crank Shaft
Torque	Nm	Dynamometer*
AirPressure	kPa	
AirFlowDP	kPa	Air Inlet
FuelConsumtion	g	Injector
CommonRailPress	Bar	After Fuel Pump
Inject Timing	°BTDC	Injector Control
Inject Duration	ms	Injector Control
Air	Deg C	Top of Air Filter
Oil	Deg C	Oil Pump
Water	Deg C	Water Pump
Air after heater	Deg C	Inlet Manifold ^a
Exhaust 1	Deg C	Exhaust Manifold
Exhaust 2	Deg C	After Exhaust Expander
Exhaust 3	Deg C	Floor Outlet
HP Fuel	Deg C	After Fuel Pump
Power	kW	Dynamometer ^b

^aNot connected, due to change in intake system

^b Calculated Values

Table 5 Dynamic Sensors

Sensor Name	Unit
CrancAngle	Deg
CylPressure	Bar
InjControl	Volts

5 PRINCIPLES OF MEASUREMENT EQUIPMENT

In the Hydra test-bed many sensors are used to have full control over the processes of the engine. These sensors are highly precise instruments that utilize simple physical principles to provide outputs of e.g. pressure, temperature, or gas composition. Understanding these principles are vital for estimations of measurement errors, and can be useful for understanding incorrect data. In the next sections a review of the basic principles behind each sensor is discussed.

Often sensors are responsible for measuring very small changes in parameters, therefore a small error in the measurement can be of large importance to the overall result of the study. Manufacturers of measuring equipment operate with quantities that describe their instruments accuracy e.g. repeatability, linearity and drift [30].

Repeatability:

Repeatability is a measure of the variation of measurements performed repeatedly on one object.

Linearity:

Linearity is a measure of the quality of result throughout the range of the instrument.

Drift or stability:

Drift is a measure of continues and systematic change of the measurement with respect to time. Often as a result of temperature change.

5.1 CRANK ANGLE AND CYLINDER PRESSURE

5.1.1 LOCATING TOP DEAD CENTER

Previously the importance of knowing the crank angle has been discussed. This may seem a trivial matter, but in reality, this is a difficult task, and if not properly done will have a large influence on results. Crank angle measurements are always taken with reference to top dead center. Locating the correct TDC position is very important because it can induce significant errors in calculations of indicated work and rate of heat release [31]. Position of TDC can be defined based on motored cylinder pressure curves. However, this is problematic because TDC will not coincide with the peak motored cylinder pressure. TDC will rather have a position after the peak motored cylinder pressure, because of heat losses and mass losses. The angle between actual TDC and the motored peak pressure is called loss angle. Figure 5-1 show the definition of the loss angle.

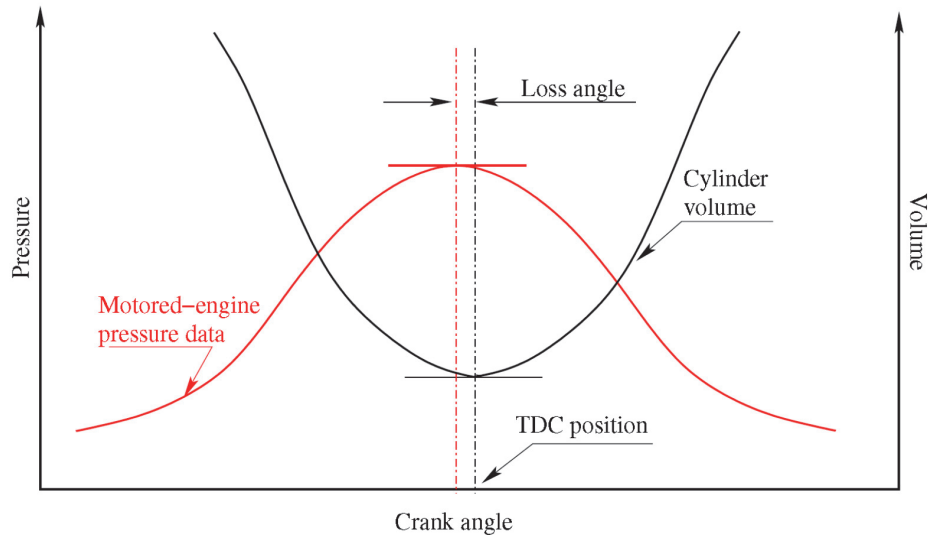


Figure 5-1 Definition of Loss angle [31]

Methods that provide sufficient accuracy when calculating loss angle has been developed. Staś [32] has for example developed a method based on net heat release rate that can be used. However, the most accurate way of determining TDC is to measure it directly. This can be done using a capacitive sensor mounted in the cylinder top [31].

5.1.2 OPTICAL ANGLE ENCODER

Crank angle measurements are performed using an optical angle encoder. The encoder operates by measuring how many increments of an incremental track that passes through a photovoltaic cell. A photovoltaic cell consists of a light source and a material that produces a small voltage if subjected to light. Each increment on the incremental track will stop light from impacting on the photovoltaic material, hence creating an oscillating signal that can be read as positions related to a reference increment (TDC). The encoder mounted to the Hydra engine has 720 increments in the incremental track, giving 1440 data points per cycle. A representation of the principles of an optical angle encoder are shown in Figure 5-2.

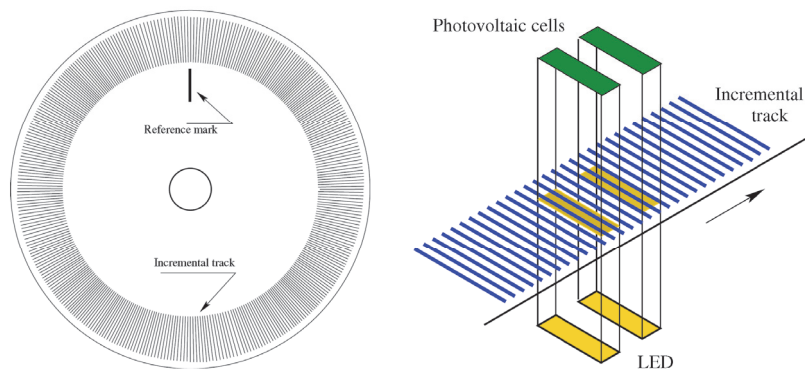


Figure 5-2 Principle of Optical Angle Encoder [31]

5.1.3 PIEZOELECTRIC TRANSDUCERS

Piezoelectric transducers are probably one of the most useful sensors for modern measurements. They can be used both as a sensor and as an actuator, and is used in in every research field from engineering to biotechnologies [33]. Piezoelectric sensors can measure a range of parameters including pressure, acceleration, vibrations, and electrical frequency. In an engine test situation, they are mostly used for in cylinder pressure measurements as well as knocking detecting sensors and as actuators in injectors [34].

The principle of piezoelectricity was first demonstrated by Pierre Curie and his brother Jacques Curie in 1880 [35]. Piezo comes from the Greek word “piezein” which means to squeeze or press. Piezoelectric material produces a small electrical potential when subject to deformation. If the material instead is subjected to a small electric potential, it will deform in the opposite direction [36]. The electric potential is directly proportional to the force that the material is subjected to, making it an easy task to convert force to an electric input to gauge force. A schematic of a typical piezoelectric pressure transducer is shown in Figure 5-3.

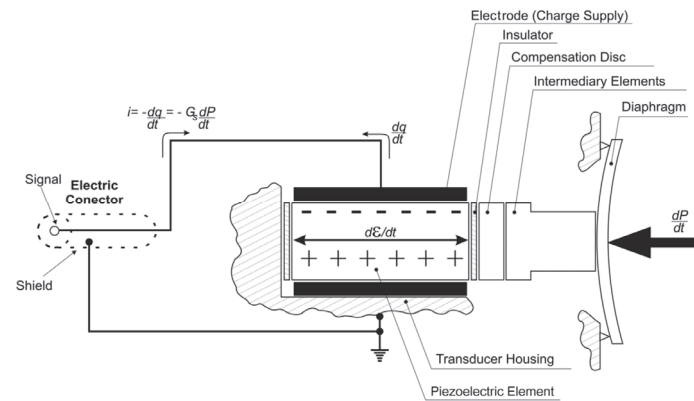


Figure 5-3 Schematic of Piezoelectric Transducer [31]

The accuracy of piezoelectric sensors is generally very high. However, the sensors are bad at measuring static forces, because the resistance of the piezoelectric material will change marginally under constant load, causing a strong tendency for drift. In addition to this, care must be taken to avoid situations that can depolarize the piezoelectric material, i.e. there are two conditions that can depolarize the material; strong electric field and high temperatures [37].

Strong electrical fields can be caused by external factors or the sensor itself. With very large pressure changes the electric potential can be so large that it depolarizes itself. This problem is often overcome by adding a capacitor to the sensor, that can work as a buffer at high loads.

If a polarized material is subjected to higher temperatures, then the materials Curie-point it will be depolarized. This implies that materials with a high Curie-point must be chosen if the sensor is subject to high temperatures. In addition to this temperature influences the internal resistance of the piezoelectric material causing bad linearity.

The piezoelectric pressure transducer used on the Hydra engine is mounted where the glow plug in cylinder top would be. The location of the pressure transducer can have a large impact on the accuracy of pressure readings. A location should be chosen in well cooled areas of the combustion chamber, to reduce thermal stresses on the transducer housing [31]. Randolph suggests several tests for determining short term drift in pressure transducers [38].

5.1.4 DYNAMIC MEASUREMENTS OF PRESSURE AND CRANK ANGLE

In the dynamic measurements, the optical crank angle encoder, the pressure transducer, and the injector comes together to create coherent data that can be used for engine analysis. The setup of the dynamic measurements is similar to that shown in Figure 5-4. Signals from both the pressure transducer and the injector are collected, and related to a specific crank angle. This data can then be used to compute for example rate of heat release.

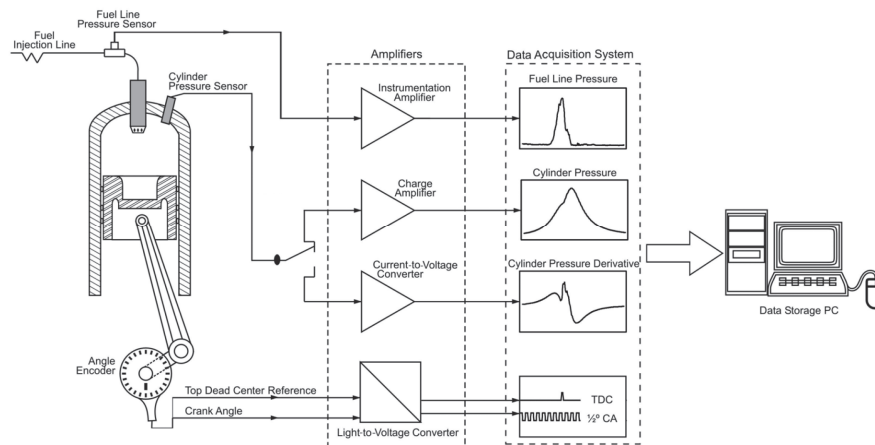


Figure 5-4 Dynamic Measurement Setup

5.2 TEMPERATURE

Temperature sensors is the most used sensor in engine research. These sensors provide vital information about the temperatures at different places in the engine or the cooling system, and can be used to derive among other things thermal efficiency of most components that dissipate heat. In an engine test-bed it is normal to have two different types of temperature sensors. Thermistors are very simple sensors that can be used for temperatures between 0 and 100 °C. Thermocouples are a little more complicated, but can measure temperatures in a much wider range than the thermistors [39].

5.2.1 THERMISTORS

Thermistors utilizes the fact that, for most conducting materials, a reduction in electrical resistance can be observed when the material is heated. Because of Ohm's law the current will increase with a reduction in resistance. This increase in current can be measured and be directly related to a specific temperature increase. Thermistors are very simple sensors that is easy and

inexpensive in use. Therefore, it is a very popular temperature sensor for automation. In engine testing situations, these sensors are mostly used for close to ambient temperature making measurements of for example charge air temperature. Thermistors is also very good at measuring very small changes in temperature [39]. Regrettably, the resistance of the thermistor can cause the thermistor to produce its own heat during measurements, which can lead to drift.



Figure 5-5 Thermistor

5.2.2 THERMOCOUPLES

Thermocouples consist of two different materials that are coupled together as shown in Figure 5-6. The sensor utilizes the Seebeck effect also called thermoelectricity, which state that if two different metals are subjected to the same heat they will create an electric potential because of dissimilar expansion of the material due to a difference in heat capacity. This method only measures differential differences in temperature, therefore a reference junction with known temperature must also be connected to the two metals [40]. This makes it possible to calculate the absolute temperature based on differential temperature in the measurement junction, and base temperature in the reference junction. The reference junction temperature is often measured using a thermistor sensor.

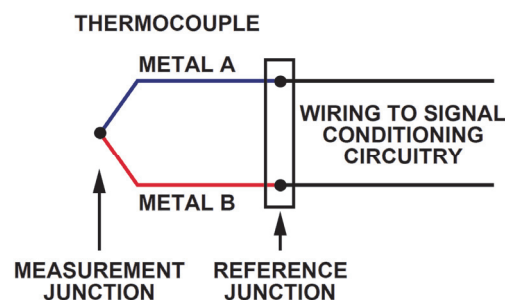


Figure 5-6 Representation of thermocouple [39]

Thermocouples can be used for measurements of temperature in a very large range from -200°C to 2500°C , this in addition to a very robust design makes them perfect for process monitoring. Thermocouples are small, and have a fast response to temperature changes, making them ideal

for use in transient behavior measurements. As opposed to thermistors they do not produce heat during measurements, which leads to a reduced chance of drift.

The disadvantages of thermocouples are coupled to signal processing. The sensor produces very small voltages, with extremely low changes depicting temperature change, ranging between 40 and 55 $\mu\text{V}/^\circ\text{C}$ depending on the materials used in the measurement junction. This means that the signal must be conditioned with gains of up to 100, which can lead to difficulties in distinguishing temperature change from noise. In addition to this the sensor is made up of two dissimilar metals, which make it a subject to corrosion [40].

5.3 HORIBA GAS ANALYZER

The gas analyzer that is available for student-experiments at NTNU is a HORIBA PG-250. This is a portable gas analyzer that can measure gas composition, using several sensors. A review of the principle used in each sensor is shown in the next sections, and are based on the HORIBA user manual [41].

5.3.1 NITROGEN OXIDES

Chemiluminescence Method (CLD):

Chemiluminescence is a term that describe chemical reactions that omit light. This is a principle that the HORIBA gas analyzer take advantage of when measuring Nitrogen Oxide emissions. The measurements are done by making ozone interact with NO and create NO_2 and O_2 as shown in equation 23. Some of the NO_2 produced is in an excited state NO_2^* . The excited nitrogen dioxide must return to a ground state. This reaction radiates light, and is shown in equation 24. If the light emitted from this reaction is measured, a determination of the NO concentration in the gas mix can be made. Measurements done using this principle can detect concentrations of NO down to 5ppt. The HORIBA PG-250 can be put in either a NO mode or a NOx mode. For the NOx mode, all NO_2 particles are put through a catalytic reduction, and is reduced to NO before it is subjected to the ozone reaction.



5.3.2 OXYGEN

Zirconia sensors also called oxygen sensors or lambda probes measure the oxygen concentration in a gas mixture. On an automotive engine, this sensor is often placed before and after the catalytic converter to give feedback to the engine control unit (ECU) about the fuel air ratio of the engine and the efficiency of the catalytic converter. A low oxygen concentration means that the engine is running rich, which means that less fuel must be injected while a high oxygen concentration means that the engine is running lean, and need a higher fuel input. This gives possibilities of fine-tuning the fuel injection. A typical lambda sensor for engine control is shown in Figure 5-7.

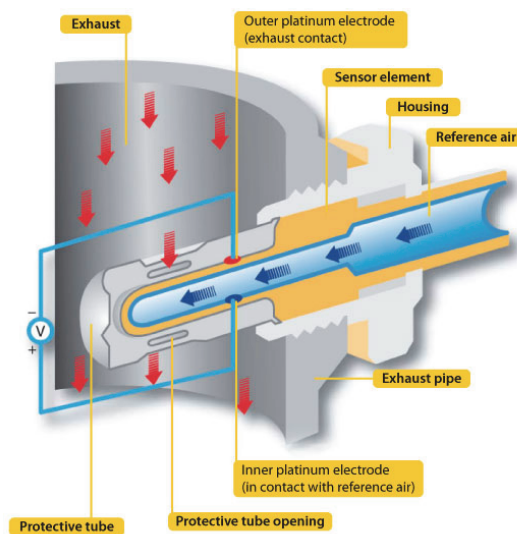


Figure 5-7 Lambda Sensor [42]

Inside gas analyzers, the oxygen sensors are more complicated, but work on the same principle as the lambda probe. The only major difference between a gas analyzer oxygen sensor and a lambda probe is that the gas analyzer can measure exact concentration due to a reference chamber with pure oxygen instead of air. The lambda probe on the other hand, can only measure oxygen concentration in comparison with the oxygen concentration of the air.

Principle of Zirconia Oxygen Sensor:

Zirconia sensors utilizes the principle of electro chemistry where the partial pressure difference between the sample gas and a reference oxygen rich gas force oxygen ions to travel through a circuit to produce an electrical potential. This potential can be measured and directly related to the difference in concentration between the reference gas and the sample gas.

Zirconia or Zirconium Dioxide with chemical formula ZrO_2 allows oxygen ions to pass freely through it at high temperatures, therefore the zirconia must be heated to approximately $800^\circ C$ before it can be used [41].

The sensor consists of a heater to get the zirconia up to temperature, a pumping cell, a sensing cell, a reference chamber and a gas detection chamber. The sensing cell is filled with close to 100% by volume of oxygen. While the pumping cell is filled with a gas with close to 0% by volume of oxygen. Figure 5-8 shows a principle drawing of a zirconia sensor.

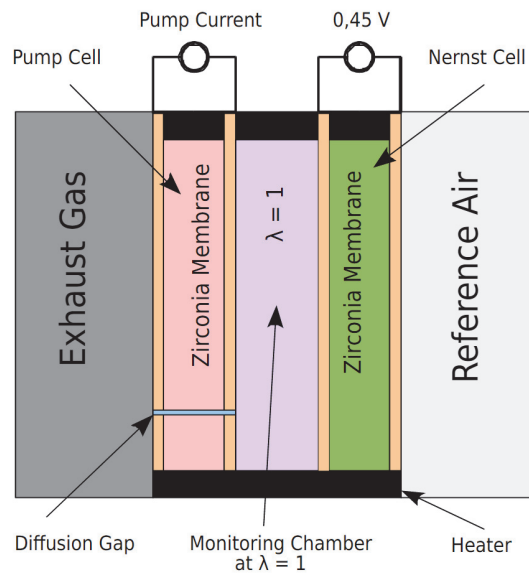


Figure 5-8 Principle of Wide Band Zirconium Sensor [43]

5.3.3 CARBON OXIDES

Non-Dispersive Infrared Sensor (NDIR):

Molecules of different substances will absorb different wave lengths of light. This principle is used to detect and size the concentrations of CO , CO_2 and SO_2 in a NDIR sensor. The sensor uses infrared light, and detect which and how much of the wavelengths that are absorbed, and can from this calculate how much of each pollutant that is present in the gas mix. A solenoid valve is altering between adding sample gas and zero gas into a measuring cell. The zero gas consist of gases that are free of pollutants that are measured, normally pure nitrogen. The infrared detector will detect how much infrared light that are absorbed in the two different gases and compare them with each other to find the concentration of the gas that are of interest. Two detectors can be coupled to each measuring cell, and several measuring cells can be active. One

reason for using several measuring cells is that some of the components will have a wavelength that slightly overlap with each other. This is circumvented using additional measuring cells with an infrared filter that filters out the wavelengths that are in an overlapping region [41]. A representation of the measuring cell is shown in Figure 5-9.

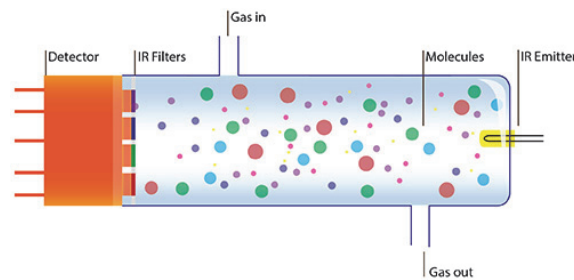


Figure 5-9 NDIR Sensor [43]

5.4 TOTAL HYDROCARBON ANALYZER

The high temperature total hydrocarbon analyzer utilizes flame ionization detection (FID) to measure the concentration of hydrocarbons in the exhaust stream. FID is a technology that compares the ionization from burning pure hydrogen, with the ionization from burning the exhaust gas. The relative difference in ionization can be directly correlated to the concentration of hydrocarbons in the exhaust stream. The combustion chamber and sampling line of the analyzer is heated to above 190°C to secure that the heavier hydrocarbons are in gaseous form [43].

5.5 AVL SMOKE METER

The AVL smoke-meter utilizes the fact that soot has a black tint, and can be captured in filters. The smoke-meter collects a specific volume of exhaust gas via a heated sample line, and uses a diaphragm pump to push the sample through a filter. The filter's reflection of light is measured before and after exhaust has been pushed through it. A clean filter is given the value of 0 and a completely black filter is given a value of 10. This method of measuring reflection from the filter is shown in Figure 5-10.

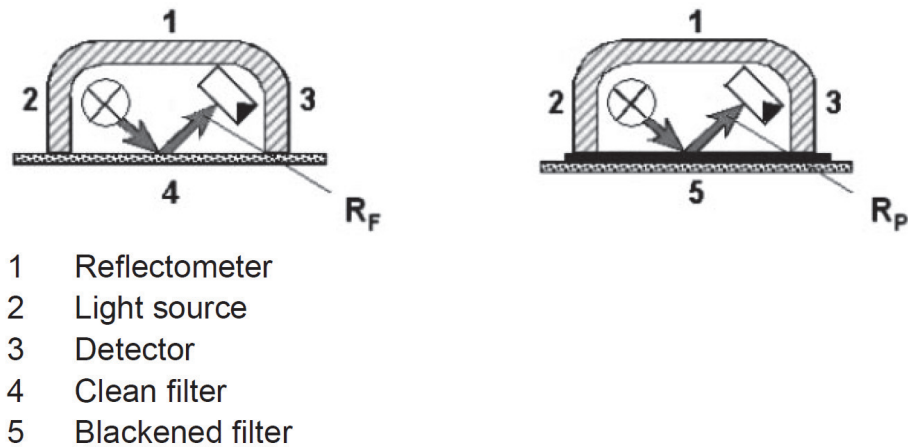


Figure 5-10 Filter reflection measurement

This is a qualitative method, which only measure the carbon fraction of particulate matter in the exhaust stream. Thus, the method does not provide any information about size distribution or other sources of particulate matter. However, it provides a simple and robust way to measure the differences in smoke emission from the combustion process. Since the same volume of exhaust is pushed through the filter, the scale for all tests is equal, and can be used for comparison. AVL suggests the following formula for calculating the carbon fraction of particle matter in the exhaust gas based on filter smoke number (FSN).

$$C = \frac{1}{0.405} * 4.95 * FSN * \exp(0.38 * FSN) \quad (25)$$

Where C is the carbon fraction of the particle matter in mg/m^3 and FSN is the filter smoke number, measured by the instrument.

6 ENGINE MAPPING

In modern engines, engine mapping is used to optimize the parameters used in engine control. This is done by providing the engine control unit (ECU) with a reference table, where optimized input can be collected for each load point. A 3D representation of the reference table is often referred to as an engine map. The ECU typically contains several maps that control different aspects of the engine operation like, for example, injection timing and exhaust gas recirculation. The maps can be represented as a function of speed and load, but are not limited to these variables. A typical map for a SI-engine with output torque as a function of engine speed and throttle opening is shown in Figure 6-1.

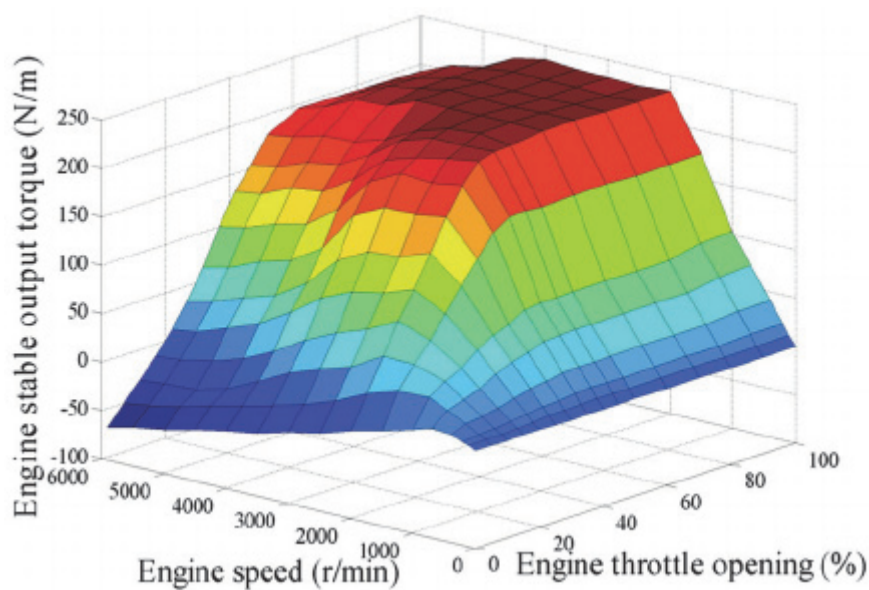


Figure 6-1 Map of output torque as function of engine speed and throttle opening [44]

The Hydra engine, in contrast to standard engines, is not controlled by engine maps. Instead, the engine-operator manually controls the inputs to the engine. This makes optimization of the engine control difficult. However, the purpose of the Hydra engine is not to operate as an optimized machine, but rather to be a platform for studying the effects of different inputs during engine operation. Therefore, the goal of mapping the engine is not to produce optimized maps, but rather to investigate limitations and stability of engine operation with variable input parameters. The maps created in this thesis (not done due to diverse failures) will therefore be more a visualization of different operating points, then an actual control map. The process of making a map and corresponding theory of curve fitting will be covered in the next sections.

6.1 PROCESS OF ENGINE MAPPING

In its most basic form an internal combustion engine is a machine that takes inputs and creates outputs. The output is dependent on both controllable and uncontrollable variables, a representation of such a system is shown in Figure 6-2. A map is a three-dimensional representation of outputs as a function of inputs and or variables.

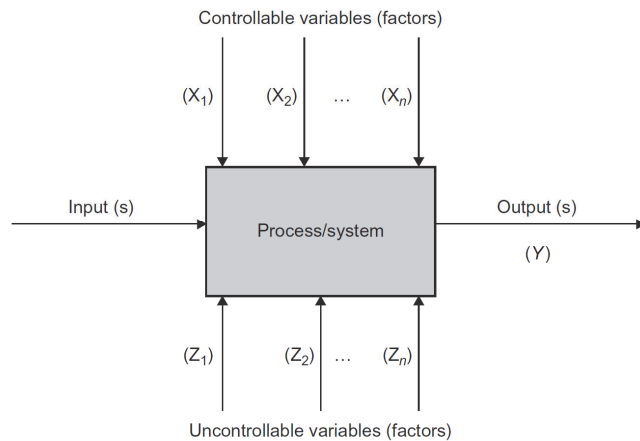


Figure 6-2 General model of engine/process/system [45]

This means that for each load point the engine has several variables that can influence the output, and each of these variables does not necessarily need to be independent. Interacting variable may increase the complexity of analysis. Figure 6-3 shows typical inputs and outputs from an engine at one specific load point. In an engine optimization situation these variables would be handled by optimization software like AVL CAMEO [46], where the software would be responsible to set up a design of experiments to optimize a certain set of outputs.

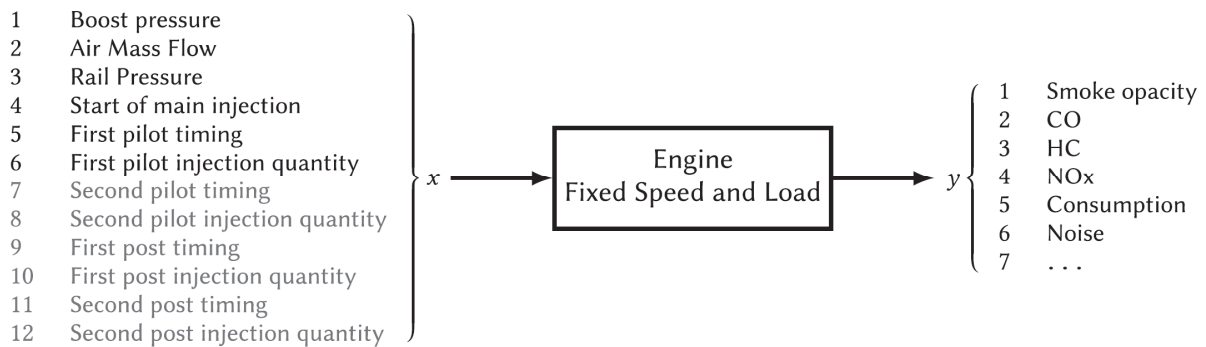


Figure 6-3 Engine inputs and outputs with fixed speed and load [47]

When dealing with engine experiments there are three factors that are very important to consider before choosing experimental methods, i.e. cost, time and accuracy. These are factors that are closely linked, but can change the character of the experiments immensely with different weightings of the factors. Both time and accuracy are highly dependent on cost, making cost the driving factor when determining the experimental procedures. Time will directly impact cost, by determining how much fuel is used, and how much the engine operators are paid. Accuracy impacts the cost through time, where additional time is used to increase accuracy. A strict balance between these factors must exist to reduce the cost as much as possible, and at the same time, produce sufficiently accurate results.

For the Hydra engine, the cost of each experiment is very low, because the engine uses very little fuel, and the operator does not require payment. Nevertheless, it is known that the engine requires a long time for each start-up procedure. This means that to reduce cost as much as possible, it is advantageous to perform as many experiments as possible for each start-up. This will increase the effective time used for experiments and will not use unnecessary amounts of energy for start-ups. To make this possible, extensive planning before each test-day is important.

6.1.1 CHOOSING LOAD-POINTS

Unfortunately, the operating profile of the test engine is not known. Therefore, the main operating profile of the engine need to be investigated. Meaning that the upper limits of load at several speeds must be found. The engine has some operational limitations, which are summarized in Table 6.

Table 6 Known engine limitations

Max Cylinder Pressure	120 bar
Max Speed	75 rps or 4500 rpm ^b
Min Speed	Around 20 rps or 1200 rpm ^a
Max Power	8 kW ^a

^aUncertain value. Must be investigated

^bNormal to use rpm as unit for engine speed, but all control of engine speed on the Hydra engine is done in rps

A load point is a point where the engine can operate at constant load and speed. As previously stated the outputs of a certain load point can be manipulated by changing settings of controllable

variables. Therefore, the controllable variables must be locked in such a way that the outputs can be compared with each other. With the Hydra engine, the most convenient variables to lock is injection timing, and injection pressure, while keeping inlet temperature close to constant. In an optimization situation, these locked variables would be subject of tweaking to improve the characteristics of the output maps.

It is important to choose load points that are contributing to a better model of the engine behavior. This can be done in a systematic way, where load points are chosen based on improvements possibilities in goodness of fit. However, this will be an iterative process, where the engine must be started and stopped between each additional load point series to allow for analysis of the data. Since the Hydra engine has a long start-up time it would be preferable to run a long series of load points as the first experiment. If the model is proven to be bad in some areas, a second series of load points must be employed in these areas, to improve the model.

6.2 CURVE-FITTING

To make a model of the data provided by the experiments, the curve-fitting tool in Matlab will be used. This tool makes it possible to make a mathematical model fitted to the collected data from the experiments, and create a surface that mimics the behavior of the engine, and can act as a visualization of the engine behavior. The curve fitting toolbox is a very versatile toolbox that can utilize several linear and non-linear regression models, to compute a mathematical model of the data provided [48]. In addition, it provides the opportunity to remove outliers from the dataset, as well as an evaluation of the correctness of the mathematical model.

6.2.1 MODELS OF FITTING

As standard, the curve fitting tool provides three different methods for fitting data: interpolation, LOWESS and polynomial.

Interpolation:

Interpolation is a method of estimating values between known data points. This can be done in several different ways, where the curve fitting tool provides six different methods of interpolation: linear, nearest neighbor, cubic spline, shape-preserving, biharmonic (v4) and thin-plate spline. Mathworks notes the following for these methods: “The linear and nearest neighbor methods are fast, but the resulting curves are not very smooth. The cubic spline and shape-preserving and v4 methods are slower, but the resulting curves are very smooth.” [49]

LOWESS:

LOWESS or locally weighted scatter-plot smoother, is a method that uses linear regression to weight data within a selected span [50]. In general, this is not a good method for engine analysis because it requires knowledge of where the dataset is more correct. In addition, the resulting surface does not provide a strictly correct picture of the dataset.

Polynomial:

Polynomial models are probably the most useful in terms of engine analysis. They are based on simple mathematical expressions of variables and coefficients. The number of coefficients and interaction between variables, is dependent on the selected degree of the polynomial. Polynomial models are given by the following expression [48]:

$$y = \sum_{i=1}^{n+1} p_i x^{n+1-i} \quad (26)$$

where p is the coefficients, x is the variables, n+1 is the order of the polynomial and n is the degree of the polynomial. The degree of the polynomial can be chosen in the range 1 to 9. For polynomials of surfaces of third degree in x direction, the expression will take the form below. Note that the sum of the degrees in x and y direction cannot exceed 9.

$$\gamma = p_{00} + p_{01}y + p_{20}x^2 + p_{11}xy + p_{30}x^3 + p_{21}x^2y \quad (27)$$

Polynomials are often used in the creation of empirical models, and have several advantages. The process is linear, which leads to simple and fast curve fitting, at the same time the process is very flexible in terms of data fitting. However, the fitting tends to be unstable at higher degrees, and can be directly wrong if extrapolation is needed. Therefore it is strongly discouraged to use polynomial models for extrapolation outside the dataset [48].

6.2.2 EVALUATING GOODNESS OF FIT

In addition to producing a mathematical model of the dataset, the curve fitting tool also provides an evaluation of the goodness of the fit for the model that is suggested. However, it is important that the fitting is checked manually for outliers and illogical behavior, before the goodness of the fit is finally evaluated. The curve-fitting tool evaluates the goodness of the fit using four different statistical models, i.e. sum of square due to error, R-square, adjusted R-square and,

root mean square error. An outline of these statistical methods are conducted below, based on documentation created by Mathworks [51].

Sum of Square due to Error (SSE):

SSE is a measure of the total deviation between the response values and the fit. A value close to zero depicts a smaller error component [51]. In mathematical terms, the SSE can be calculated according the following formula:

$$SSE = \sum_{i=1}^n w_i (y_i - \hat{y}_i)^2 \quad (28)$$

R-Square:

R-square depicts the goodness of fit in terms of variation of the data. It is defined as the ratio between the sum of squares of the regression (SSR) and the total sum of squares (SST) [51]. R-square takes a value between 0 and 1, where a value close to 1 indicates that a large portion of the variance in the data is accounted for in the model. The mathematical definition of SSR, SST and R-square is given by equations below:

$$SSR = \sum_{i=1}^n w_i (\hat{y}_i - \bar{y})^2 \quad (29)$$

$$SST = \sum_{i=1}^n w_i (y_i - \bar{y}_i)^2 \quad (30)$$

$$Rsquare = \frac{SSR}{SST} = 1 - \frac{SSE}{SST} \quad (31)$$

Degrees of Freedom Adjusted R-Square:

The adjusted R-square considers that the value of R-square tends to increase with the number of fitted coefficients in the model, despite no practical improvement in the fit. The adjusted R-square is the best indicator of fit quality, where a series of fits with different degrees are compared to each other. In mathematical terms, the adjusted R-square is described as follows:

$$\text{adjusted Rsquare} = 1 - \frac{SSE(n - 1)}{SST(v)} \quad (32)$$

where v is defined as $(n - m)$ and n is the number of response values and m is the number of fitted coefficients.

Root Mean Square Error (RMSE):

RMSE is also known as the standard error of the fit, and is the estimated standard deviation of the random component of the data. A RMSE with a value close to 0 indicates a fit that is more useful for prediction. RMSE is defined as follows:

$$RMSE = s = \sqrt{MSE} \quad (33)$$

where MSE is the mean square error of the residual mean square.

$$MSE = \frac{SSE}{v} \quad (34)$$

7 METHODOLOGY

The experiments of this thesis will be conducted in NTNU's machinery laboratory at Marinteknisk senter. The main purpose of the experiments will be to identify problems with the Hydra engine test-bed and make an evaluation of its ability to provide the correct measurement data. As an additional bonus the experiments will be used as a basis of understanding for making an engine guide for the Hydra engine.

The test-bed and sensors has been covered in detail in chapter 4 and 5, therefore no more consideration will be shown in this regard. The next section will give some additional information related to actual test setup, fuel, planned tests, and data processing.

7.1 TEST SETUP

An illustration of the test setup is shown in Figure 7-1. It was not possible to mount the AVL-smoke meter at the time of these experiments due to a shortage of laboratory personnel.

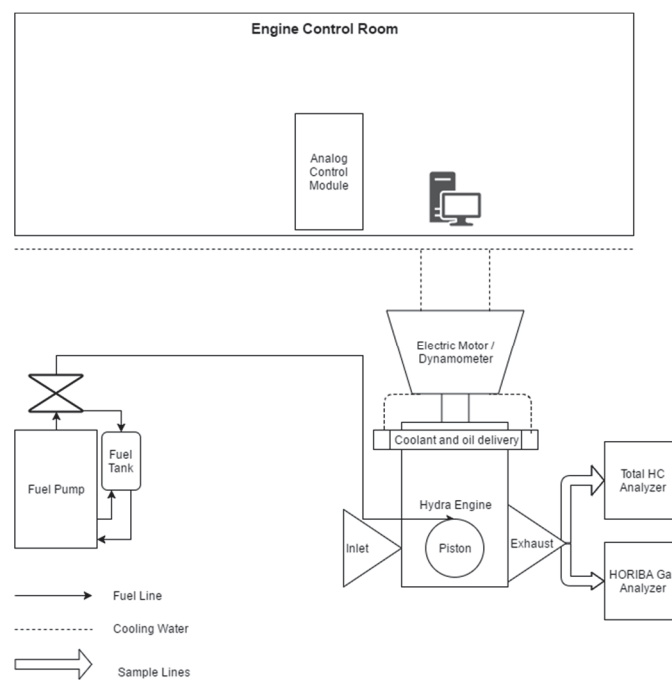


Figure 7-1 Illustration of test setup

7.2 FUEL

Marine gas oil (MGO) is used for the all conducted experiments. The diesel fuel can be assumed to have the properties shown in Table 7. The datasheet for the fuel used, can be found in appendix H.

Table 7 Typical Properties of MGO [52]

Lower Heating Value [MJ/kg]	42.8
Cetane Number	< 51.0
Density @15°C [kg/m ³]	855
Viscosity @40°C [mm ² /s]	3
Flash Point [°C]	<65.0
Sulfur Content [% (m/m)]	>0.05

7.3 TESTING METHODS

The testing of the engine can be divided into the following six stages.

1. Fault diagnostics
2. Function checks
3. Motored tests
4. Engine stability
5. Limit identification
6. Engine mapping

Fault diagnostics uses up a large amount of time in this project, however it is difficult to document every step of this process. The problems that need fixing is summarized in chapter 3, an effort will be made to fix all these problems within the time scope of this project. However, it is possible that a solution to all problems will not be found in the allocated time. A summary of what has been done and which problems that have been fixed will be shown in the results section. The fault diagnostics is highly reliant on the expertise of the laboratory personnel, and involves both fixing of mechanical problems and control system problems. The method used for fault diagnostics is an iterative process where each fault is subject to a systematic removal of problem contributors as shown in Figure 7-2.

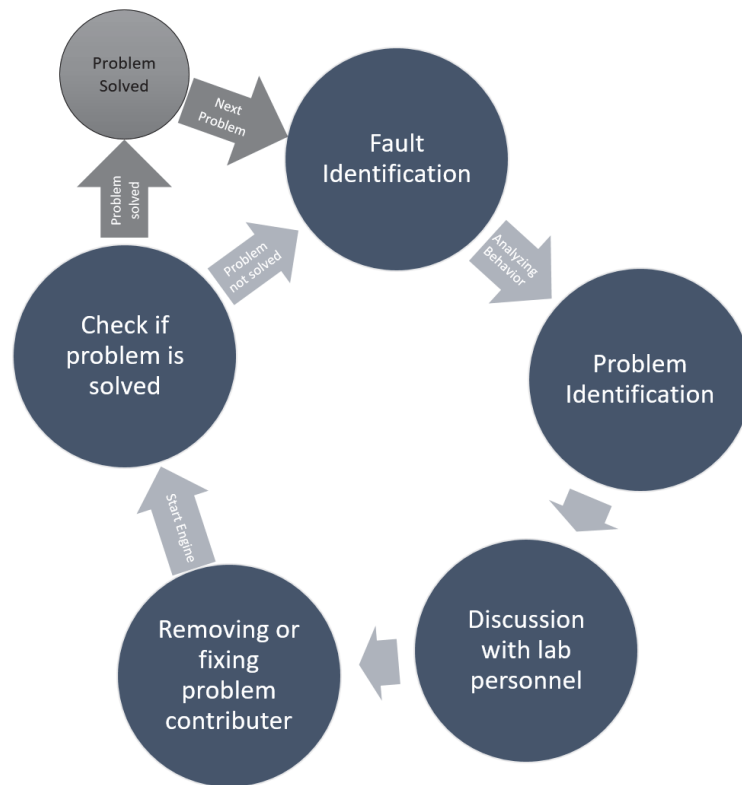


Figure 7-2 Fault diagnostics process

The rest of the stages, i.e. *function check, motored, stability, operational limits, and engine mapping*, are more conventional experiments with a preset procedure for each experiment. The procedure for these experiments, including planned load-points and achieved objectives can be found in appendix A. The next subsections will go into details about the motive behind each experiment, and important aspects with each experiment.

7.3.1 FUNCTION CHECK

The Hydra test-bed has several functions that need to be checked thoroughly to prove that the test-bed functions safely and within specifications. Some of these functions will be checked in the fault diagnostics session, and some will be tested as separate functions. The engine will in the future be used by students that have little to no experience with engines. This means that it should be close to impossible to do something wrong when using the test-bed. The functions that need to be tested are shown in list below.

1. Max engine speed trip
2. Max pressure trip
3. Max injector pressure trip
4. Coolant and oil temperature trip

5. Injector control, i.e. pressure, timing, and duration
6. Inlet air heater
7. Logging of data happens as expected
8. Check for possible pinch hazards
9. Stupidity check. What can be done wrong?
10. Checking consistency of P-V diagram

7.3.2 MOTORED TEST

As described in section 2.1.2, the mechanical efficiency can be measured by motoring the engine without combustion. To get an estimate of mechanical efficiency at different speed, the engine will be motored at load-point with increments of 5 rps from 20 to 75 rps. This will give a give information about how the mechanical efficiency develops over time, and the consistency of the P-V diagram can be checked over a range of speeds. Additionally, the behavior of the volumetric efficiency can be checked during this experiment.

7.3.3 TIME UNTIL STABILITY EVALUATION

To measure steady state load-points, the engine must reach stability. If the load or speed of the engine is changed, the engine will use some time to operate stably. Stability in this context means that the engines delivers close to constant outputs. The time until stability influences strongly the expected time for each experiment, and knowing the approximate time the engine uses to reach stability can help reducing the total cost of the experiments.

The time until stability will be tested by logging static measurements during a change in load with constant speed. The load will be changed from motored conditions to 4 kw for the first experiment, and from 1kW to 4 kW for the second experiment. The engine will be judged as stable when the fluctuations in NO_x or exhaust temperature are close to zero. The engines approximate time until stability will be the longest time measured from these tests.

7.3.4 FINDING OPERATIONAL LIMITS

To prepare for the gridding of the engine, the last part of the engine stability test-day will be used to evaluation of the upper limits of operation. This will be done by trying to push as much power as possible from the engine at a set of speeds. Where the operational limit will be defined at the black smoke limit. The black smoke limit is where the engine starts to produce large amounts of black smoke, due to lower combustion efficiency. The black smoke limit is found

by having a live video feed of the exhaust outlet. When a large change in the exhaust color is detected, the black smoke limit is reached. The engine will be tested in its whole operational range from 20 to 75 RPS, with increments of 10 RPS. The tests will be performed with a rail pressure of 1000 bar. This will establish the upper limits of the grid. The reason for doing this on a separate test-day is that the engine needs to be warm and ready to be pushed, in addition the limit of operation must be known before the rest of the gridding can be planned.

7.3.5 ENGINE MAPPING USING GRIDDED TEST-POINTS

To be completely sure that the engine operates as expected at every possible load point, a mapping of the engine will be conducted. This will secure that the engine has been through all expected load points, and will give information about how the test-bed performs over time. In addition, load points that can give problems with for example vibrations or low accuracy can be found. It exists several methods for identifying load points for engine mapping. The simplest and most robust of these methods are gridding. Gridding is when load points are chosen as part of a grid, with the outer points selected at the limits of operating range. A large number of points will of course give a more detailed picture than fewer points.

As previously stated, in chapter 6, the most effective method of conducting a gridding of the Hydra engine is to first run a grid with a relatively large number of load points, and run additional points if the model is unstable in certain areas. The first grid will be composed of 25 load points in the operational area. For each speed 5 points will be defined at 20, 40, 60, 80 and 100% of the operational limit.

7.4 PREPARATION AND CALIBRATION

Before the testing can be started, all the equipment used in the test must be heated up to operational temperature. One of the first tasks of the test day is to start the AVL smoke-meter and, the HORIBA gas analyzer. Both instruments require a long time (up to two hours) to heat up and be ready for calibration. The next step is to heat up the engine, the heat up process is covered in detail in the Operation Manual, which can be found in appendix B.

Before each test day, calibrations of the gas analyzer will be conducted. The calibration will be conducted by the laboratory personnel. If the testing period exceeds 4 hours, a second calibration should be performed.

When all equipment is ready for testing the alteration of injection duration and speed can start. When the desired load point is reached, the engine will be left on that point until a stability of the parameters measured from different sensors can be seen. A good indicator of stable operation is NO_x emission measurements, the stability evaluation will give good insight in the behavior of the test-bed in this regard. When stability is reached the logging of static and dynamic data can start. This procedure will be repeated for each test/load point.

7.5 DATA PROCESSING

For each load point the LabVIEW interface produces two files, one for static and one for dynamic measurements. These files must be conditioned before it is possible to use them for plotting purposes. MATLAB is used to process the data from the experiments. Each load point is imported as a set of variables into the MATLAB environment. This results in one variable for each sensor output. For the static data, these variables are measurements performed over a certain period. To get usable points for plotting, the static data must be averaged. The averaged data is collected together with the variance of outputs in two matrixes, and are saved as a MAT-file. This MAT-file can then later be loaded as a workspace to a script that performs the needed plotting procedures and needed calculations of for example efficiencies, and fuel consumption. All relevant MATLAB scripts can be found in appendix C to F.

8 RESULTS AND DISCUSSION

In this section, the results from the performed experiments will be presented, accompanied by a short discussion about the implications of the results. In addition, the performed modification done to the Hydra engine will be covered, where special attention to the process of fixing each issue will be shown.

8.1 PERFORMED MODIFICATIONS

The modification process was much more complex than initially anticipated. A range of problems surfaced as the project progressed, and resulted in a somewhat tight time schedule. All required modifications were performed within the middle of May, although some of the modifications of lesser importance were neglected due to limited time. Below follows a description of all modifications that were performed, and how they affected the operation of the engine. The modifications that were not performed, and their impact on the engine operation are discussed in the next subchapter.

Oil Leaks:

The oil leaks were a large concern. During the operation of the engine, large amounts of oil was pouring out of the engine, which was both a fire hazard and hazard related to lubrication starvation.

The oil leaks were first thought to be a result of a bad top fitting. The camshaft cover was removed and a new fitting was installed in addition to some fitting sealant on difficult locations. This resulted in reduced leaks, but a much larger leak was discovered behind the exhaust manifold. To investigate further, the exhaust manifold was dismantled. A six-millimeter hole was discovered behind the exhaust manifold, going directly into the cylinder liner. When the engine reached operating temperature, oil poured out of this hole. The hole is not documented in any drawings, but are possibly made to measure cylinder liner temperature. The hole was sealed with a plug and some sealant paste as shown in Figure 8-1. The modification was successful and the oil leak was severely reduced. After this the oil and the oil filter were changed, this was of great importance since the old oil filter was seven years old. After some additional tests a small leak has been detected from the seal between the oil heater and the crank case. This leak should be shown attention at the next oil change.



Figure 8-1 Sealed hole behind exhaust manifold

Fuel System:

The fuel system quickly became the largest problem during the modification period of the engine. The system did not operate even close to what was expected. The problems both with slow response time, small controllable window and no measurements of fuel consumption was dealt with.

The small controllable window meant that a very small change in the input to the fuel pump could be the difference between maximum and minimum pressure-increase. This made it impossible to control the pressure with a PID controller in the control system, therefore manual control was needed. Even with manual control it was impossible to make the system work close to one specific pressure. Initially the response time was seen as a possible contributor, therefore one of the pulse-dampeners was removed, to give the system a faster response time. This alteration lead to some improvement in the controllability of the system, but was not enough to conclude that the system was operational.

The fuel pump mounted in the system is originally made for a Toyota Avensis, which have four injectors, that together inject much more fuel then the injector mounted on the Hydra engine. A possible reason for the uncontrollable behavior could be that the pump could not be controlled during a much smaller output flow then the pump was designed for. Therefore, it was decided that a controlled leak could solve the problems. Unfortunately, the valves available in the lab did not have sufficient tolerance, and provided a much larger leak then the pump could handle.

This resulted in the acquisition of a micrometer-controlled leak valve. The leak valve was mounted to the system, and the system started to behave much more like expected. However, with the controlled leak temperature in both the valve and the fuel tank became a concern. During even short operation a considerable rise in shell temperature on the leak valve was detected. Therefore, a CPU cooling rib with a cooling fan was mounted to the valve to provide some cooling. As an additional safety precaution a temperature sensor was mounted in the fuel tank to provide information about fuel temperature.

Fuel flow measurement was not available, and after the addition of a leak it became apparent that it was impossible to have a flow measurement in a conventional way (using a Coriolis type flowmeter). This would be highly complex with measurements of three to four different flows, and would be inaccurate, expensive and time consuming. Therefore, it was decided that the best option was to measure the weight of the fuel tank in real time. This will provide an adequate estimate of the fuel consumption on stable load. A force cell was mounted to the fuel tank, and connected to the logging system to be logged together with static measurements. To improve the correctness of this measurement a smaller tank was installed. This tank has the added benefit of being transparent, which makes it possible to monitor fuel level. For future improvement of the test-bed a possible option for fuel measurements is to calibrate the injector to provide flow estimations as a function of injection pressure and duration.

Air Flowmeter Calibration:

Very little information was available on the air flowmeter mounted on the Hydra engine. It was not known what type of flow meter it was, nor which company that has manufactured the flowmeter or how often it has been cleaned. This made it impossible to determine the flow based on the pressure difference in the flow meter. To solve this problem the flowmeter was first dismantled and cleaned, the condition of the flowmeter was very poor, where the mesh was filled with metal shavings and particulates. After cleaning, the flowmeter was subjected to a calibration up against a correct flowmeter.

The calibration was performed by connecting a vortex type flowmeter to the inlet of the laminar flowmeter via a plastic tube. The laminar flow meter was then calibrated up against the vortex flowmeter. Initially it was thought that the flow could be provided by motoring the Hydra engine. However, since the Hydra engine is a one-cylinder engine, this provided a too unstable flow for calibration. Therefore, an external compressor was used to provide a more stable flow.

After calibration, the engine was started up, and motored to check the consistency of the calibration. It was found that the calibration was not even close to correct, the reason for the incorrectness of the calibration is uncertain. At this point, time became a large issue. Therefore, a temporary solution was devised, where a known flowmeter was connected to the engine instead of the existing flowmeter.

Dynamic measurements:

The Hydra engine has been subjected to some “cannibalization” during its lifetime. As a result of this the pressure transducer encoder for in cylinder pressure measurements was missing. A new encoder was found and installed. During this process, it was found that the computer that controls the engine has filled all connection points for dynamic control. This means that it is not possible, with the current setup, to add control of multiple injections.

Control System:

Some minor changes were done to the control system. The changes are summarized in the following list.

1. Initiation of safe shutdown of fuel system when injector is rendered inactive
2. Possibility for adding or removing timestamp from filenames
3. PID controller for common rail pressure

8.2 MODIFICATIONS NOT PERFORMED

Due to short time schedule, some of the planed modifications where not performed. The modifications that was not performed is summarized in the following list.

1. No relocation of fuel system
2. Safety cover on fuel pump not installed
3. Fuel filter not changed
4. No analog emergency-stop of fuel pump
5. No calculation of ROHR in logging system

8.3 FUNCTION CHECK

Function checks were performed during the experiments, and during warm-up of the engine. The checklist below was used during the function check process.

Table 8 Checklist for function check

Check	Performed	Comments
Max engine speed trip	Yes	Engine does not trip during high speeds
Max pressure trip ^a	No	Not able to reach
Max injector pressure trip	Yes	Stopped by control system at 1300 bar
Injector Control	Yes	Working properly
Inlet air heater	No	Not mounted
Logging of data	Yes	Working properly
PV- diagram ^a	Yes	Consistent, but not changing properly
Stupidity-check	Yes	Safety cover on fuel pump, possible to add enormous amounts of fuel

^a Pressure sensors was later found to be bad. More on this in the next section.

The most notable findings during the function check is that there is no speed trip installed. However, since the engine has a very noticeable change in sound when altering speed, it is very unlikely that the engine operator unaware of the change. Nevertheless, it is worth noting that the electrical dynamometer has the capabilities of rotating the engine well above the highest advisable engine speed.

The stupidity-check revealed that the fuel pump should be covered. It is very easy to forget that the fuel pump is running, since it only emits a low constantly pitched sound. The fuel pump is rotating at a speed of 900 rpm, and is a considerable risk when personnel is near it.

During the smoke limit test of the engine it became apparent that one may inject much more fuel into the combustion chamber than the engine could handle. This can cause flooding of the engine, and subsequently lead to fires. The only way to monitor if too much fuel is injected into the combustion chamber is to have gas analyzers connected to the engine, where CO and HC can be monitored. In the future, this problem can be circumvented by altering the control system to allow maximum injection duration based on engine speed, injection timing and common rail pressure.

8.4 MOTORED TEST

The motored test was performed by motoring the engine at the speeds shown in Figure 8-2. The engine operated as expected, except for logging of pressure data at 75 RPS. This load point was repeated several times, with the same result, therefore it has been replaced with the 70 RPS load point. A possible reason for this logging problem can be a bug in the control system. The engine sound drops significantly above speeds of 33 RPS.

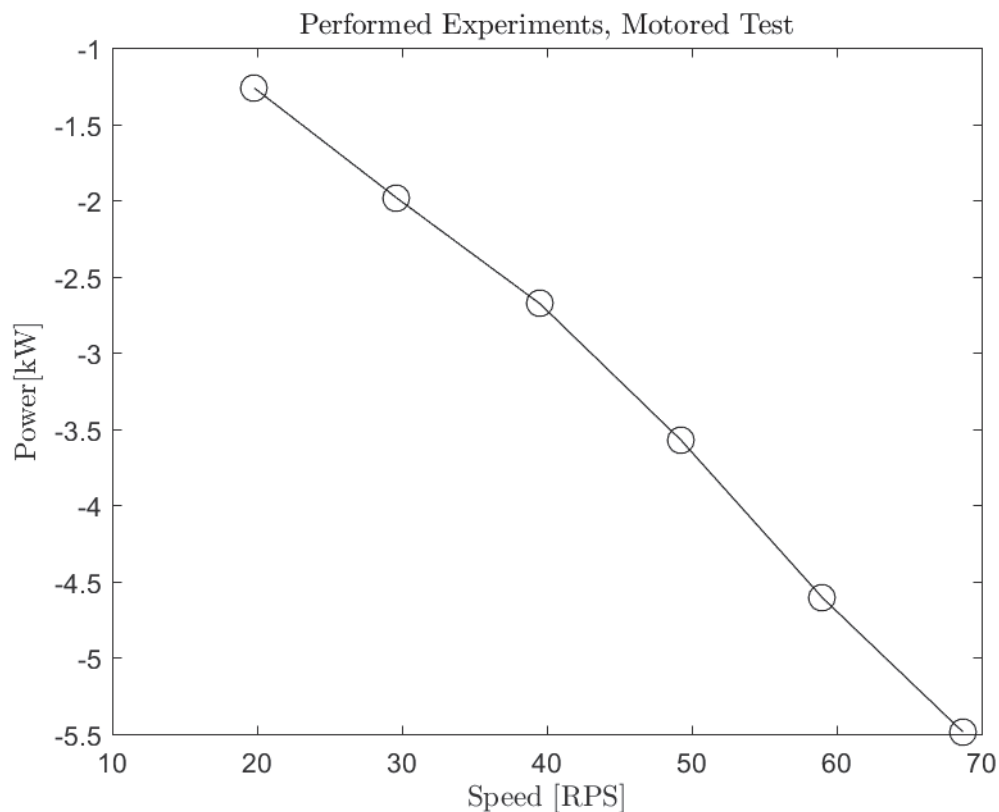


Figure 8-2 Performed experiments, motored test

8.4.1 VOLUMETRIC EFFICIENCY AND FLOW RESTRICTIONS

The volumetric efficiency of the engine has been calculated based on the measured inlet air flow, and the theoretical maximum ideal gas that the engine can pump based on its rotational speed and displacement volume, this has also been defined in chapter 2.1.2. The volumetric efficiency for each measured speed is shown in Figure 8-3.

Volumetric efficiency for an internal combustion engine are typically in the range 80 to 90 % according to Heywood [7]. From Figure 8-3 it can be seen that the volumetric efficiency is in the expected range with speeds between 20 and 50 RPS. However, the volumetric efficiency is drastically reduced between 50 and 70 RPS. Although a reduction of the efficiency at elevated

speeds are expected, this decrease is so severe and sudden that it can only be explained by a flow restriction somewhere in the system or that the engine is sucking false air (air that has not passed through the flow meter). No candidates for false air was found. The obvious candidates for a flow restriction is the inlet flow meter and the exhaust manifold. However, the rating of the flow meter and the considerable available cross-sectional area of the inlet system eliminates it as a suspect. Therefore, the exhaust manifold was checked for choked flow conditions.

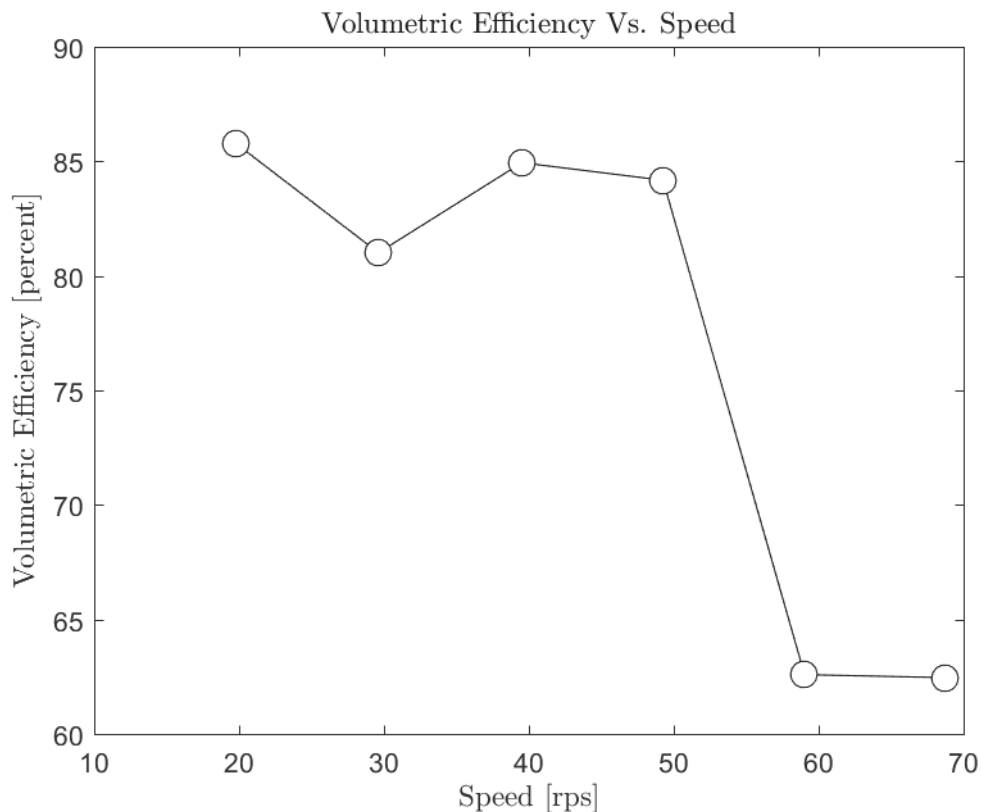


Figure 8-3 Volumetric efficiency, motored test

To check the exhaust manifold for choked flow proved to be a challenge. The biggest problem was that the pressures on both sides of the exhaust manifold is unknown, meaning that the analysis is leaning strongly on assumptions. However, the analysis show that the exhaust manifold configuration is a problem for the gas exchange process of the engine. The flow is not choked, but is only 1/6 of choked conditions, when only the reduction in diameter is accounted for. In addition to this the pressure drop in the exhaust manifold was calculated based on the Darcy-Weisbach equation. This resulted in a peak pressure drop of 59 kPa at the highest engine speed, only accounting for the diameter reduction and the first 90-degree bend. The system behaves appropriately at a pressure drop below 40 kPa, which indicates that the exhaust manifold should be improved to have a pressure drop below 40 kPa for the whole operational

range of the engine. This can probably be achieved by replacing the sharp bend with a gentler elbow, and possibly increase the diameter of the pipe entering the elbow. Note that this is a very crude analysis, which is based on uncertain values, and can only be used to exclude possible reasons for flow restrictions. Based on the above numbers, the exhaust manifold cannot be excluded as a suspect.

8.4.2 MECHANICAL EFFICIENCY AND PRESSURE MEASUREMENTS

One of the main advantages with motored tests is that the frictional forces of the engine can be measured, in combination with pressure measurements this can result in good estimations of mechanical efficiency. Regrettably the pressure transducers were found to be completely wrong during the analysis of the data. The first indication of this fault was that the logged pressure measurements started on around negative 3 bar. This could be as simple as that the pressure transducers zero-point was set to an incorrect value. This was corrected for by adding the error to the pressure measurements. However, it was later found that in addition to this error, the pressure decreased with increasing speed. This should not be the case, and results in a mechanical efficiency over 100 % because imep is decreasing with speed. The raw data of the pressure data has been checked for each conducted experiment, and the fault was found in each data set. The implication of this is that imep, mechanical efficiency and ROHR calculations are incorrect and cannot be used in this thesis. However, this problem can be relatively easily fixed by replacing the pressure transducer with a functioning one. Before this is done it should be checked for problems in the logging system. During the experiments, the live dynamic pressure measurements was monitored, and no fault in the pressure transducer was detected. It is possible that the fault is as simple as a logging error. The mechanical efficiency was calculated with the methods introduced in chapter 2.1.2.

8.5 STABILITY TEST

The stability test was conducted with two different tests. In the first test, the engine was motored, and then the injection duration was increased until power reached 4 kW. The second test started at 1 kW, where the injection duration was increased to reach a power of 4 kW. Both tests were conducted at speeds of 40 RPS, and both tests were stopped when a subjective stability of NO_x and exhaust temperature was found. The tests were first conducted with a rail pressure of 1000 bar, but a bizarre fault in the injector caused an injector shutdown when the injection duration was increased above 0.42 ms. This was first thought to be a control system bug, but this was later disproven by checking error messages in the system. Some experts on the department of marine engineering suggested that this behavior may be a result of a bad piezoelectric element. To circumvent this problem the rail pressure was lowered to 800 bar, which produced no similar fault. The performed experiments are shown in Figure 8-4, where a measurement is taken every second.

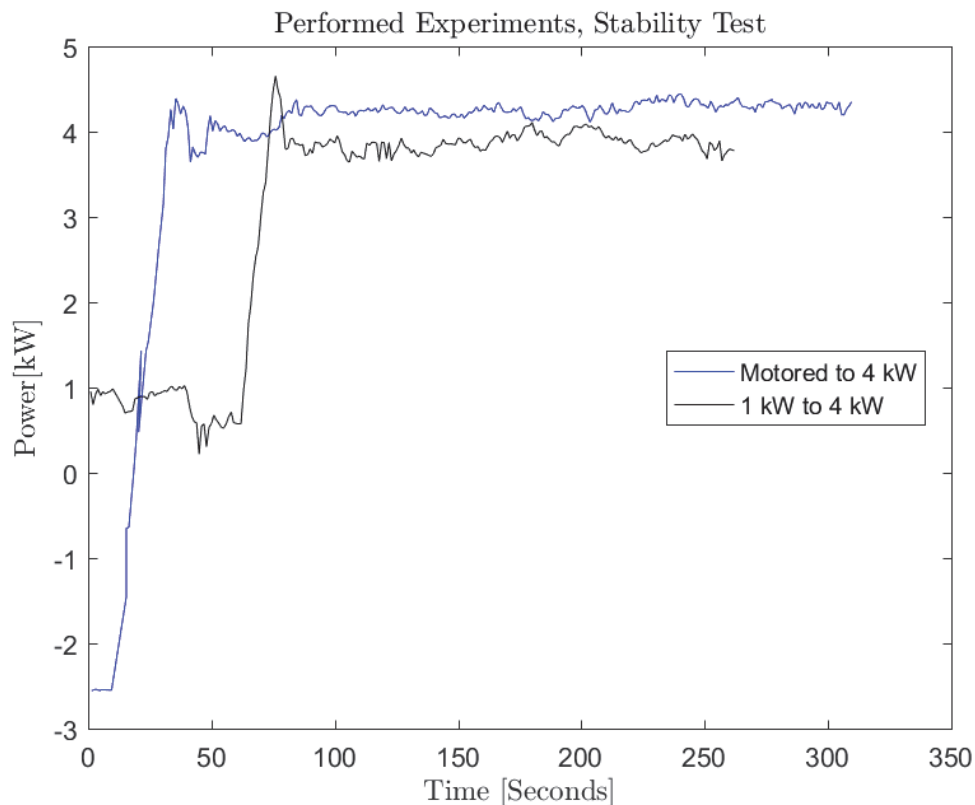


Figure 8-4 Performed experiments, Stability test

It can be seen from Figure 8-4 that it was not possible to hit the exact power of the previous test, even if the injection duration and speed was set to the exact same number. This can be explained by a difference in engine oil temperature, as can be seen from Figure 8-5. Which

could lead to a slight difference in the internal friction of the engine, in addition to better autoignition conditions. Later it was learned that the engine temperature could be controlled by changing the flowrate of the cooling water. This results in a much more stable engine temperature. Control of engine temperature can become a significant factor when completely similar load points are needed for comparison.

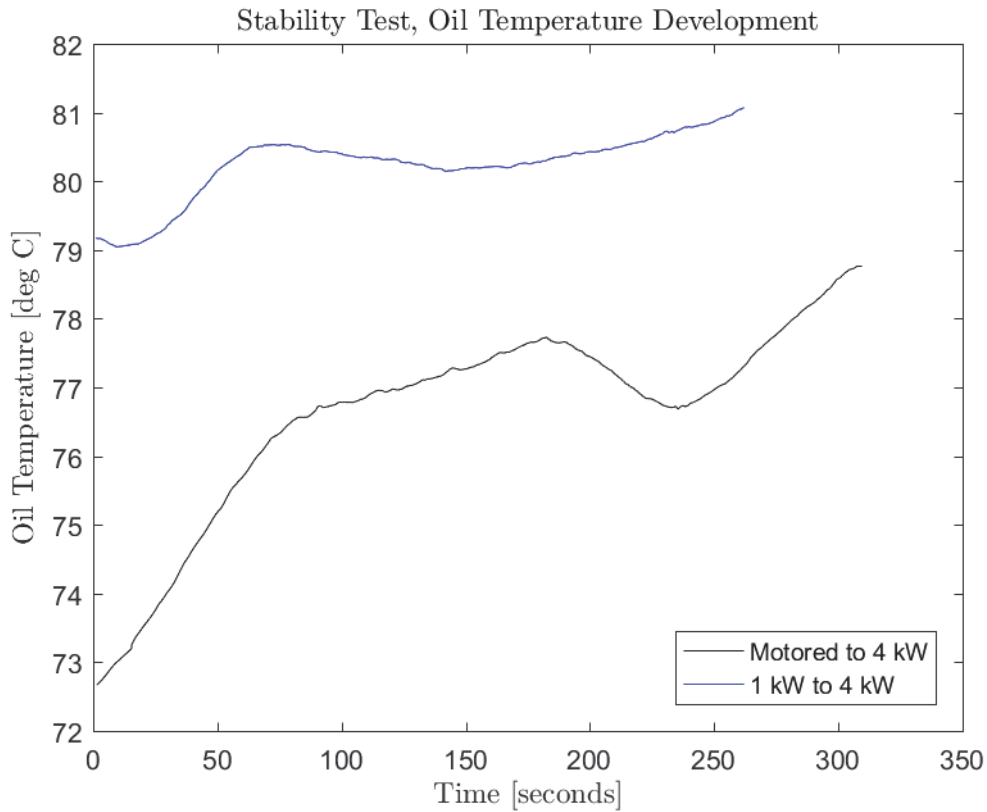


Figure 8-5 Oil temperature, Stability test

8.5.1 STABILITY OF NO_x AND SPEED

The goal of these tests was to see how long time the engine uses to reach stability. This was done by looking at the change in NO_x. When these two variables are stable, one can argue that the engine is stable. Nevertheless, as pointed out in the previous section, other variables like engine temperature may become a contributing factor to the engine stability.

With older eddy-current dynamometers an instability of engine speed is often seen as a result of unstable resistance in the dynamometer. This is for example seen in the Scania test-bed (tested in project thesis). As can be seen from Figure 8-6 the electrical motor/generator mounted to the Hydra engine provides extremely stable engine speeds. The measurements only differ a maximum of 0.19 RPS.

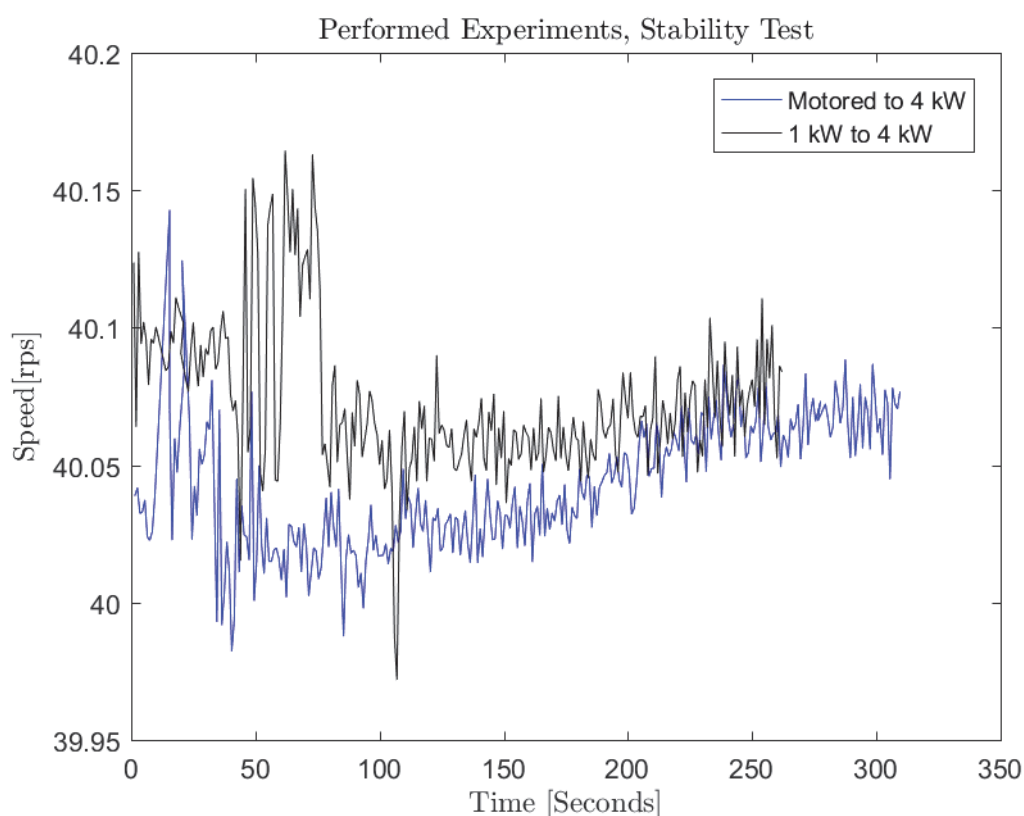


Figure 8-6 Engine speed, Stability test

Figure 8-7 show the measured NO_x level as function of time for the two stability tests. Both graphs behave as expected, where an increase in NO_x happens as the load is increased. This is a direct result of increased combustion and exhaust temperatures. When the load is increased from motored conditions to 4 kW, the NO_x level uses approximately 200 seconds or 3 min and 20 seconds to reach stability. When load is increased from 1 to 4 kW the NO_x level uses

approximately 130 seconds or 2 min and 10 seconds to reach stability. During repetition of these tests (due to diverse logging problems) it was found that the time until stability could be greatly reduced between load points by not motoring the engine between load points. This would keep the exhaust temperature more stable, and result in a faster acquisition of results. As a result of these tests it can be concluded that the engine should be running at a specific load point for at least 4 min from motored conditions, and at least 3 min from an already loaded conditions (adding time to increase robustness of this suggestion). If the engine is running even longer than this, even more stable outputs are expected. In addition to this it is important that the engine operator checks the HORIBA gas conditioner flow rate. This instrument has a tendency to cut flow-rate over time, which results in directly wrong results. It can be smart to check the flow rate indicator at each new load point.

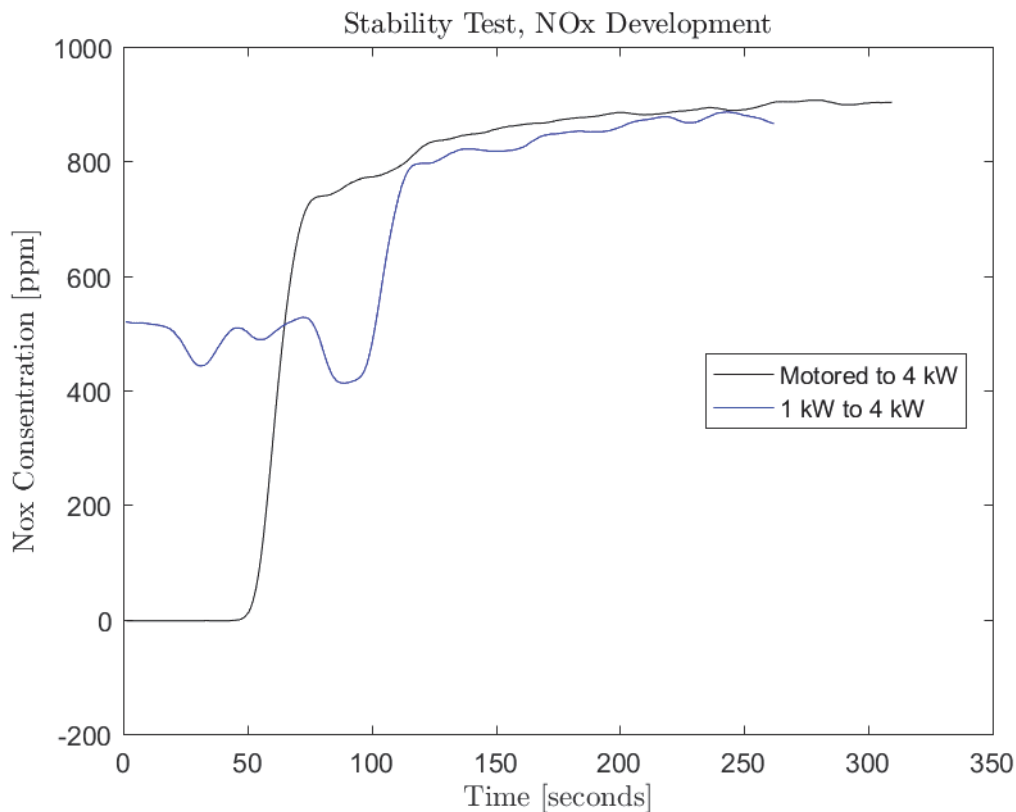


Figure 8-7 NOx, stability test

8.6 INVESTIGATION OF OPERATIONAL LIMITS

The smoke limit is normally found by monitoring the blackness of the smoke from the exhaust outlet. This was found to be impossible with the Hydra engine. A camera was mounted to the exhaust outlet, but it was not possible to detect any change in smoke color. The exhaust smoke is probably too diluted by the time it reaches the exhaust outlet. As an alternative to monitoring of exhaust color, the HORIBA gas analyzer and the THC analyzer was used to measure levels of CO as well as HC. When a sharp increase in these two variables was detected, the injection duration was lowered slightly, and the top load with current inputs was defined.

The engine had the following locked inputs: injection timing 10° BTDC, rail pressure 800 bar. The experiments were planned over the whole operational range of the engine, but needed to be aborted due to an injector malfunction. Therefore, the operational limits were only found in the range 20 to 60 RPS. The result of the tests is shown in Figure 8-8.

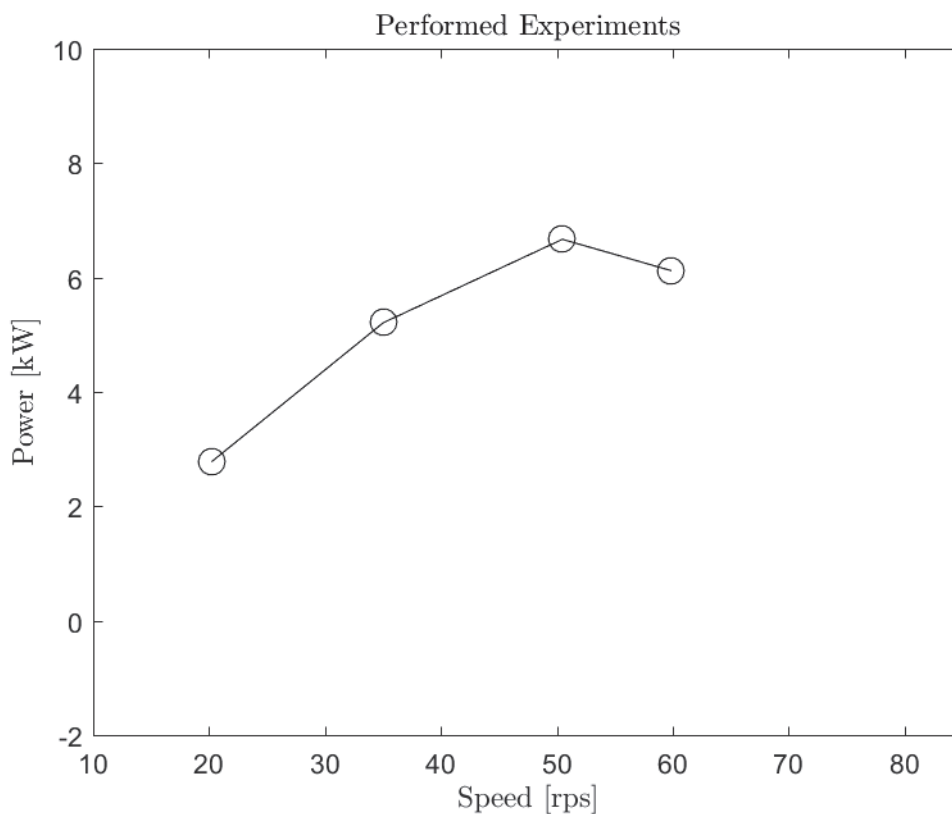


Figure 8-8 Operational Limits

The injector malfunction was detected by a sharp drop in rail pressure, this invoked an inspection in the engine room, where it was found that the injector had released a very large quantity of fuel into its return line. The fuel system and engine was immediately shut down.

When the injector is working properly it should only release very small quantities of fuel into its return line. If this is not the case it can be an indication of injector failure. The reason for this failure is probably related to wear, but it is difficult to determine the exact cause without having an expert dismantle the injector. The failure of the injector caused the engine to be inoperable, and the engine would only become operable if a new or serviced injector was installed. It was concluded that no further tests should be conducted in relation to this thesis because of the uncertainty in time usage for injector replacement.

8.6.1 VOLUMETRIC EFFICIENCY AND FUEL FLOW

To verify the findings in the motored tests, the volumetric efficiency was calculated. Figure 8-9 show that the volumetric efficiency behaves in a similar manner as in the motored test, thus solidifying the theory of flow restrictions in the exhaust system.

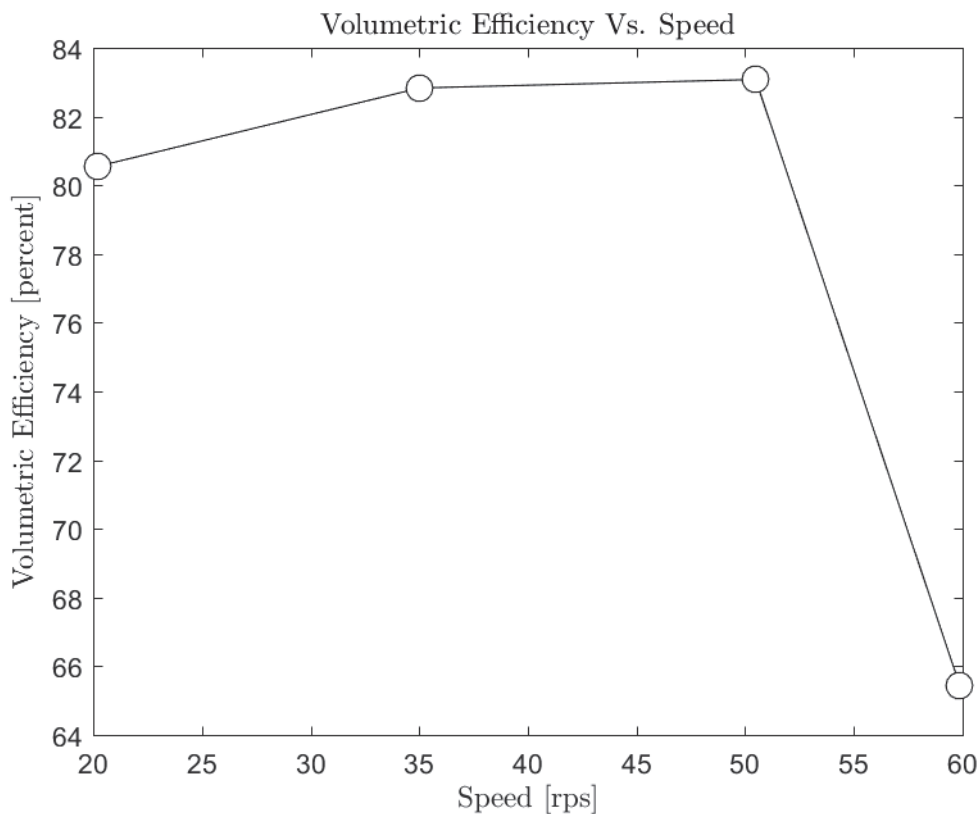


Figure 8-9 Volumetric efficiency, Limit test

The fuel system has undergone severe modifications, it was of interest if these modifications provided an improvement of the overall fuel system, and if it was possible to measure fuel flow in a reasonable fashion. The common rail pressure was in these tests set to 800 bar. Review of the logged data show that the rail pressure varied at a maximum of 3.14 bar. This is a variation

of 0.39%, which can be said to be within what we can expect for such a system. Heating of the fuel tank was a concern, and was monitored during the tests. The maximum fuel tank temperature measured was 33°C after several hours of operation at high pressure. The modification to the pressure system is by other words a success.

The calculated fuel flow, based on measurements of change in fuel tank weight, is shown in Figure 8-10. As expected the fuel flow is increased with increasing load. Without measurements, of rate of heat release it is difficult to validate the flow rate without using several assumptions. If conservative mechanical (0.8), combustion (0.9) and thermal efficiencies (0.35) are employed, the theoretical output based on fuel consumption can be calculated. These values are near the actual output. However, this becomes only speculation since none of the efficiencies are known. The fuel flow measuring system is functioning, but how accurate results it produces are difficult to say. Nevertheless, the results could become better if the retune line from the injector was routed to the fuel tank. This would on the other hand mean that no indication of injector failure would be present, which would mean that periodical tests of the injector should be employed.

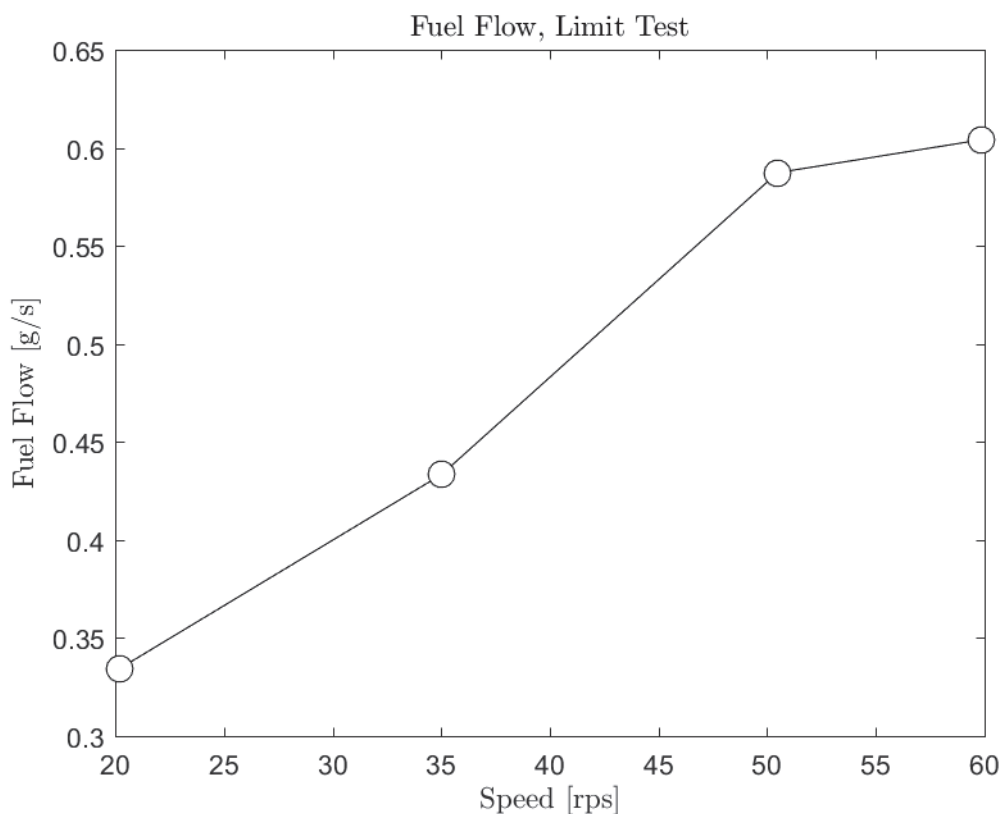


Figure 8-10 Fuel flow measurement, Limit test

8.7 RECOMMENDATION FOR TEST-BED IMPROVEMENT

The following improvements must be done to get the Hydra engine back in operational conditions.

1. New or serviced injector
2. New or recalibrated pressure transducer, first check if this is a logging problem

The following improvements would increase the usability of the engine. Ranked from most important to least important. The locations of improvements 1,2 and 4 can be seen in Figure 8-11 and Figure 8-12.

1. Exhaust flow improvements, longer elbow, less reduction in pipe diameter
2. Injector return routed to fuel tank
3. Shorter step control of injection duration
4. Safety cover on fuel pump
5. ROHR calculation in logging system
6. Possibility for multiple injections per power stroke
7. Injector duration limit dependent on speed a common rail pressure
8. Timer on duration of static measurements

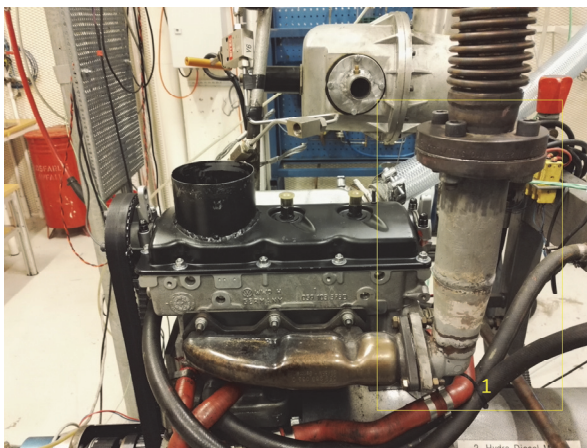


Figure 8-12 Location of improvement nr.1



Figure 8-11 Location of improvement nr.2 and 4.
Yellow line is proposed route for fuel return.

8.8 TIPS AND TRICKS LEARNED FROM EXPERIMENTS

The Hydra engine has been out of operation for a long time, this has caused information about how to operate the engine in an efficient manner to fade away. During the experiments performed in this thesis several tricks have been learned about both maintenance and engine operation. In an effort to preserve this information, and pass it on to be used in the future life of the engine, a list of tricks and tips are posted below.

Maintenance tips

1. Oil level should be checked with the oil pump turned off. The oil pump uses significant amounts of oil, filling up oil when the oil pump is running will cause overfilling.
2. Coolant does not need to be topped all the way up. This will cause large amounts of coolant to flow out of the overflow tube. Coolant should be filled to approximately half the height of the cooling tower top.

Engine operation tips

1. Common rail pressure should be increased in steps of 50 bar. Wait for approximate stability before further increase is employed.
2. During change of load point, it can be smart to continue injecting fuel to the engine. Motoring the engine will cause rapid cooling of the exhaust system.
3. The cooling water flow can be closed during warm-up of the engine. This will greatly reduce warm-up time.
4. The engine oil temperature can be stabilized on a specific level by controlling the cooling water flow. Turn the lower valve slightly to increase the water flow. Look at the temperatures of cooling water and oil. After some time, these values will balance each other. This is very important if good repeatability is required.
5. Always double-check that the logging system is writing to the correct file.
6. Do not delete the previous logged file. This will invoke an error, where a control system restart is needed.

9 CONCLUSION

This thesis has aimed to be a driving factor in the restoration of the Hydra engine, where a key goal was to make the engine ready for student-experiments. Regrettably the engine has not become ready for student-experiments since the experiments in this thesis needed to be aborted due to unforeseen failures. Nevertheless, the engine is very close to being ready for use, and many of the modification done to the engine this semester was successful.

The motored test of the engine revealed a very low volumetric efficiency at engine speeds above 50 RPS. It is very likely that this problem is due to flow restrictions in the exhaust system. In addition, it was found that the pressure transducer mounted to the engine was incorrect. This resulted in no calculation of mechanical efficiency, and also meant that it was not possible to compute rate of heat release for the proceeding tests.

The stability test was eventually a success, where the engine was found to have a very stable speed and common rail pressure. The engine reaches emission stability after approximately 4 minutes, but this time can be reduced by continuing to inject fuel as a new load point is acquired. It was also learned that the produced power output is very dependent on the oil temperature of the engine. This temperature can be controlled by controlling the cooling water flow into the engine. To improve measurements of emissions it is advised to check the flow in the gas conditioner mounted the HORIBA gas analyzer. With each new load point the flow tended to be reduced, this induced unstable results, but could easily be avoided by turning the flow control knob on the conditioner.

The limit test was limited to only four points because of an injector failure. The injector failure materialized in a large leak of fuel into the return line of the injector. All further tests were aborted, due to a long injector repair time. This means that no mapping of the engine was conducted. Nevertheless, the limit test revealed several important factors in the engine operation. The problem with both the volumetric efficiency and the pressure transducer was verified. It was found that it was possible to inject much more fuel than what is possible to burn. Additionally, it was established that the fuel consumption measuring system was working properly. Despite this more experiments should be conducted, where the measurement can be compared with rate of heat release.

If the unforeseen errors with the fuel injector and the pressure transducer is fixed, the engine will be operational from 20 to 50 RPS. If additionally, the exhaust system is improved, the engine will ascertain its original operational area from 20 to 75 RPS.

The Hydra engine is a very versatile engine, with enormous research potential due to its many variable parameters. Furthermore, the engine has no comparable alternative in the machinery lab. Because it is the only engine in the lab that is fitted with a common rail fuel system, the labs position as a research facility will be strengthened if the restoration is completed.

9.1 FURTHER WORK

This section will suggest further work on the Hydra engine. Recommendation for further modifications to the engine can be found in chapter 8.7. No further suggestions for engine restoration will be made, instead the focus here will be on further testing and improvements of the engine related to future master thesis work.

1. Development of safer injection control

The current setup of the control system allows for injection of a surplus fuel. This can be avoided by clearly state the boundaries of engine operation in the control system. Such a task would include experiments for determining boundaries at different speeds, injection pressures and injection timings, and would involve some programming of the injector control to suite the findings in the experiments.

2. Develop control maps for more standardized testing

The engine could be controlled using a control map instead of manual control. Making such a map would be a considerable challenge, and can contribute to the versatility of the engine.

3. Validation of fuel consumption measuring system and mapping of engine

It was not possible to verify the correctness of the fuel consumption measuring system in this thesis, due to problems with the pressure transducer. This is something that must be done, and can probably be done while mapping the engine.

10 REFERENCES

1. Tschoke, H., K. Mollenhauer, and K.G.E. Johnson, *Handbook of Diesel Engines*. 2010, Dordrecht: Springer.
2. Diesel, R., *Internal-combustion engine*. 1898, Google Patents.
3. Gardiner, R. and A. Greenway, *The Golden Age of Shipping: The Classic Merchant Ship, 1900-1960*. 1994: Conway Maritime Press.
4. Thomas, D.E., *Diesel: Technology and Society in Industrial Germany*. 1987: University of Wales Swansea.
5. Corbett, J.J. and H.W. Koehler, *Updated emissions from ocean shipping*. *Journal of Geophysical Research: Atmospheres*, 2003. **108**(D20): p. n/a-n/a.
6. Congress, G.C. *Panasonic Develops New Higher-Capacity 18650 Li-Ion Cells; Application of Silicon-based Alloy in Anode*. 2009 [cited 2017; Available from: <http://www.greencarcongress.com/2009/12/panasonic-20091225.html>].
7. Heywood, J.B., *Internal combustion engine fundamentals*. McGraw-Hill series in mechanical engineering. 1988, New York: McGraw-Hill.
8. Mock, R., K. Lubitz, and R. Mock, *Piezoelectric Injection Systems*. Vol. 114. 2008. 299-310.
9. Bosch. *Bosch History*. 2017; Available from: http://www.bosch.com/en/com/bosch_group/history/theme_specials/journey_through_our_history/journey_through_our_history.html.
10. Registry, D.E. *2-Stroke vs. 4-Stroke Engines*. 2015 30.01.17]; Available from: <https://dieselengineregistry.wordpress.com/2-stroke-vs-4-stroke-engines/>.
11. de Klerk, A., *Diesel Fuel*, in *Fischer-Tropsch Refining*. 2011, Wiley-VCH Verlag GmbH & Co. KGaA. p. 283-299.
12. Song, C., C.S. Hsu, and I. Mochida, *Chemistry of diesel fuels*. Applied energy technology series. 2000, New York: Taylor & Francis.
13. Çengel, Y.A., M.A. Boles, and M. Kanoğlu, *Thermodynamics : an engineering approach*. 7th ed. in SI units. ed. McGraw-Hill series in mechanical engineering. 2010, Singapore ; New York: Mc-Graw-Hill.
14. Europe, A.N. *Injector wars: piezo vs. solenoid*. 2006; Available from: <http://europe.autonews.com/article/20061113/ANE/61109031/injector-wars:-piezo-vs.-solenoid>.
15. Koyanagi, K., et al., *Optimizing Common Rail-Injection by Optical Diagnostics in a Transparent Production Type Diesel Engine*. 1999, SAE International.
16. Park, S., et al., *Effect of injector type on fuel-air mixture formation of high-speed diesel sprays*. *Proceedings of the Institution of Mechanical Engineers D, Journal of Automobile Engineering*, 2006. **220**(D5): p. 647-659.
17. Pickett, L.M. and D.L. Siebers, *Soot in diesel fuel jets: effects of ambient temperature, ambient density, and injection pressure*. *Combustion and Flame*, 2004. **138**(1-2): p. 114-135.
18. Magdi K. Khair, H.J. *Diesel Fuel Injection*. 2013; Available from: https://www.dieselnet.com/tech/diesel_fi.php.
19. Bosch, *Common-rail injection systems CRS2-25 diesel common-rail system with solenoid valve injectors and 2,500bar* 2017.
20. Eastwood, P., *Particulate Emissions from Vehicles*. RSP. Vol. v.20. 2008, Hoboken: Wiley.
21. Colbeck, I.L., *Aerosol Science : Technology and Applications (1)*. 2013, Somerset, GB: Wiley.
22. Aoyagi, Y., et al., *A Gas Sampling Study on the Formation Processes of Soot and NO in a DI Diesel Engine*. 1980, SAE International.

23. WHO, W.h.o., *Health Aspects of Air Pollution with Particulate Matter, Ozone and Nitrogen Dioxide*. 2003, WHO.
24. Baukal, C.E., *Industrial combustion pollution and control*. Environmental science and pollution control series. 2004, New York: Marcel Dekker.
25. Danping, W. and H.A. Spikes, *The lubricity of diesel fuels*. *Wear*, 1986. **111**(2): p. 217-235.
26. Wadumesthrige, K., et al., *Investigation of Lubricity Characteristics of Biodiesel in Petroleum and Synthetic Fuel*. *Energy Fuels*, 2009. **23**: p. 2229-2234.
27. Ricardo, *Hydra Engine Modifications*. 1999.
28. Cussions, *Ricardo Single Cylinder Research Engines, Technical Specifications*. 1973.
29. Denso, *Service Manual - Common Rail System (CRS) - Diesel Injection Pump*. 2007.
30. Kalantar-zadeh, K., *Sensors : An Introductory Course*. *Sensors*. 2013, Dordrecht: Springer.
31. André V. Bueno, J.A.V.a.L.F.M., *Internal Combustion Engine Indicating Measurements*, in *Applied Measurement Systems*. 2012.
32. Staś, M.J., *An Universally Applicable Thermodynamic Method for T.D.C. Determination*. 2000, SAE International.
33. Steinem, C. and A. Janshoff, *Piezoelectric Sensors*. Springer Series on Chemical Sensors and Biosensors. Vol. v.5. 2007, Dordrecht: Springer.
34. Bishop, R.H., *The Mechatronics handbook : [1] : Mechatronic systems, sensors, and actuators : fundamentals and modeling*. 2nd ed. ed. The Electrical engineering handbook series. Vol. [1]. 2008, Boca Raton, Fla: CRC Press.
35. Curie, J. and P. Curie, *Phénomènes électriques des cristaux hémiedresa faces inclinées*. 1882.
36. Heywang, W., K. Lubitz, and W. Wersing, *Piezoelectricity: Evolution and Future of a Technology*. Evolution and Future of a Technology. Vol. 114. 2008, Berlin, Heidelberg: Springer Berlin Heidelberg, Berlin, Heidelberg.
37. APC. *Piezoelectric Ceramics: Principles and Applications*. 2016; Available from: <https://www.americanpiezo.com/knowledge-center/piezo-theory.html>.
38. Randolph, A.L., *Methods of Processing Cylinder-Pressure Transducer Signals to Maximize Data Accuracy*. 1990, SAE International.
39. Mukhopadhyay, S.C., *Intelligent Sensing, Instrumentation and Measurements*. Smart Sensors, Measurement and Instrumentation. Vol. v.5. 2013, Berlin: Springer.
40. Duff, M. and J. Towey, *Two Ways to Measure Temperature using thermocouples feature simplicity, accuracy, and flexibility*. *Analog Dialogue*, 2010. **44**(10): p. 1-6.
41. HORIBA, *HORIBA PG-300 Instruction Manual*. 2011.
42. NGK. *Zirconium dioxide lambda sensor*. 2016; Available from: <https://www.ngk.de/en/products-technologies/lambda-sensors/lambda-sensor-technologies/zirconium-dioxide-lambda-sensor/>.
43. Engineering, J.U.M., *FID model 3-200, Product Brochure*. 2009.
44. Li, L., et al., *Identification of a driver's starting intention based on an artificial neural network for vehicles equipped with an automated manual transmission*. *Proceedings of the Institution of Mechanical Engineers, Part D: Journal of Automobile Engineering*, 2016. **230**(10): p. 1417-1429.
45. Antony, J., *Design of experiments for engineers and scientists*. 2014: Elsevier.

-
46. Martyr, A.J. and M.A. Plint, *Engine Testing : The Design, Building, Modification and Use of Powertrain Test Facilities*. 4th ed. ed. Engine Testing. 2012, Burlington: Elsevier Science.
 47. Lefebvre, N., *Lecture note 1 TMR4535 DoE/Engine calibration, Basic elements*. 2016, NTNU. p. 26.
 48. Mathworks. *Linear and Nonlinear Regression Curve fitting tool box*. 2017 17.03.17]; Available from: <https://se.mathworks.com/help/curvefit/linear-and-nonlinear-regression.html>.
 49. Mathworks. *Interpolation Methods, Curve fitting tool box*. 2017 17.03.17]; Available from: <https://se.mathworks.com/help/curvefit/interpolation-methods.html>.
 50. Mathworks. *Lowess, Curve fitting tool box*. 2017 17.03.17]; Available from: <https://se.mathworks.com/help/curvefit/lowess-smoothing.html>.
 51. Mathworks. *Evaluating Goodness of Fit. Curve fitting tool box*. 2017 17.03.17]; Available from: http://se.mathworks.com/help/curvefit/evaluating-goodness-of-fit.html#bq_5kwr-3.
 52. AS, S.F.R.M., *Datablad Statoil Marine Gassolje LS*.

APPENDIX

The appendix section contains documents with individual page numbers.

APPENDIX A – PLANED AND CONDUCTED TESTS

The next pages contain the test plan used during the conducted experiments of this thesis.

Function Check							
Test #	What to do	Performed?	Comments:				
1*	Max engine speed trip	y	Engine does not trip during high speeds				
2*	Max pressure trip	n	Not able to reach				
3*	Max injector pressure trip	y	Stopped by coontrol system at 1300 bar				
4*	Injector Control	y	Working properly				
5*	Inlet air heater	n	Not mounted				
6*	Logging of data	y	Working properly				
7*	Consistency of PV diagram	n					
8*	Stupidety check	y	Nothing found but the safety cover on fuel pump				
Motored Test							
Test #	Name	Speed [rps]	Data logged?	Comments:			
1	Mech1	20	y	Loud sound, but stable			
2	Mech2	30	y	Sound on around 23 rps, but good at 30			
3	Mech3	40	y	Drop in sound afther 33 rps, more vibrations in floor. Still			
4	Mech4	50	y	Nothing to report			
5	Mech5	60	y	Nothing to report			
6	Mech6	70	y	Nothing to report			
7	Mech7	75	y	No pressure data recorded. 3x retest conducted. 1 of 3 was successfull			
Time Until Stability Evaluation							
Test #	Name	Speed 1 [rps]	Load 1 [kW]	Speed 2 [rps]	Load 2 [kW]	Static logged?	
8	Stab1	40	motored	40	4	y	
9	Stab2	40	1	40	4	y	
Operational Limits Investigation							
800 bar common rail pressure							
Test #	Name	Speed 1 [rps]	Load	Limit Load [kW]	Comments:	Inj dur	Inj timing
11	Limit1	20	Smoke Limit	2.7	ok	0.43	10 atdc
12	Limit2	35	Smoke Limit	5.2	ok	0.49	10 atdc
13	Limit3	50	Smoke Limit	6.6	ok	0.54	10 atdc
14	Limit4	60	Smoke Limit	6.2	ok	0.52	10 atdc
15	Limit5	70	Smoke Limit	N/A	Injector Malfunction		10 atdc

No further tests made. Planed mapping point are shown in next page.

Engine Mapping				
Test #	Name	Speed [rps]	Load [%]	Load [kW] from Limit test
21	Map1	20	20	0.54
22	Map2	20	40	1.08
23	Map3	20	60	1.62
24	Map4	20	80	2.16
25	Map5	35	20	1.04
26	Map6	35	40	2.08
27	Map7	35	60	3.12
28	Map8	35	80	4.16
29	Map9	50	20	1.32
30	Map10	50	40	2.64
31	Map11	50	60	3.96
32	Map12	50	80	5.28
33	Map13	60	20	1.24
34	Map14	60	40	2.48
35	Map15	60	60	3.72
36	Map16	60	80	4.96
37	Map17	75	20	Limit Missing
38	Map18	75	40	Limit Missing
39	Map19	75	60	Limit Missing
40	Map20	75	80	Limit Missing

Verification points				
41	Map21	27.5	30	
42	Map22	42.5	50	
43	Map23	67.5	70	
44	Map24	67.5	30	

APPENDIX B – OPERATION MANUAL

The next pages contain the operational manual for startup and operation of the Hydra engine. This document is based on the experiences during the development of this thesis. The first chapter has been removed from this document because it has much resemblance with chapter 4 in this thesis.

PREFACE

This manual has been made to make the process of starting and performing experiments with the Hydra engine easier. The manual features a simple guide for preparations and start-up of the engine, in addition to a control guide on how to operate the engine. To give the reader a basic understanding of the complete operation of the test-bed, the manual starts with an in depth review of the most important components of the test-bed.

CONTENTS

PREFACE.....I

CONTENTS.....II

FIGURE LISTIII

1 START-UP GUIDE4

 1.1 HEAT-UP AND PREPARATIONS 4

 1.2 START UP 7

 1.3 SHUTDOWN..... 7

2 CONTROL GUIDE.....8

 2.1 INJECTION CONTROL..... 9

 2.1.1 *Common Rail Pressure*..... 9

 2.1.2 *Injection Timing and Injection Duration*..... 10

 2.2 LOGGING DATA 11

 2.3 DEALING WITH ERROR MESSAGES 12

3 TIPS AND TRICKS13

 3.1 MAINTENANCE TIPS 13

 3.2 ENGINE OPERATION TIPS..... 13

FIGURE LIST

FIGURE 1-1 FUSE BOX SWITCH.....	4
FIGURE 1-2 ANALOG CONTROL MODULE	4
FIGURE 1-3 COOLANT CAP.....	5
FIGURE 1-4 STRAP WRENCH TIGHTENED AROUND DRIVESHAFT.....	5
FIGURE 1-5 PRESSURE ENCODER	6
FIGURE 1-6 FREQUENCY CONVERTER FOR FUEL PUMP MOTOR	6
FIGURE 1-7 ENGINE SPEED KNOB, DIALED TO 20 RPS	7
FIGURE 2-1 MAIN CONTROL SYSTEM WINDOW.....	8
FIGURE 2-2 INJECTION CONTROL	9
FIGURE 2-3 LOGGING INTERFACE	11
FIGURE 2-4 REOCCURRING ERROR MESSAGE	12
FIGURE 2-5 CHASSIS RESET	12

1 START-UP GUIDE

1.1 HEAT-UP AND PREPARATIONS

Visual inspection of the engine and engine room:

Look for leaks and other discrepancies that can influence the engine operation. Some oil can be expected. Look and smell for diesel leaks. Check if safety covers are installed.

Engage fuse box for Hydra engine:

The control panel for the engine fuse box can be found in head-height to your left when entering the control room. Rotate the switch marked with “Hydramotor” from 0 to 1 (Figure 1-1). The light above the switch will light up, and a summing sound will be heard.



Figure 1-1 Fuse box switch

Start oil and coolant heater and pump:

Press down the four orange buttons, marked with “Oil Heater”, “Oil Pump”, “Coolant pump” and “Coolant Heater”, on the analog control module shown in Figure 1-2. The buttons should glow orange, and a summing from the pumps can be heard.

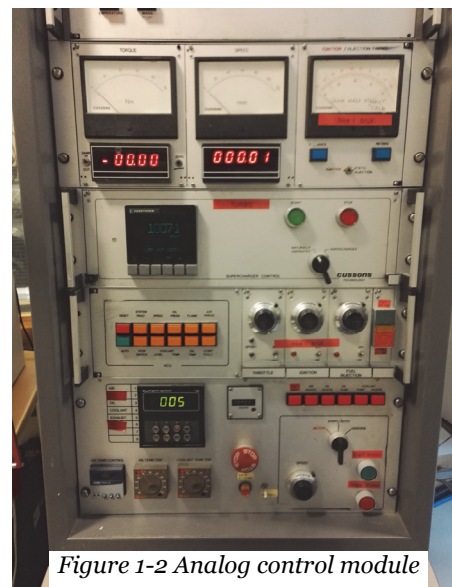


Figure 1-2 Analog control module

Systems check:

The following systems must be checked before the starting procedure can continue.

Oil level:

Open the oil cap, check if the oil level is between the indicators on the stick. If oil level is too low, add oil from the can in the spare parts cabinet. The oil cap is located at the right side of the crankcase.

Coolant pump:

Open the coolant cap (Figure 1-3), and check if the blue colored liquid inside is moving. This will ensure that the coolant pump is functioning. The coolant cap is located between the Hydra engine and the dynamometer.



Figure 1-3 Coolant cap

Rotate engine:

Open the access panel on the driveshaft between the Hydra engine and the dynamometer. Find the strap wrench on the wall over the workshop table, and tighten it around the driveshaft (Figure 1-4). Rotate the driveshaft two times. This secures that there is nothing blocking the engine from rotating.

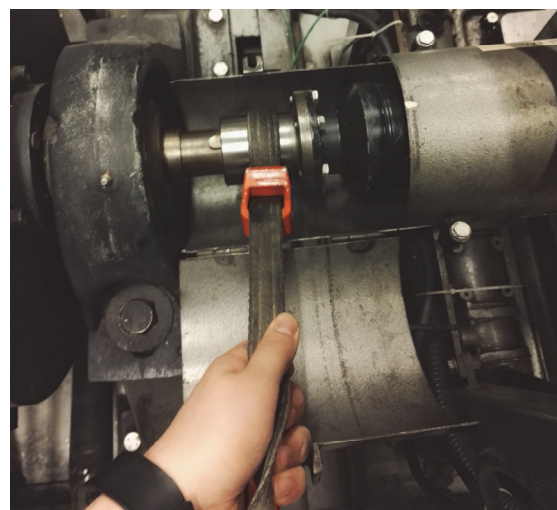


Figure 1-4 Strap wrench tightened around driveshaft

Pressure encoder:

Check that the pressure encoder is online, (the operate light should be green). If it is not online, press the reset button (red button). The encoder (Figure 1-5) is located above the window to the control room, at the left side of the engine.



Figure 1-5 Pressure encoder

Diesel level:

Check that the fuel tank has sufficient fuel level, and that both pipes from the fuel pump is in contact with the fuel.

Start fuel pump:

Open the white box beside the fuel pump. The frequency converter for the electric motor driving the fuel pump is located inside. Press “run” and check that the rotational speed is set to around 800 rpm. If this is not the case, rotate the white knob carefully until the correct speed is shown.



Figure 1-6 Frequency converter for fuel pump motor

1.2 START UP

Before the engine can be started it must be ensured that the engine has reached a temperature above 50°C. This can be checked both on the analog control module and in the control system in LabVIEW. Do not continue unless a temperature above 50°C has been noted.

Set engine speed to 20 rps:

The start up speed for the engine is recommended to 20 rps. This speed is set by turning the speed knob, which are located to the left of the start button on the analog control module. Note that the upper number dial, shows the ten's place and the lower number dial shows the one's place.



Figure 1-7 Engine speed knob, dialed to 20 rps

Start the engine:

This is done in two steps. First press the reset button, this will check for errors in the system, and give a 10 second window to press the start button. When the start button is pushed, the engine should star. If not, check if the emergency stop buttons located at the analog control module and the Hydra test-bed are pressed down.

1.3 SHUTDOWN

1. Remove load (turn of injector)
2. Lower speed to 20 rps
3. Press stop engine button

2 CONTROL GUIDE

The control system is opened by clicking on the desktop shortcut called “Hydra Control System”. This will open the LabVIEW window shown in Figure 2-1. To make the interface live, click on the arrow in the upper left corner. In the upper left corner, the measured values are showed in real time. Below that is the calculated values, which are based on the measured values. At this moment only power is calculated hear. To the right of the calculated values, the PID controller gains are found. These values can be manipulated to get different responses for the control of fuel pressure. However, the present values work acceptably. In the big window to the right the measured cylinder pressure and injection timing and duration is shown in real time. The graphs in this window should be monitored closely during operation of the engine. Below the in-cylinder pressure window, the logging of data and file allocation happens. Logging and injection control will be covered in the next sections.

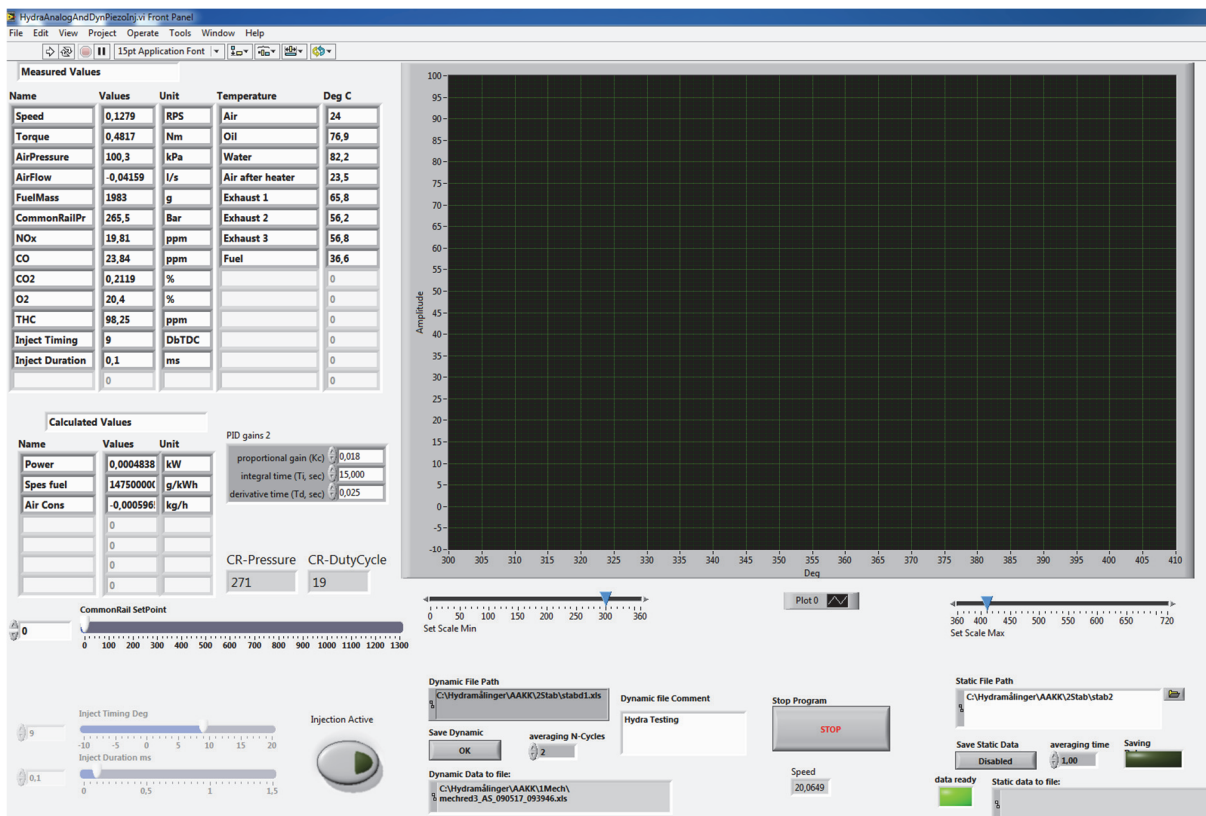


Figure 2-1 Main Control System Window

2.1 INJECTION CONTROL

The injection is controlled by the interface in the bottom left corner of the LabVIEW window. The interface is shown in a close view in Figure 2-2. In this interface three main parameters can be controlled; fuel pressure, injection duration and injection timing. Furthermore, there is a button called “Injection Active” in the bottom right corner of Figure 2-2. This button is used to turn off and on the injector. In the picture below this interface is in the off position. When button is in the on position the button acquires a green light, in addition the inject timing and duration bar will become unshaded. The injector can be turned on even if the engine has no rotational speed. Since the injection timing is dependent on the crank angle position, no fuel will be injected in this state. When the button is pressed to turn off the injector, all parameters are automatically set to zero.

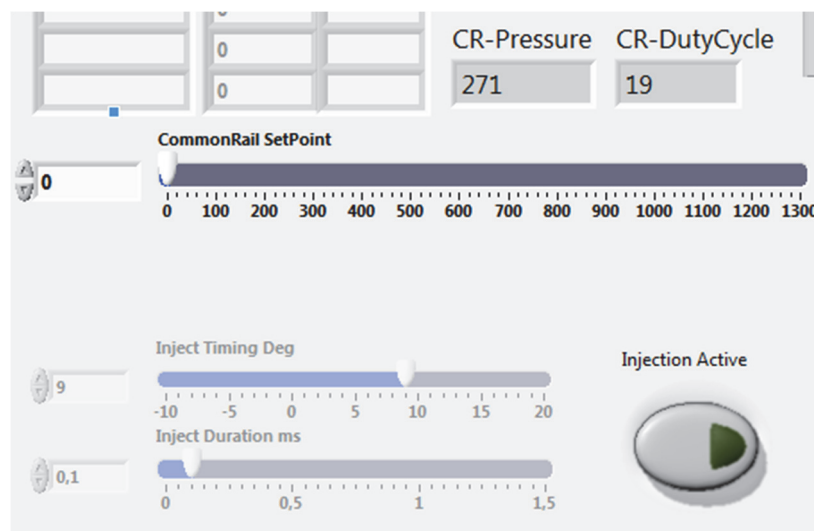


Figure 2-2 Injection Control

2.1.1 COMMON RAIL PRESSURE

Before common rail pressure is controlled, be sure that the fuel pump is running. The common rail pressure is controlled by increasing the common rail set point, this must be done in incremental steps, to avoid large pressure variations. Use steps of 50 bar, and wait for the value in the “CR-Pressure” window to stabilize, continue increasing the pressure until the desired pressure is reached.

2.1.2 INJECTION TIMING AND INJECTION DURATION

Injection timing is initially always set to 9° ATDC. This value can be changed at any point, but it could be smart to manipulate this value while combustion is present. This makes it possible to monitor the impact timing change has on the pressure curve. This is in general good practice during every interaction with the engine. Always keep an eye on the pressure data, power and temperatures.

The injection duration controls how long the injector is open at each power stroke. This value can in principle be set much higher than what the engine can handle. Therefore it much care must be shown when this value is altered. The limits of the engine tend to be above 0.4 ms with a timing of 10° ATDC and a rail pressure of 800 bar. This will of course vary with speed, timing and fuel pressure. Nevertheless, extra care must be shown close to 0.4 ms, meaning that HC and CO emissions must be monitored closely, if these values increase sharply the engine has reached its limit. Note that these values (especially CO) has a slow reaction, therefore allow some time at each duration close to the limit to check these values.

When the desired load point has been acquired the engine should be left on this point for at least 4 minutes before data is logged. This is done to let the engine reach stability. Shorter stability time can be achieved by sustaining injection of fuel during change to a new load point. Motoring the engine between load points will cool the exhaust system rapidly, the engine will hence use more time to warm up the exhaust system at the new load point.

2.2 LOGGING DATA

Data is logged using the lower right part of the LabVIEW window, which is shown in Figure 2-3. The logging system is divided into a dynamic and a static part. The dynamic part logs measurements of crank angle, cylinder pressure and injector volt inputs. The static part logs measurements of temperatures, engine speed, emissions, and flowrates. The location and the filename of the logged files is controlled by altering the file path for static and dynamic logging.

Static data is logged by clicking the button called “Save Static Data”, this button will then change from displaying “Disabled” to displaying “Enabled”. Data is now being logged in steps defined by the “averaging time” window. When sufficient data is collected, press the “Save Static Data” button again to terminate the logging process. Observe that the correct file has been written by inspecting the path in the “Static data to file” window.

Dynamic data is logged by pressing the button called “Save Dynamic”. The data is averaged over the number of cycles specified in the “averaging N-Cycles” window. Observe that the correct file has been written by inspecting the path in the “Dynamic Data to file” window.

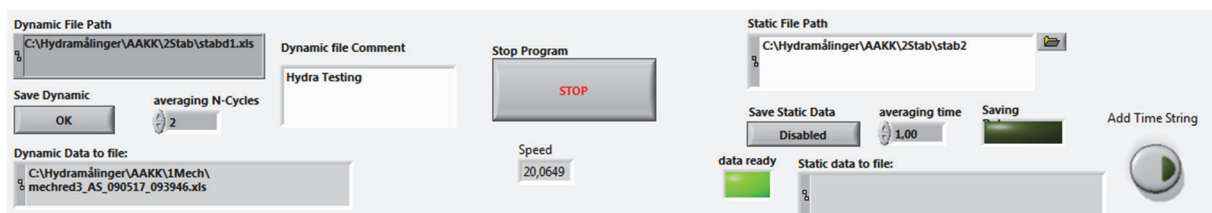


Figure 2-3 Logging Interface

2.3 DEALING WITH ERROR MESSAGES

There is one reoccurring error message that needs to be handled every time the fuse box is turned on. The error is displayed in Figure 2-4. The error happens because the chassis that handles the sensors has not been reset.

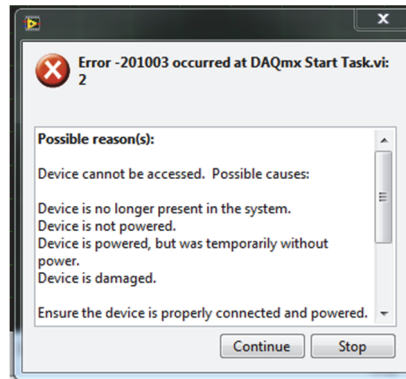


Figure 2-4 Reoccurring Error Message

The chassis is reset by opening the program called “NI – measurement & Automotive Explorer”. Open the slider called “Devices and Interfaces” proceed with opening the slider called “Network Devices”. Click on “Reset Chassis” as shown in Figure 2-5. Now restart the LabVIEW interface.

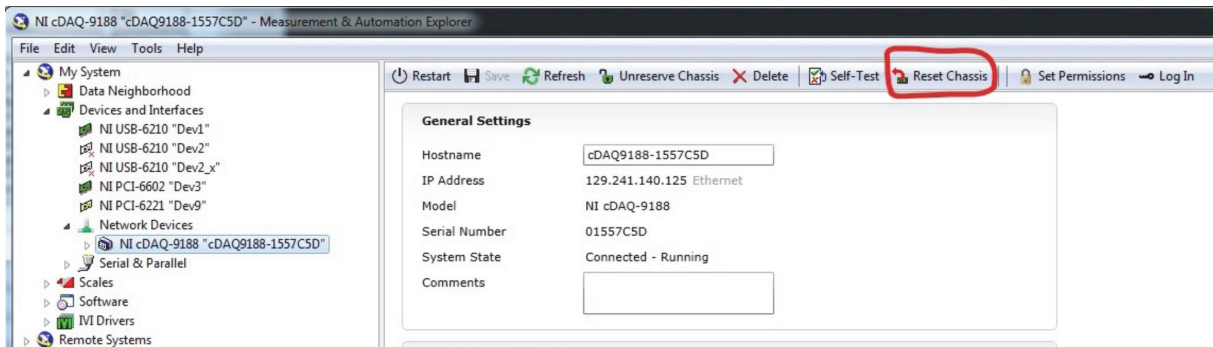


Figure 2-5 Chassis Reset

3 TIPS AND TRICKS

3.1 MAINTENANCE TIPS

1. Oil level should be checked with the oil pump turned off. The oil pump uses significant amounts of oil, filling up oil when the oil pump is running will cause overfilling.
2. Coolant does not need to be topped all the way up. This will cause large amounts of coolant to flow out of the overflow tube. Coolant should be filled to approximately half the height of the cooling tower top.

3.2 ENGINE OPERATION TIPS

1. Common rail pressure should be increased in steps of 50 bar. Wait for approximate stability before further increase is employed.
2. During change of load point, it can be smart to continue injecting fuel to the engine. Motoring the engine will cause rapid cooling of the exhaust system.
3. The cooling water flow can be closed during warm-up of the engine. This will greatly reduce warm-up time.
4. The engine oil temperature can be stabilized on a specific level by controlling the cooling water flow. Turn the lower valve slightly to increase the water flow. Look at the temperatures of cooling water and oil. After some time, these values will balance each other. This is very important if good repeatability is required.
5. Always double-check that the logging system is writing to the correct file.
6. Do not delete the previous logged file. This will invoke an error, where a control system restart is needed.

APPENDIX C – MATLAB SCRIPT - READING DATA

The next pages contain the Matlab script used to read data produced by the logging system of the Hydra engine. This script was made before any of the data was collected, therefore it will appear more complicated than strictly needed.

Contents

- [Info:](#)
- [Reading files](#)
- [Conditioning file names](#)
- [Reading Static Variables](#)
- [Reading Dynamic Variables. Remember to add ROHR and accuROHR, when ready.](#)
- [Matrix Conditioning](#)
- [Inserting mean and range of static variables in each matrix](#)
- [Fuel Evaluation](#)
- [Dynamic data processing:](#)
- [Saving workspace](#)

Info:

This script is made to read all values collected in the LabView interface, where focus is on versatility and not efficiency. It is thought to be a script that can be used for different purposes with a easy way to change names of variables and there collums. This is a slow script, mainly because of the slowness of the xls read command. Some changes must be made to the script to make it work in any situations.

```
clear
clc
close all
```

Reading files

Prompting file names and iteration conditions

```
Namestat = input('Input static name\n');
Namedyn = input('Input dynamic name\n');
Namestat = input('Input dynamic name\n');
teststart = 1;
testend = input('Enter number of files to be read\n');
testlength = testend-teststart+1;
testnumb_start = 1;
testnumb_end = testlength;

for i=teststart:testend
```

Conditioning file names

```
%Note that the tab should have the same name as the file
eval(sprintf('file%d = '%s%d%s'';',i,Namestat,i, '.xlsx'));
eval(sprintf('filed%d = '%s%d%s'';',i,Namedyn,i, '.xlsx'));
eval(sprintf('tab%d = '%s%d'';',i,Namestat,i));
eval(sprintf('tabd%d = '%s%d'';',i,Namedyn,i));
```

Reading Static Variables

```
%Change collumn that is collected if needed
```

```

eval(sprintf('x_value%d = xlsread(file%d,tab%d,'A26:A1000');',i,i,i));
eval(sprintf('speed%d = xlsread(file%d,tab%d,'B26:B1000');',i,i,i));
eval(sprintf('torque%d = xlsread(file%d,tab%d,'C26:C1000');',i,i,i));
eval(sprintf('airpress%d = xlsread(file%d,tab%d,'D26:D1000');',i,i,i));
%Jumping over unused variables
eval(sprintf('airflow%d = xlsread(file%d,tab%d,'E26:E1000');',i,i,i));
eval(sprintf('fuelmass%d = xlsread(file%d,tab%d,'F26:F1000');',i,i,i));
eval(sprintf('railpress%d = xlsread(file%d,tab%d,'G26:G1000');',i,i,i));
eval(sprintf('nox%d = xlsread(file%d,tab%d,'H26:H1000');',i,i,i));
eval(sprintf('co%d = xlsread(file%d,tab%d,'I26:I1000');',i,i,i));
eval(sprintf('co2%d = xlsread(file%d,tab%d,'J26:J1000');',i,i,i));
eval(sprintf('o2%d = xlsread(file%d,tab%d,'K26:K1000');',i,i,i));
eval(sprintf('thc%d = xlsread(file%d,tab%d,'L26:L1000');',i,i,i));
eval(sprintf('air%d = xlsread(file%d,tab%d,'M26:M1000');',i,i,i));
eval(sprintf('oil%d = xlsread(file%d,tab%d,'N26:N1000');',i,i,i));
eval(sprintf('water%d = xlsread(file%d,tab%d,'O26:O1000');',i,i,i));
eval(sprintf('airaheater%d = xlsread(file%d,tab%d,'P26:P1000');',i,i,i));
eval(sprintf('exhaust1%d = xlsread(file%d,tab%d,'Q26:Q1000');',i,i,i));
eval(sprintf('exhaust2%d = xlsread(file%d,tab%d,'R26:R1000');',i,i,i));
eval(sprintf('exhaust3%d = xlsread(file%d,tab%d,'S26:S1000');',i,i,i));
eval(sprintf('power%d = xlsread(file%d,tab%d,'U26:U1000');',i,i,i));

```

Reading Dynamic Variables. Remember to add ROHR and accuROHR, when ready.

```

eval(sprintf('crankangle%d = xlsread(file%d,tab%d,'A9:A1450');',i,i,i));
eval(sprintf('cylpressure%d = xlsread(file%d,tab%d,'B9:B1450');',i,i,i));
eval(sprintf('injctrldyn%d = xlsread(file%d,tab%d,'C9:C1450');',i,i,i));

```

end

Matrix Conditioning

```

%Conditioning matrixes for faster computation
air = zeros(1,testlength);
airr = zeros(1,testlength);
airpress = zeros(1,testlength);
airpressr = zeros(1,testlength);
airaheater = zeros(1,testlength);
airaheaterr = zeros(1,testlength);
co = zeros(1,testlength);
cor = zeros(1,testlength);
co2 = zeros(1,testlength);
co2r = zeros(1,testlength);
exhaust1 = zeros(1,testlength);
exhaust1r = zeros(1,testlength);
exhaust2 = zeros(1,testlength);
exhaust2r = zeros(1,testlength);
exhaust3 = zeros(1,testlength);
exhaust3r = zeros(1,testlength);

```

```

thc = zeros(1,testlength);
thcr = zeros(1,testlength);
injtiming = zeros(1,testlength);
injtimingr = zeros(1,testlength);
nox = zeros(1,testlength);
noxr = zeros(1,testlength);
o2 = zeros(1,testlength);
o2r = zeros(1,testlength);
oil = zeros(1,testlength);
oilr = zeros(1,testlength);
power = zeros(1,testlength);
powerr = zeros(1,testlength);
railpress = zeros(1,testlength);
railpressr = zeros(1,testlength);
speed = zeros(1,testlength);
speedr = zeros(1,testlength);
torque = zeros(1,testlength);
torquer = zeros(1,testlength);
water = zeros(1,testlength);
waterr = zeros(1,testlength);
x_value = zeros(1,testlength);
x_valuer = zeros(1,testlength);
mf = zeros(1,testlength);
x_rate = zeros(1,testlength);
airflow = zeros(1,testlength);
airflowr = zeros(1,testlength);

```

Inserting mean and range of static variables in each matrix

range can in most cases be skipped here

```

for i = teststart:testend
    for i = testnumb_start:testnumb_end

```

```

air(i) = eval(sprintf('mean(air%d);',i));
airr(i) = eval(sprintf('range(air%d);',i));
airpress(i) = eval(sprintf('mean(airpress%d);',i));
airpressr(i) = eval(sprintf('range(airpress%d);',i));
airaheater(i) = eval(sprintf('mean(airaheater%d);',i));
airaheaterr(i) = eval(sprintf('range(airaheater%d);',i));
airflow(i) = eval(sprintf('mean(airflow%d);',i));
airflowr(i) = eval(sprintf('range(airflow%d);',i));
co(i) = eval(sprintf('mean(co%d);',i));
cor(i) = eval(sprintf('range(co%d);',i));
co2(i) = eval(sprintf('mean(co2%d);',i));
co2r(i) = eval(sprintf('range(co2%d);',i));
exhaust1(i) = eval(sprintf('mean(exhaust1%d);',i));
exhaust1r(i) = eval(sprintf('range(exhaust1%d);',i));
exhaust2(i) = eval(sprintf('mean(exhaust2%d);',i));
exhaust2r(i) = eval(sprintf('range(exhaust2%d);',i));
exhaust3(i) = eval(sprintf('mean(exhaust3%d);',i));
exhaust3r(i) = eval(sprintf('range(exhaust3%d);',i));
thc(i) = eval(sprintf('mean(thc%d);',i));
thcr(i) = eval(sprintf('range(thc%d);',i));
nox(i) = eval(sprintf('mean(nox%d);',i));
noxr(i) = eval(sprintf('range(nox%d);',i));
o2(i) = eval(sprintf('mean(o2%d);',i));
o2r(i) = eval(sprintf('range(o2%d);',i));

```

```

oil(i) = eval(sprintf('mean(oil%d);',i));
oilr(i) = eval(sprintf('range(oil%d);',i));
power(i) = eval(sprintf('mean(power%d);',i));
powerr(i) = eval(sprintf('range(power%d);',i));
railpress(i) = eval(sprintf('mean(railpress%d);',i));
railpressr(i) = eval(sprintf('range(railpress%d);',i));
speed(i) = eval(sprintf('mean(speed%d);',i));
speedr(i) = eval(sprintf('range(speed%d);',i));
torque(i) = eval(sprintf('mean(torque%d);',i));
torquer(i) = eval(sprintf('range(torque%d);',i));
water(i) = eval(sprintf('mean(water%d);',i));
waterr(i) = eval(sprintf('range(water%d);',i));
x_value(i) = eval(sprintf('mean(x_value%d);',i));
x_valuer(i) = eval(sprintf('range(x_value%d);',i));

```

Fuel Evaluation

```

mf(i) = eval(sprintf('range(fuelmass%d);',i));
x_rate(i) = eval(sprintf('max(x_value%d);',i));

```

```

end
end
mf_rate = mf./x_rate;

```

Dynamic data processing:

```

%Zeroes:
crankangle = zeros(1442,testlength);
cylpressure = zeros(1442,testlength);
injctrldyn = zeros(1442,testlength);
% Collect in matrixes:
for i = teststart:testend
    crankangle(:,i) = eval(sprintf('crankangle%d(1:1442);',i));
    cylpressure(:,i) = eval(sprintf('cylpressure%d(1:1442);',i));
    injctrldyn(:,i) = eval(sprintf('injctrldyn%d(1:1442);',i));
end

```

Saving workspace

Save the variables that are needed for analysis

```

save(FileName, 'air', 'airr', 'co', 'cor', 'co2', 'co2r', 'exhaust1', ...
'exhaust1r', 'exhaust2', 'exhaust2r', 'exhaust3', 'exhaust3r',...
'nox', 'noxr', 'o2', 'o2r', 'oil', 'oilr', ...
'power', 'powerr', 'railpress', 'railpressr', 'speedr', 'torque', ...
'torquer', 'water', 'waterr', 'x_value', 'x_valuer', 'speed',...
'mf_rate', 'testlength', 'airpress', 'airpressr', 'airaheater',...
'airaheaterr', 'airflow', 'crankangle', 'cylpressure', 'injctrldyn'...
, 'railpress1', 'railpress2', 'railpress3', 'railpress4',...
'x_value1', 'x_value2', 'x_value3', 'x_value4');
% Confirming finished script and file name
disp('Script completed. All needed variables are saved in in the following file:')
disp(FileName)

```

APPENDIX D – MATLAB SCRIPT – MOTORED TEST

The next pages contain the Matlab script used to plot and calculate relevant data from the motored tests.

Contents

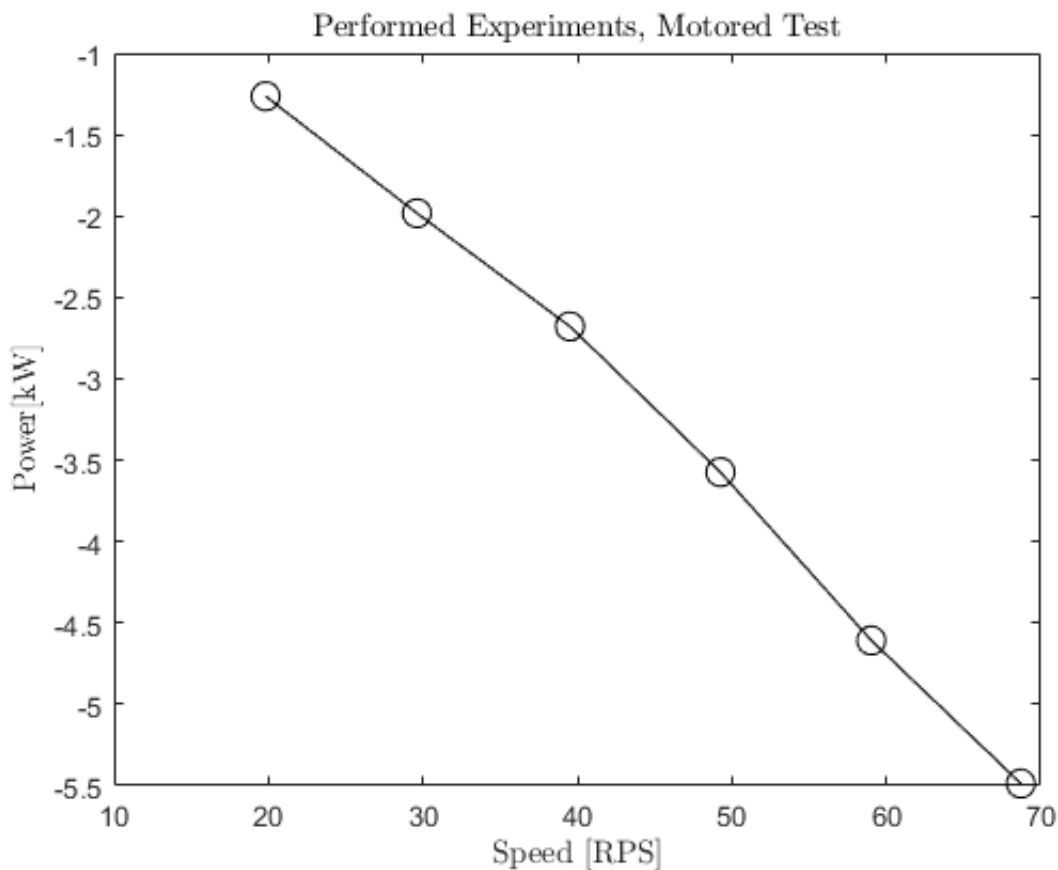
- Mechanical Efficiency
- Plot of Experiments
- Engine parameters
- Plot PV-Curve
- Efficiency Calculations
- Plot bmep, imep and mechanical efficiency
- Volumetric efficiency
- Engine temp
- Chocked Flow
- Pipe flow

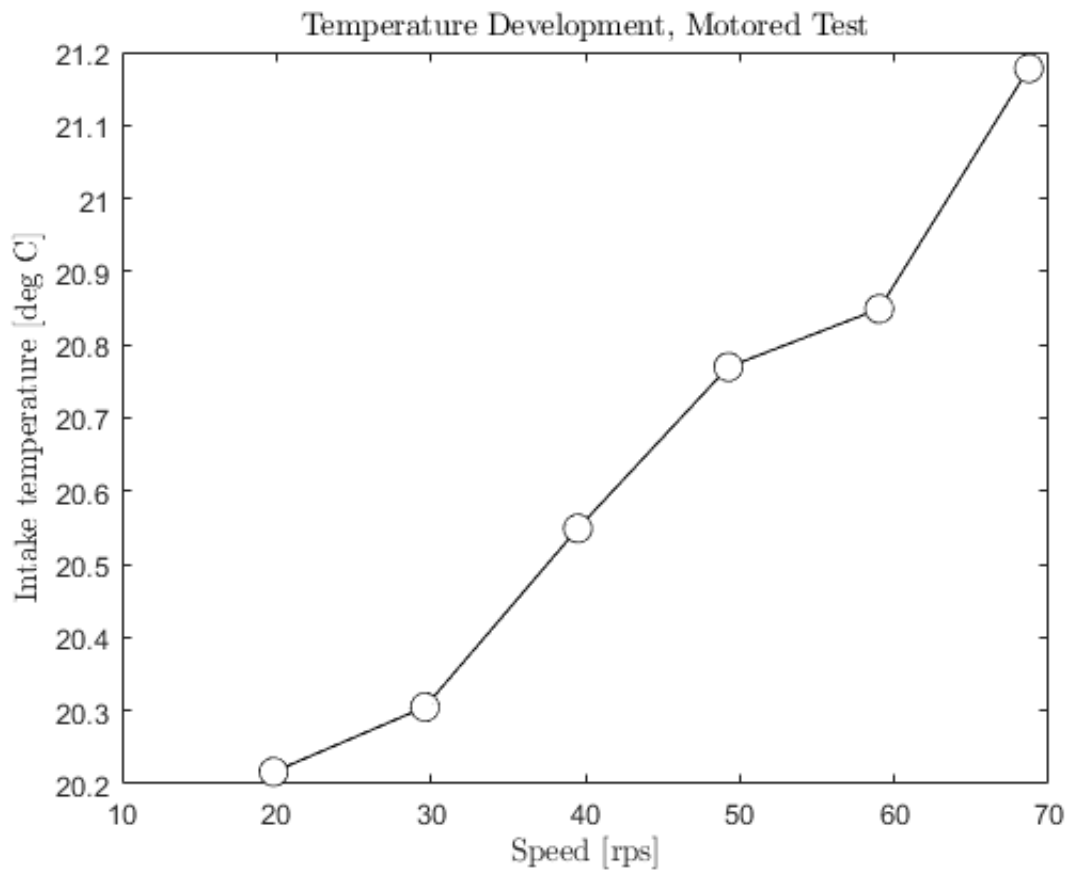
Mechanical Efficiency

```
load('Efficiency.mat')
presscorrect = xlsread('Pressurecorrection.xlsx','A723:F723');
cylpressure = (cylpressure + abs(presscorrect));
```

Plot of Experiments

```
power_calc = 2*3.14*speed.*torque*10^-3;
P_experimentsMECH(speed,power_calc);
TempDevMECH(speed,airaheater);
```





Engine parameters

```

nr = 2; % two cycles per power stroke
Vd1 = 0.4286; %dm^3
Vc = 0.02136*10^-3;%m^3
B = 78.35*10^-3; %m
S = 88.9*10^-3; %m
Cr = 20;
r = 0.5*S;
l = 156*10^-3;%156*10^-3; %144mm?
R = l/r;

l_conrod = 156*10^-3;
Vd = (pi/4)*B^2*S;
epsilon = 20; %compression ratio q2w

l_crankarm = S/2;
lambda = l_crankarm/l_conrod; %crank ratio
kappa = 1.4;

%Allocation of vectors
V = zeros(size(crankangle));

```

```

for i = 1:size(crankangle)
    cr_ang(i) = crankangle(i,1)*(pi/180);

end

for i = 1:length(V)
    for j = 1:length(V)
        V(i,1:6) = Vc+(Vd+Vc)-...

```

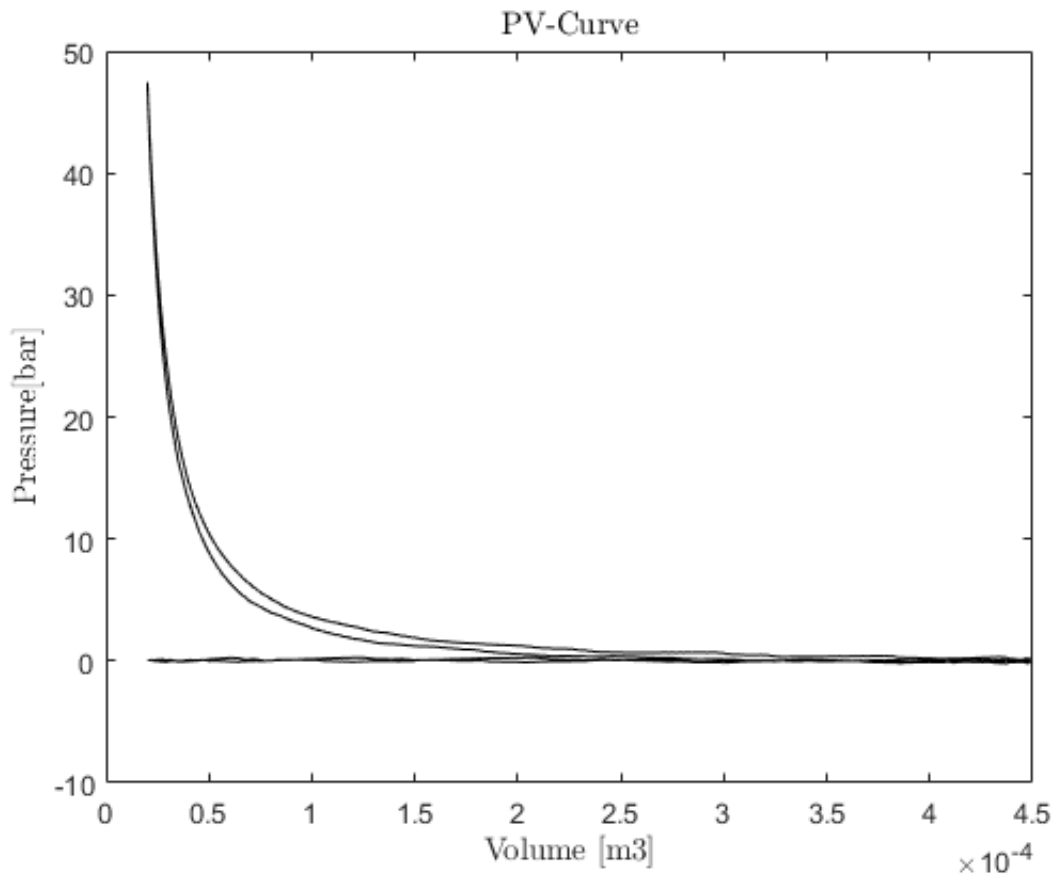
```

(Vd*((1/(epsilon-1))+0.5*(1-cos(cr_ang(i)+pi)+(1/lambda)...
*(1-sqrt(1-(lambda*(sin(cr_ang(i)+pi))^2)))));
end
end

```

Plot PV-Curve

```
PV_Curve(V(:,1),cylpressure(:,1))
```



Efficiency Calculations

```

%kW
bmep = ((6.28*torque*nr)./(Vd1));
for i= 1:6
imep_gross(1,i) = 10^5*((trapz(cylpressure(540:721,i),...
V(540:721,i)))-(trapz(cylpressure(722:900,i),V(722:900,i))));
end
eff_mech = 100*abs(bmep./imep_gross);

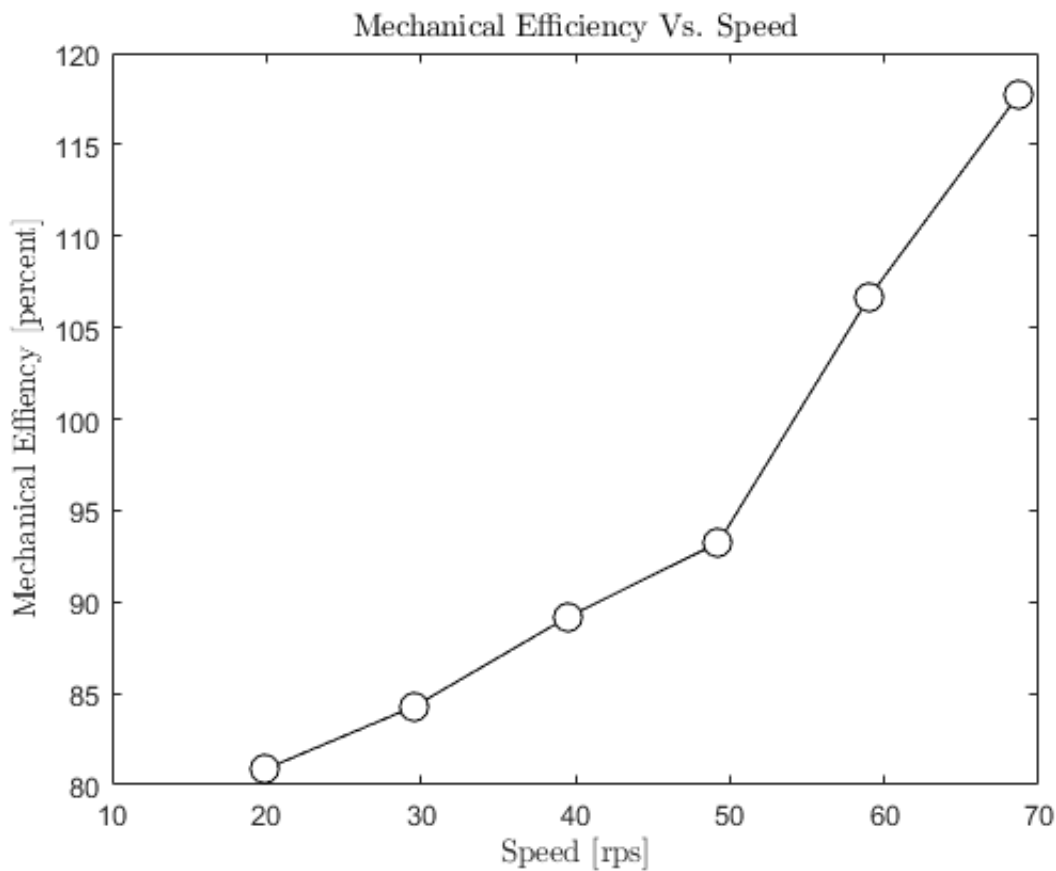
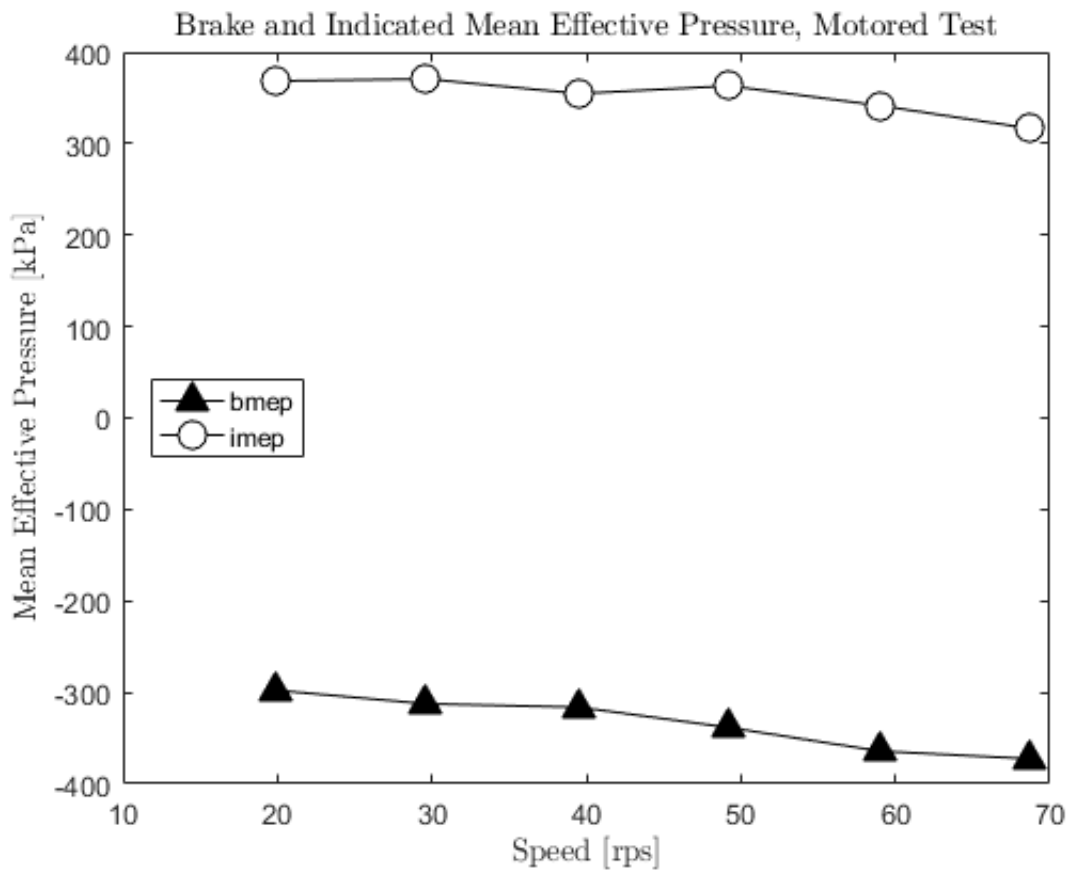
```

Plot bmep, imep and mechanical efficiency

```

IBMEP(speed,bmep,speed,imep_gross)
MECHEFF(speed,eff_mech)

```



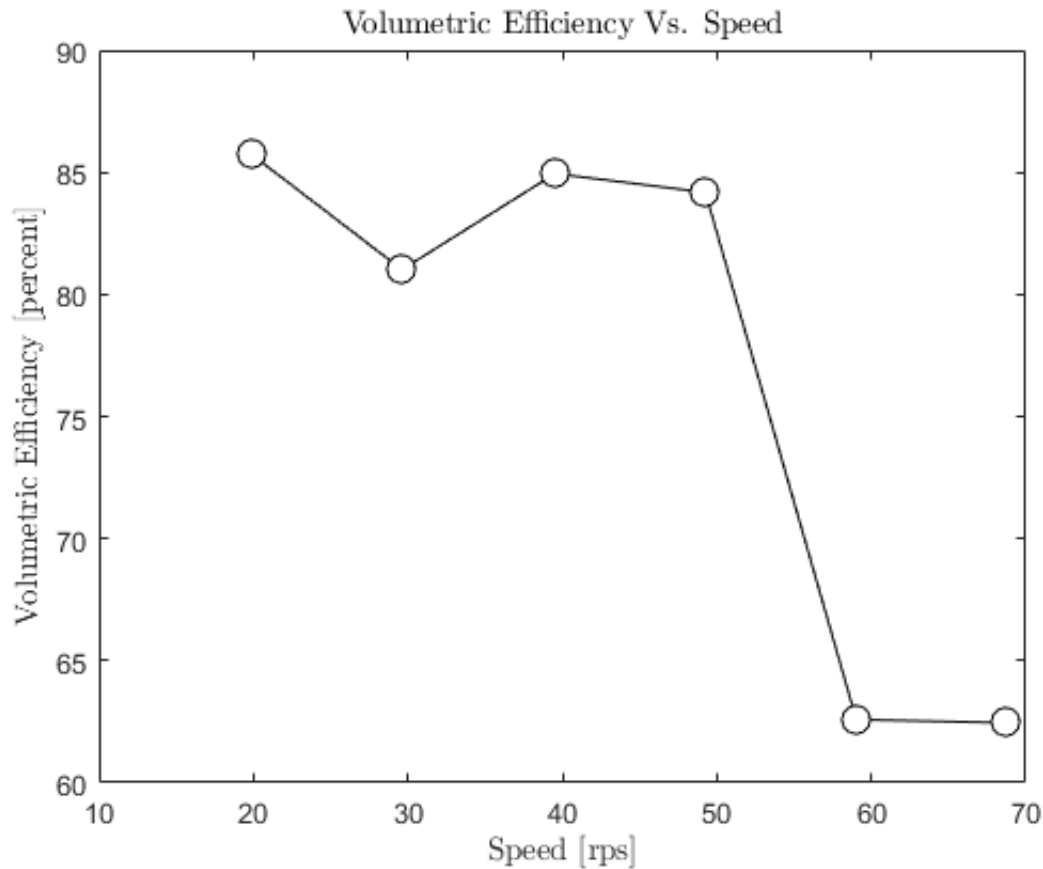
Volumetric efficiency

```
R = 287.058; %J/kgK
v_a_dot = airflow; % l/s
rho_a = mean((airpress*10^3)./(R*(airaheater+273)));
```

```

eff_vol = 100*(v_a_dot./ ((Vd1/2).*speed));
% Plot:
VOLEFF(speed,eff_vol)
print -dpng Volumetric_Efficiency_Mech.png

```



Engine temp

```

%Oil
figure1 = figure('Color',[1 1 1]);
% Create plot
plot(speed,oil,'MarkerFaceColor',[1 1 1],'MarkerSize',10,'Marker','o',...
      'Color',[0 0 0]);

% Create xlabel
xlabel('Speed [rps]','Interpreter','latex');

% Create title
title('Oil Temperature Development , Motored Test','Interpreter','latex');

% Create ylabel
ylabel('Oil Temperature [deg C]','Interpreter','latex');

box('on');
grid('off');
set(gcf, 'PaperPositionMode','auto')
print -dpng oiltempMECH.png

% Exhaust
figure1 = figure('Color',[1 1 1]);
% Create plot
plot(speed,exhaust1,'MarkerFaceColor',[1 1 1],'MarkerSize',10,'Marker','o',...
      'Color',[0 0 0]);

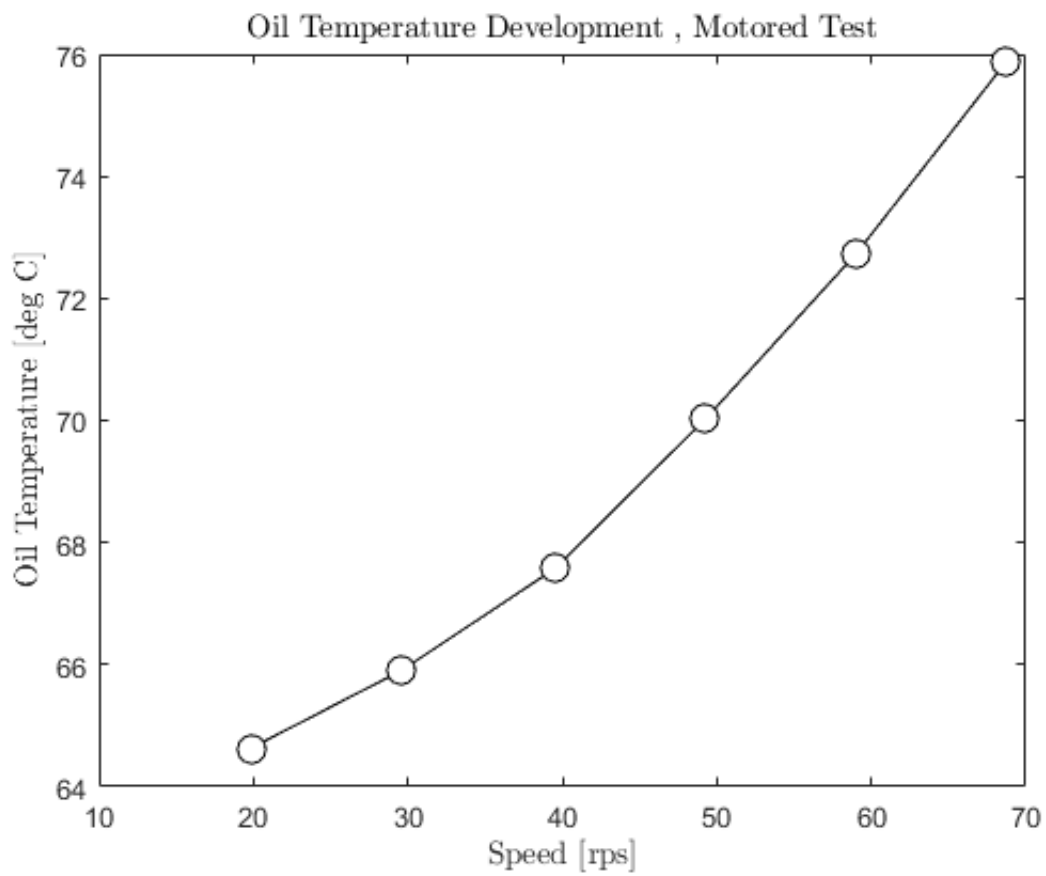
```

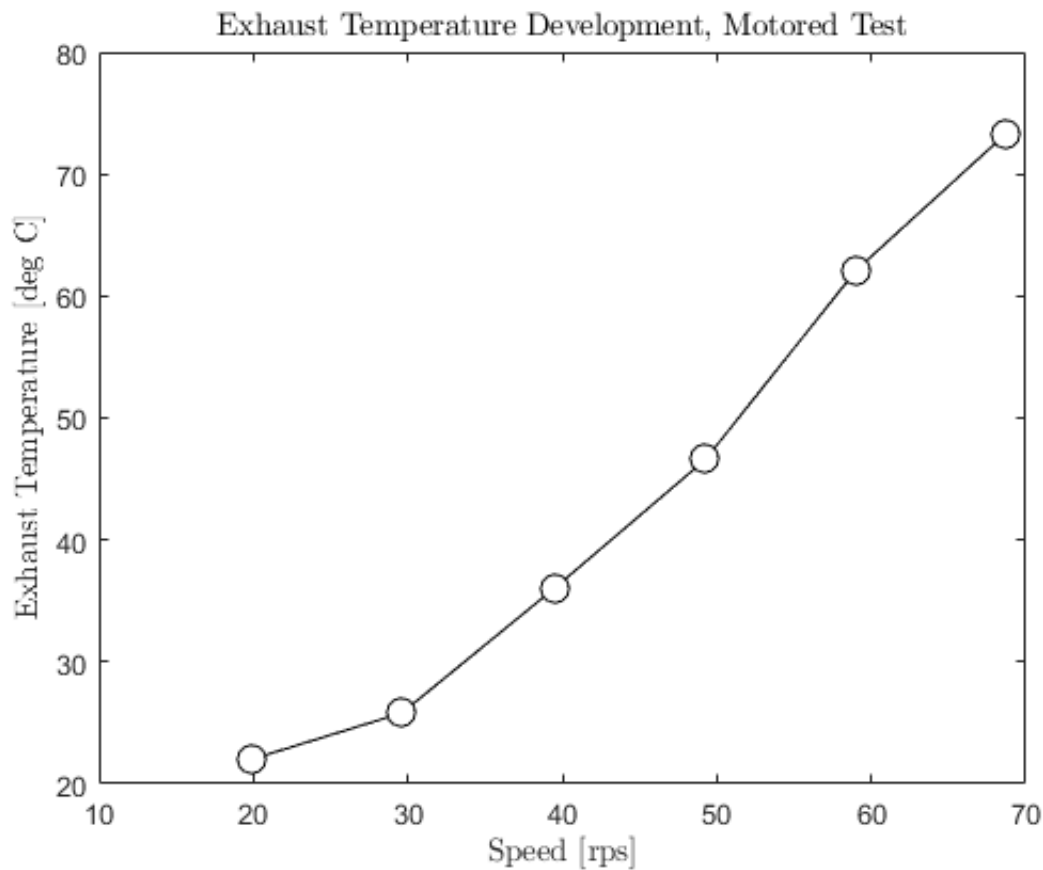
```
% Create xlabel
xlabel('Speed [rps]','Interpreter','latex');

% Create title
title('Exhaust Temperature Development, Motored Test','Interpreter','latex');

% Create ylabel
ylabel('Exhaust Temperature [deg C]','Interpreter','latex');

box('on');
grid('off');
set(gcf, 'PaperPositionMode','auto')
print -dpng extempMECH.png
```





Chocked Flow

```

rho_ex = mean((airpress*10^3)./(R*(exhaust1+273)));
m_rate = v_a_dot*rho_ex*10^-3; %kg/s
Cd = m_rate/(rho_ex*10^-3*v_a_dot);
d = 0.019; % m, 25mm wide, unkown wall thickness, assumed 3mm
A = (3.14/4)*d^2;
k = 1.4; %ratio of spesific heat
P0 = 101*10^3; %kPa
m_rate_exhaust_max = Cd*A*sqrt(k*rho_a*P0*(2/(k+1))^(k+1)/(k-1));
m_rate_actual = m_rate;
disp(m_rate_exhaust_max )
disp(m_rate_actual)

```

649.2023

37.3238 53.9193 76.6267 95.3639 84.6318 98.7939

Pipe flow

```

dminor = 0.019; % 0.019
dmajor = 0.060; % measuered outer 65    60
beta = dminor/dmajor;
Kred = 0.8*sin(15)*(1-beta^2);

K = 0.81; % from table
n = 1;
ft = 8*((2.457*log(3.707*d)))^-2;
Kb = (n-1)*(0.25*3.14*ft*(r/d)+0.4*K)+K;

```

```
dP = (Kred + Kb)*((rho_ex*v_a_dot.^2)/(2*9.81)); % head loss
dPpas = dP*9.81; %kPa
disp(dPpas)
```

9.3869 18.7033 36.6031 55.8562 44.3326 59.8196

APPENDIX E – MATLAB SCRIPT – STABILITY TEST

The next pages contain the Matlab script used to plot and calculate relevant data from the stability tests.

Contents

- Stability
- Plot of Experiments
- NOx Stability With Same speed
- Exhaust Temp
- Oil temp

Stability

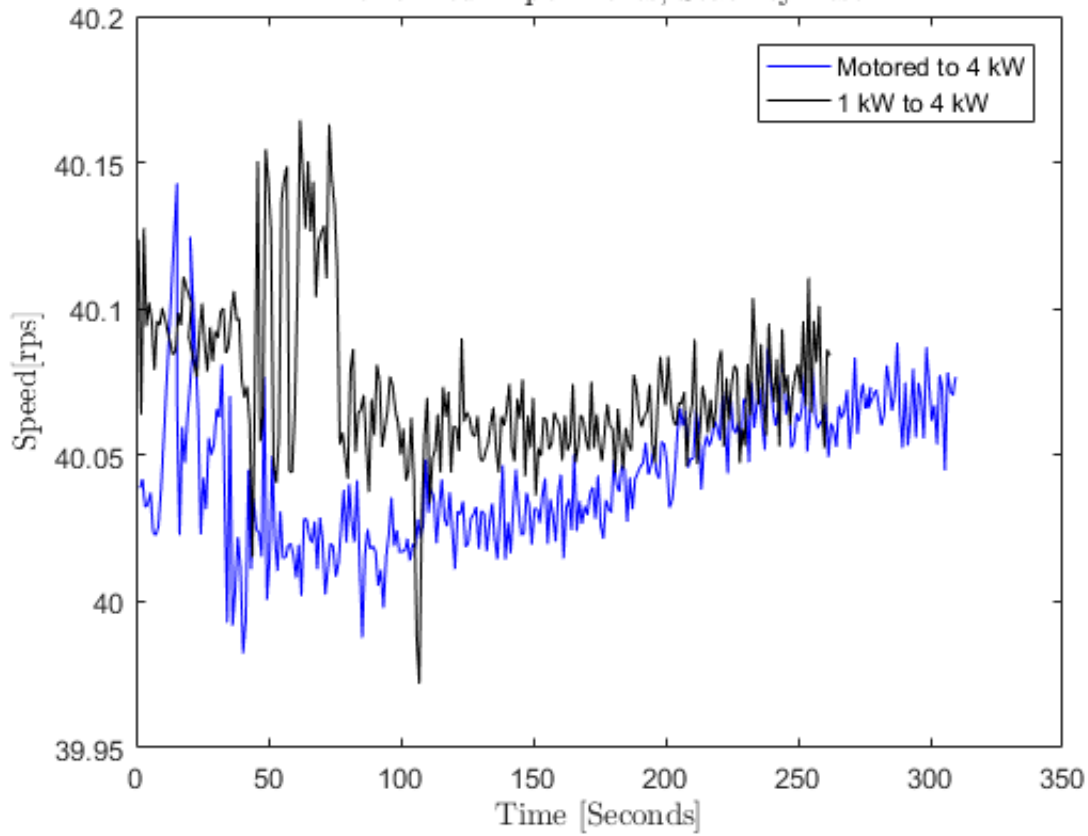
```
%load('Stability.mat');  
load('Stability.mat')
```

Plot of Experiments

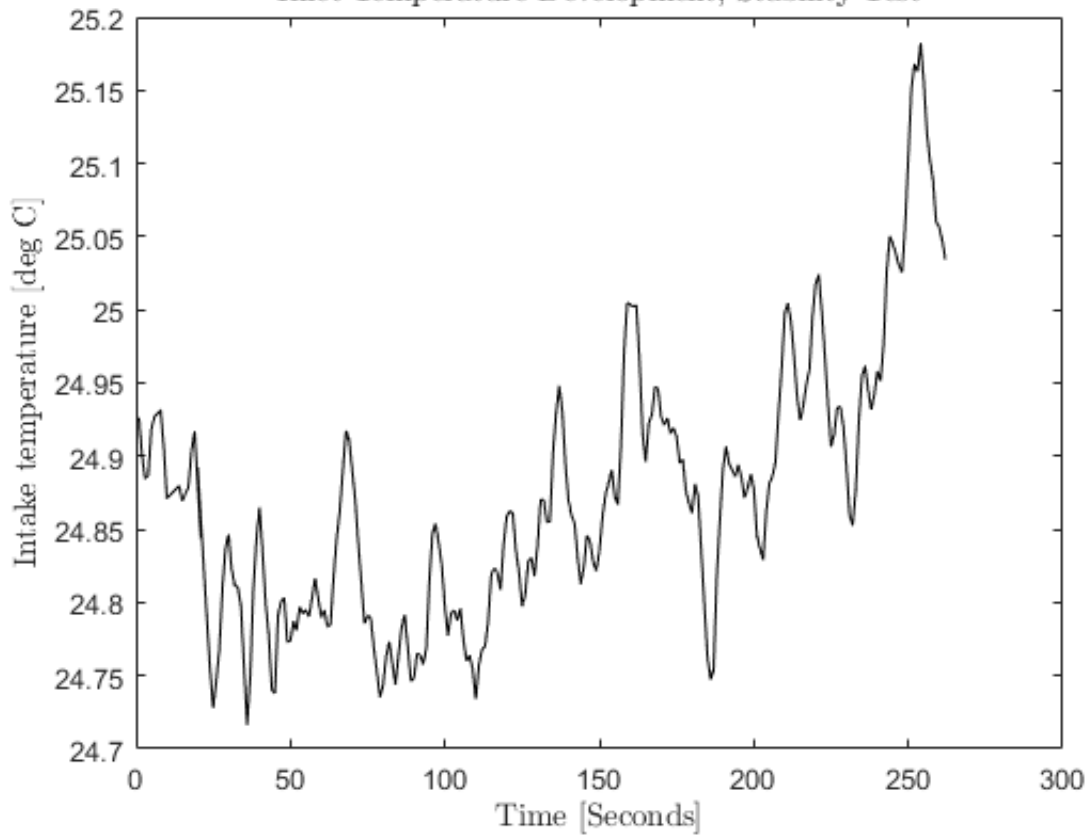
```
powercalc1 = 2*3.14*speed1.*torque1*10^-3;  
powercalc2 = 2*3.14*speed2.*torque2*10^-3;  
StabPower(x_value1,powercalc1,x_value2,powercalc2);  
P_experimentsSTAB(x_value1,speed1,x_value2,speed2);  
TempDevSTAB(x_value1,airaheater1,x_value2,airaheater2);
```



Performed Experiments, Stability Test



Inlet Temperature Development, Stability Test



NOx Stability With Same speed

```
figure1 = figure('Name','NOx Stability');
```

```

plot(x_value1,nox1,'Color',[0 0 0],'DisplayName','Motored to 4 kW');
hold on
plot(x_value2,nox2,'Color','b','DisplayName','1 kW to 4 kW');

% Create xlabel
xlabel('Time [seconds]','Interpreter','latex');

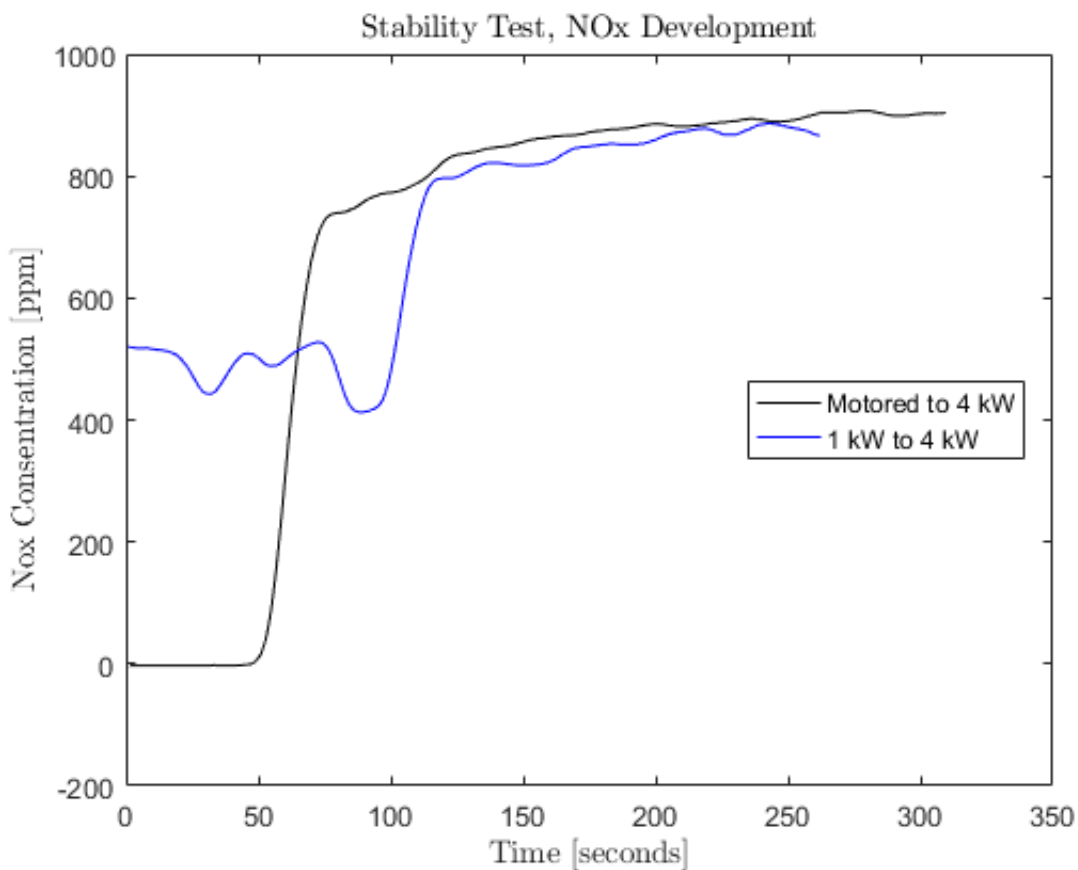
% Create title
title('Stability Test, NOx Development','Interpreter','latex');

% Create ylabel
ylabel('Nox Concentration [ppm]','Interpreter','latex');

box('on');
legend('show')
set(legend,'Location','east');

grid off
print -dpng Stability_NOx.png

```



Exhaust Temp

```

figure1 = figure('Name','Exhaust Stability');

plot(x_value1,exhaust11,'Color',[0 0 0],'DisplayName','Motored to 4 kW, EX1');
hold on
plot(x_value2,exhaust12,'Color','b','DisplayName','1 kW to 4 kW, EX1');
hold on
plot(x_value1,exhaust21,'Color','c','DisplayName','Motored to 4 kW, EX2');
hold on

```

```

plot(x_value2,exhaust22,'Color','r','DisplayName','1 kW to 4 kW, EX2');
hold on
plot(x_value1,exhaust31,'Color','g','DisplayName','Motored to 4 kW, EX3');
hold on
plot(x_value2,exhaust32,'Color','y','DisplayName','1 kW to 4 kW, EX3');

% Create xlabel
xlabel('Time [seconds]','Interpreter','latex');

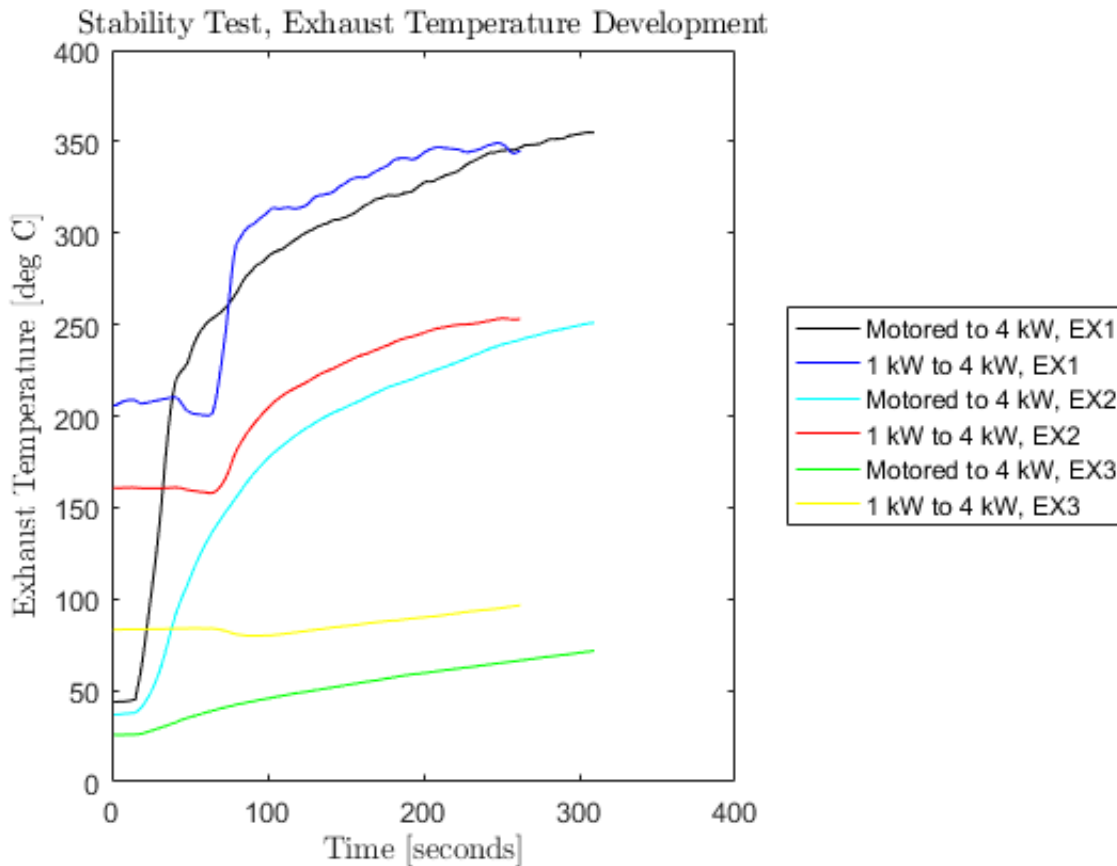
% Create title
title('Stability Test, Exhaust Temperature Development','Interpreter','latex');

% Create ylabel
ylabel('Exhaust Temperature [deg C]','Interpreter','latex');

box('on');
legend('show')
set(legend,'Location','eastoutside');

grid off
print -dpng Stability_Ex1.png

```



Oil temp

```

figure1 = figure('Name','Oil Stability');

plot(x_value1,oil1,'Color',[0 0 0],'DisplayName','Motored to 4 kW');
hold on
plot(x_value2,oil2,'Color','b','DisplayName','1 kW to 4 kW');

```

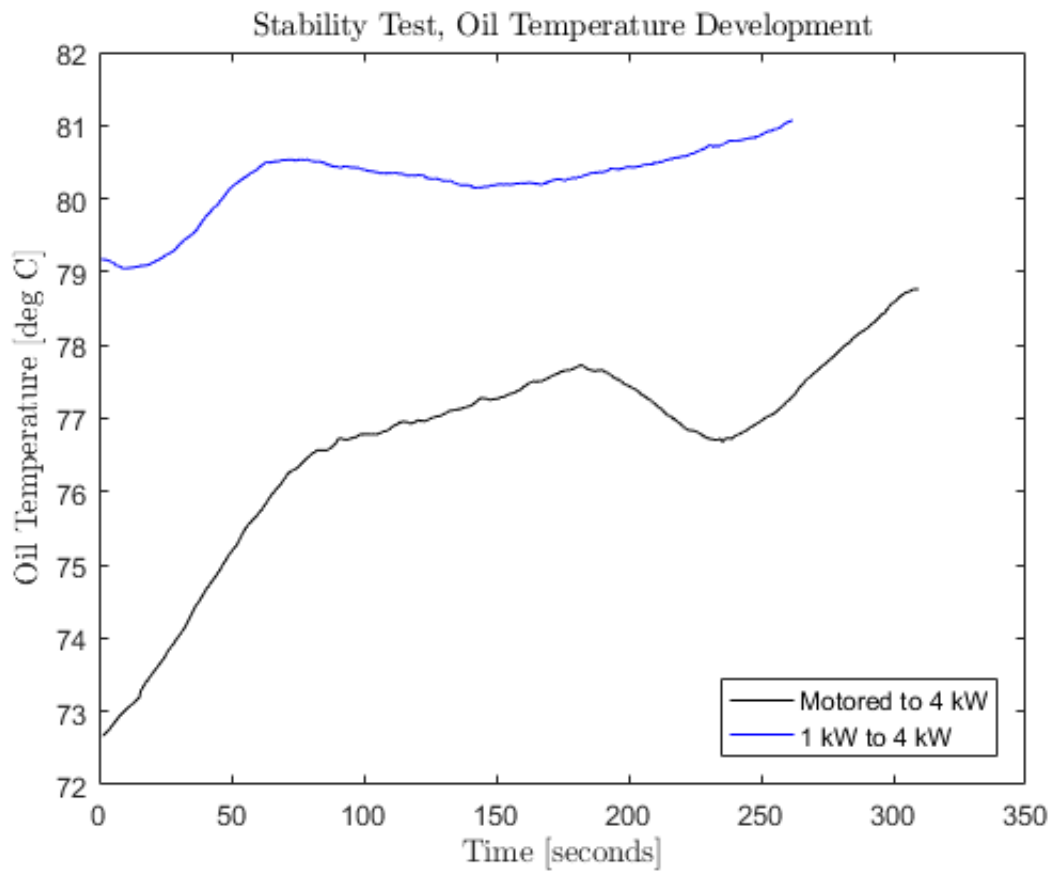
```
% Create xlabel
xlabel('Time [seconds]','Interpreter','latex');

% Create title
title('Stability Test, Oil Temperature Development','Interpreter','latex');

% Create ylabel
ylabel('Oil Temperature [deg C]','Interpreter','latex');

box('on');
legend('show')
set(legend,'Location','southeast');
grid off

print -dpng Stability_Oil.png
```



APPENDIX F – MATLAB SCRIPT – LIMIT TEST

The next pages contain the Matlab script used to plot and calculate relevant data from the limit tests.

Contents

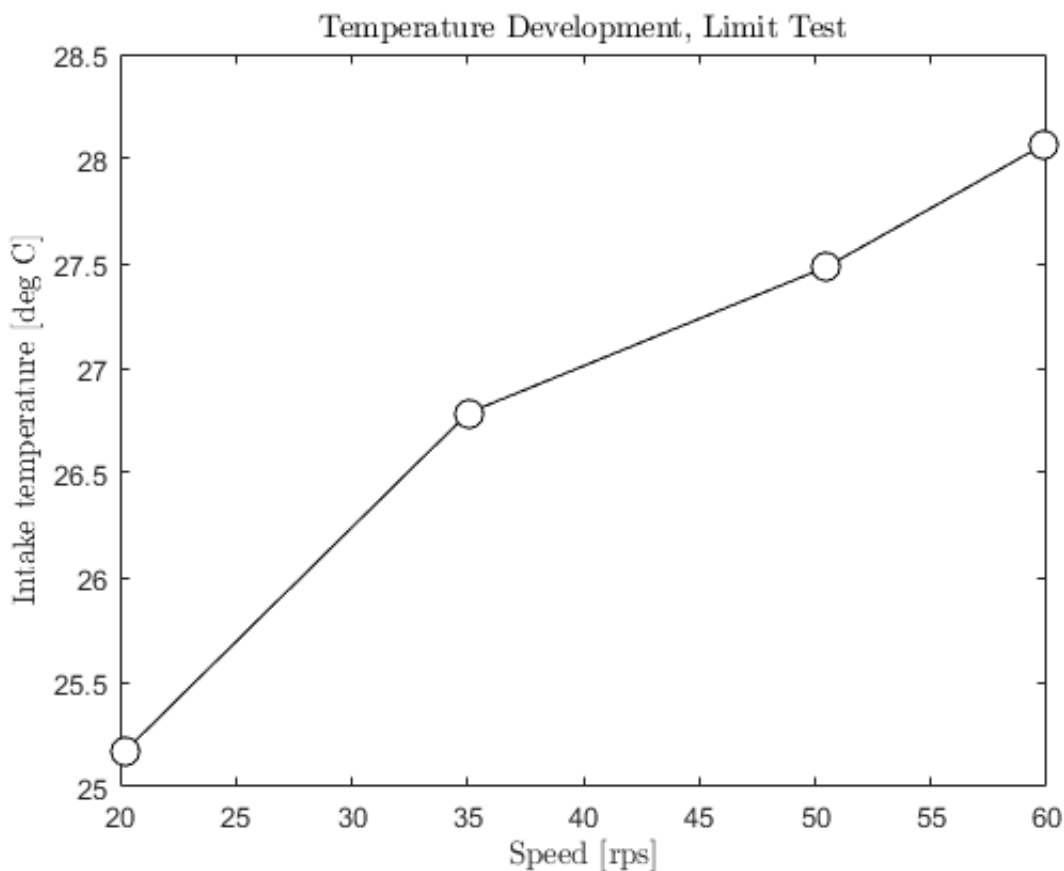
- Limits
- Plot of Experiments
- Plot of operational area. As function of speed and load
- Volumetric efficiency
- Rate of Heat Release
- Engine temp
- Fuel Flow
- Exhaust temp
- Energy in fuel mass:

Limits

```
load('OPLimits.mat')
```

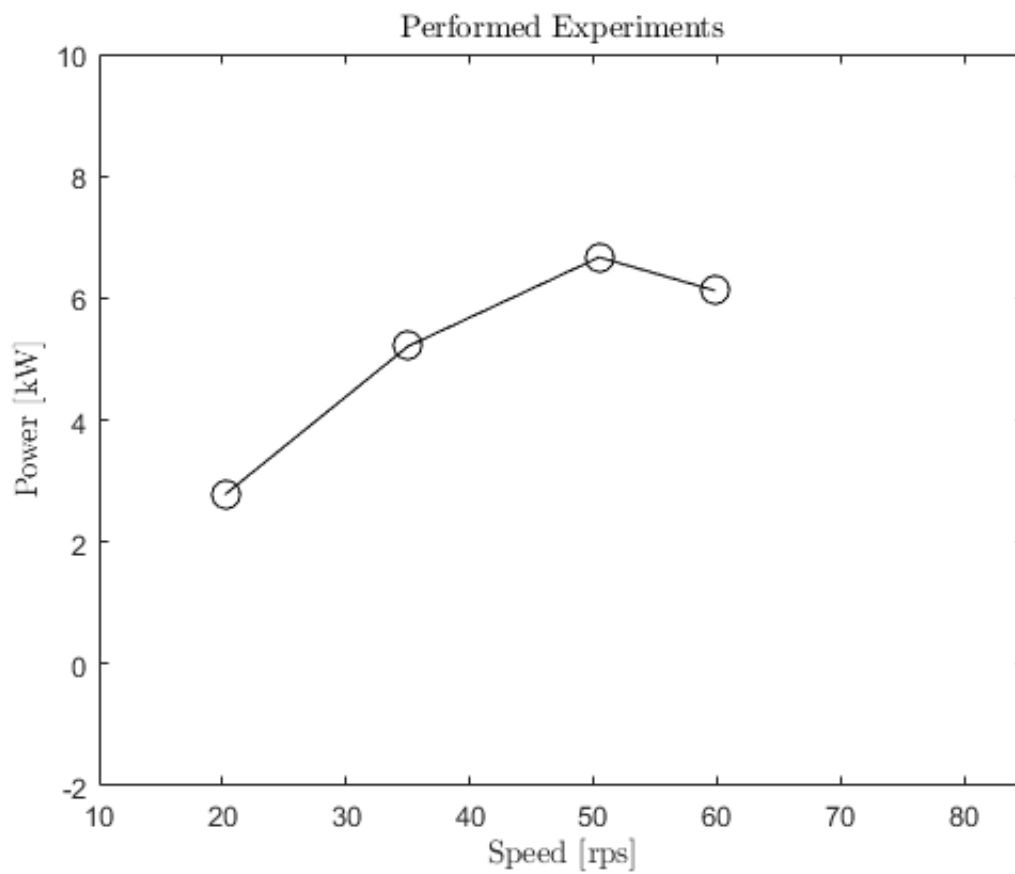
Plot of Experiments

```
power_calc = 2*3.14*speed.*torque*10^-3;  
% P_experimentsLIMIT(speed,power_calc);  
TempDevLIMIT(speed,airaheater);
```



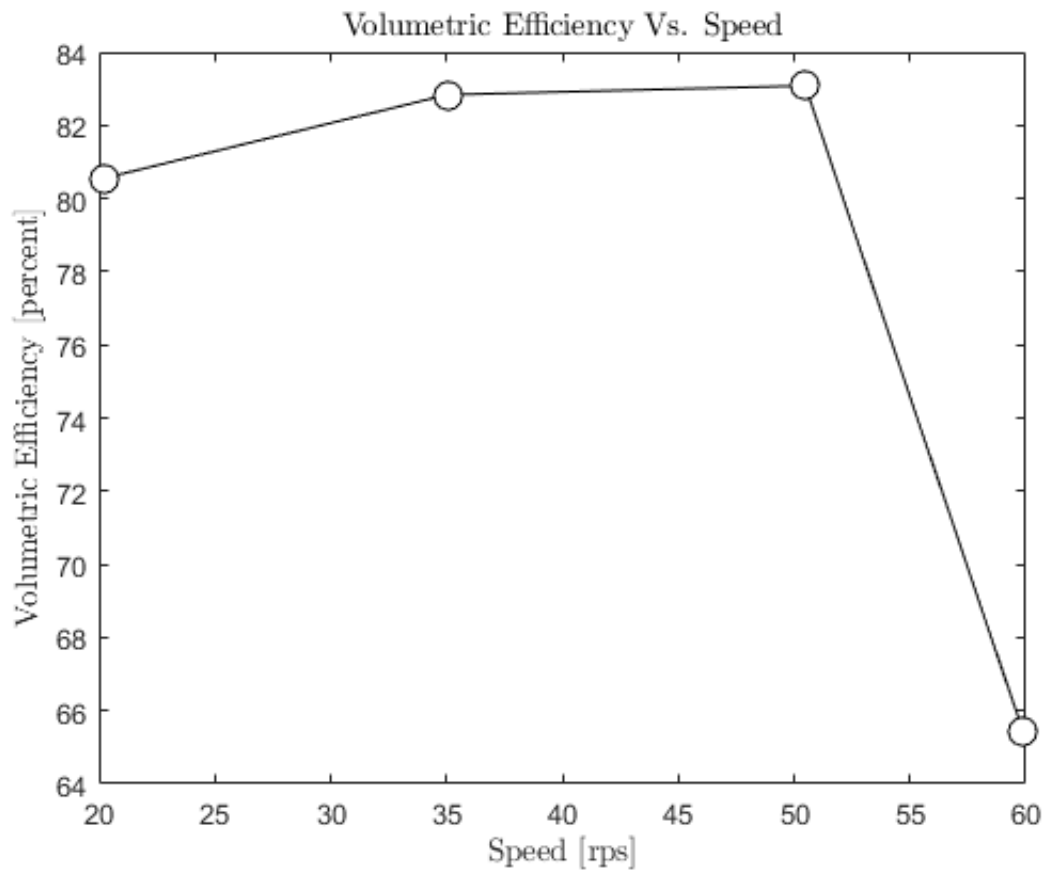
Plot of operational area. As function of speed and load

```
Limitations(speed,power_calc);
```

Volumetric efficiency

```
R = 287.058; %J/kgK
v_a_dot = airflow; % l/s
rho_a = airpress*10^3/(R*(oil+273));
eff_vol = 100*(v_a_dot./ ((Vd/2).*speed));
% Plot:
VOLEFF(speed,eff_vol)
print -dpng Volumetric_Efficiency_Limit.png
```



Rate of Heat Release

Not plotted due to pressure transducer problems

```
%Change load point dependent on which pressuredata to plot
loadpoint =1;

%ROHR1(crankangle,cylpressure,loadpoint)

% figure
% plot(cylpressure(:,1:3),'DisplayName','cylpressure')
% figure
```

Engine temp

```
%Oil
figure1 = figure('Color',[1 1 1]);
% Create plot
plot(speed,oil,'MarkerFaceColor',[1 1 1],'MarkerSize',10,'Marker','o',...
      'Color',[0 0 0]);

% Create xlabel
xlabel('Speed [rps]','Interpreter','latex');

% Create title
title('Oil Temperature Development , Limit Test','Interpreter','latex');

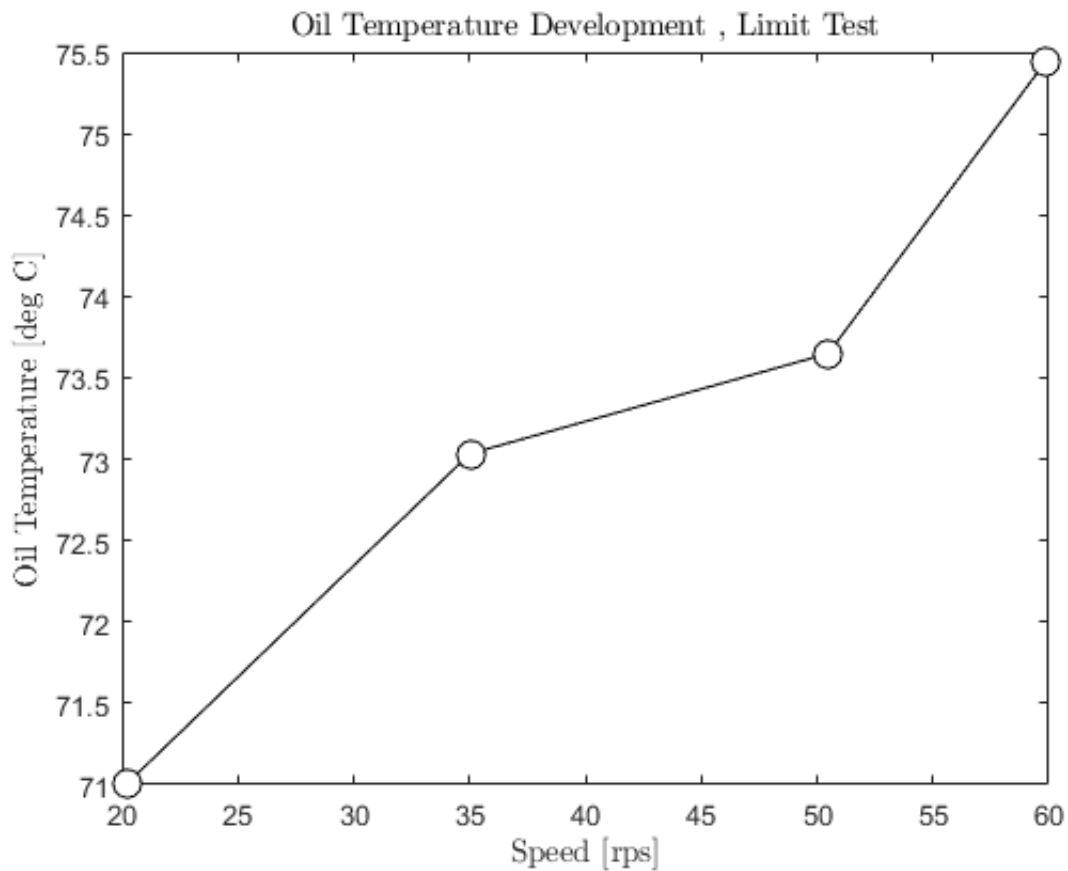
% Create ylabel
ylabel('Oil Temperature [deg C]','Interpreter','latex');

box('on');
```

```

grid('off');
set(gcf, 'PaperPositionMode','auto')
print -dpng oiltempLimit.png

```



Fuel Flow

```

figure1 = figure('Color',[1 1 1]);
% Create plot
plot(speed,mf_rate,'MarkerFaceColor',[1 1 1],'MarkerSize',10,'Marker','o',...
     'Color',[0 0 0]);

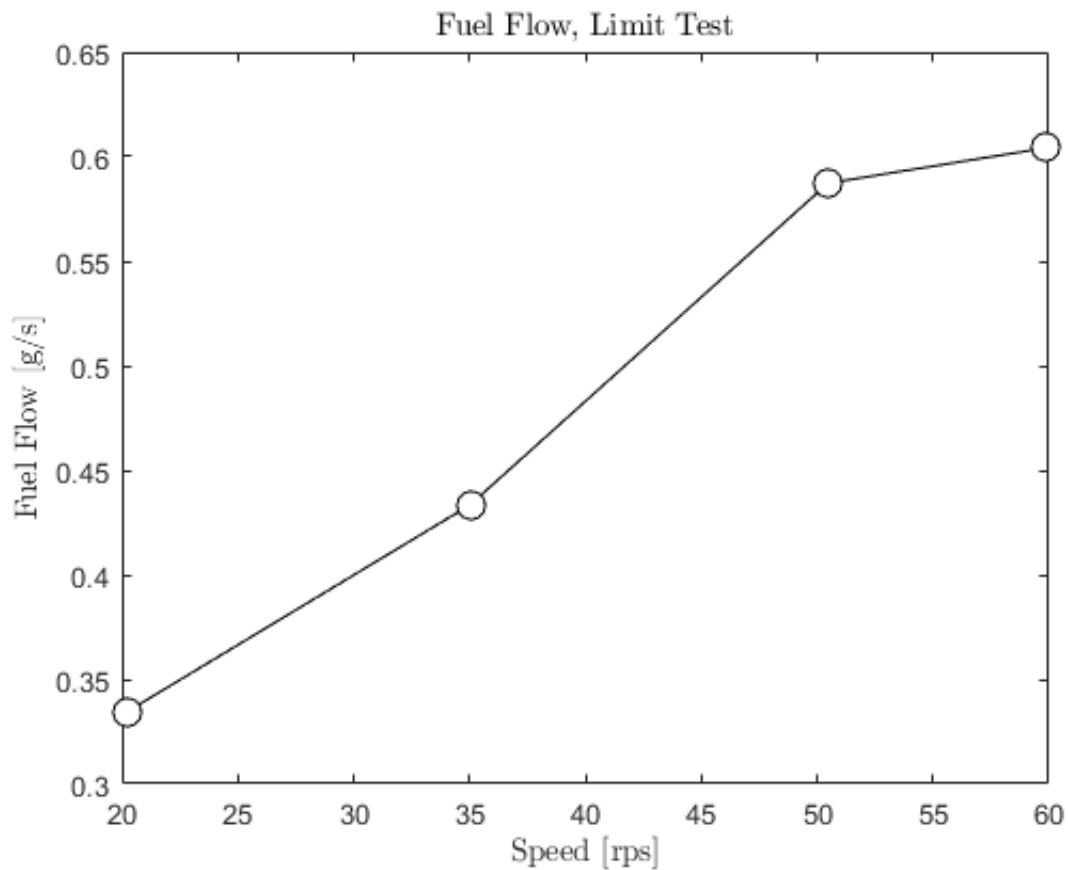
% Create xlabel
xlabel('Speed [rps]','Interpreter','latex');

% Create title
title('Fuel Flow, Limit Test','Interpreter','latex');

% Create ylabel
ylabel('Fuel Flow [g/s]','Interpreter','latex');

box('on');
grid('off');
set(gcf, 'PaperPositionMode','auto')
print -dpng fuelflowLIMIT.png

```



Exhaust temp

```

figure1 = figure('Color',[1 1 1]);
% Create plot
plot(speed,exhaust1,'MarkerFaceColor',[1 1 1],'MarkerSize',10,'Marker','o',...
      'Color',[0 0 0]);

% Create xlabel
xlabel('Speed [rps]','Interpreter','latex');

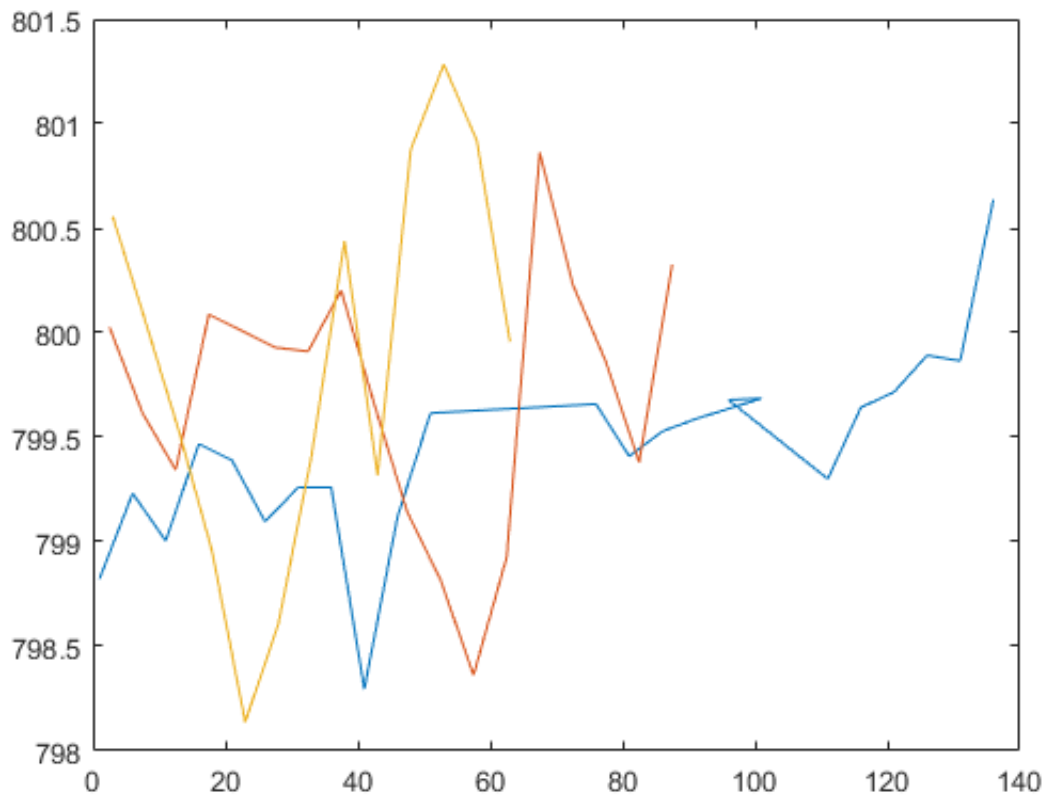
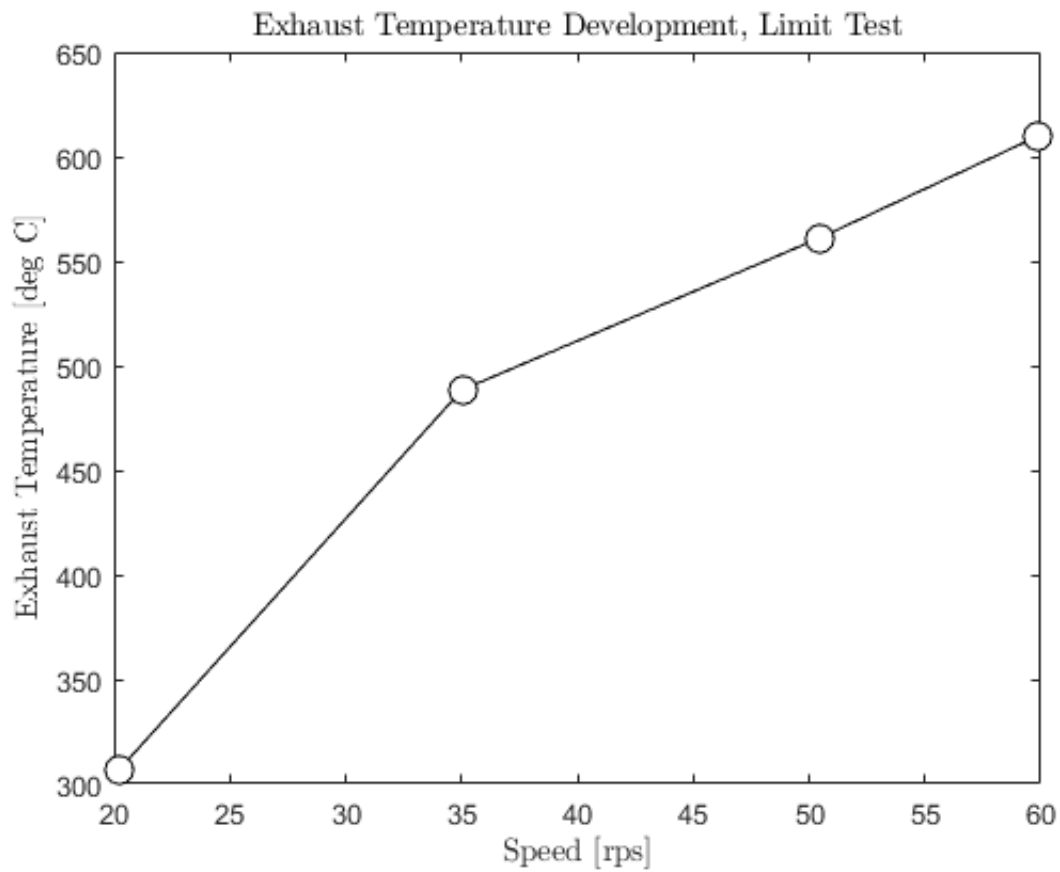
% Create title
title('Exhaust Temperature Development, Limit Test','Interpreter','latex');

% Create ylabel
ylabel('Exhaust Temperature [deg C]','Interpreter','latex');

box('on');
grid('off');
set(gcf, 'PaperPositionMode','auto')
print -dpng extempLimit.png

figure
plot(x_value2,railpress2,x_value3,railpress3,x_value4,railpress4)

```



Energy in fuel mass:

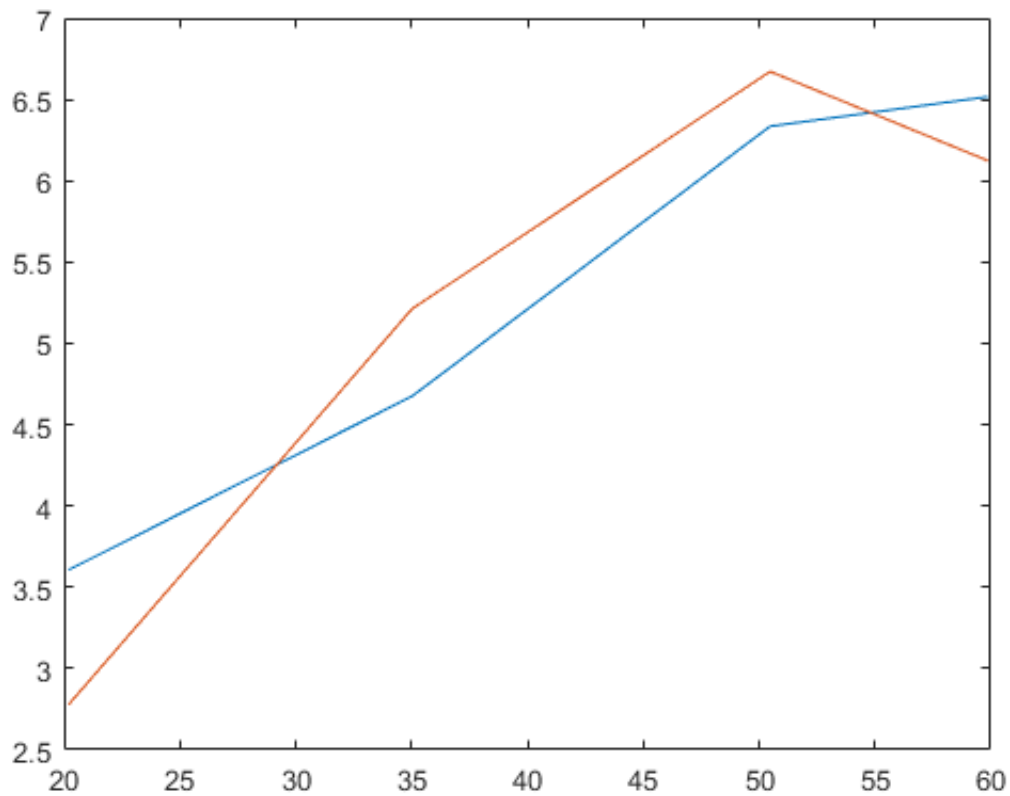
```

lhv = 42.8*10^-3; % MJ/g
Energy = lhv*mf_rate*10^3; %kJ/s = kW
disp(Energy)

```

```
% Thermal, mechanical, combustion
Meff = 0.8;
Ceff = 0.9;
Teff = 0.35;
Energy_out = Energy*Meff*Ceff*Teff;
disp(Energy_out)
disp(power)
figure
plot(speed,Energy_out,speed,power)
```

14.3121	18.5499	25.1377	25.8586
3.6066	4.6746	6.3347	6.5164
2.7789	5.2121	6.6719	6.1230



APPENDIX G – REVIEW OF PREVIOUS INTAKE SYSTEM

In the next pages a review of the old intake system is shown. A similar system would be advisable to use in the future.

1.1 Air Intake

The air inlet fitted to the Hydra engine has a very special design. Figure 1 shows the first part of the air inlet. One may notice that there are two different inlets. In the green rectangle, the air filter for the naturally aspirated inlet port can be seen. Below this rectangle there is a red handle, this handle can be actuated to close the naturally aspirated port, making it possible to use pressurized inlet air. In the black rectangle, the inlet port for pressurized air is shown, a hose from a compressor in the basement can be connected to this port to allow for a constant elevated inlet pressure. This compressor is however at the present moment not in operation, and will not be in operation during the testing period of this thesis. In the blue rectangle, the flowmeter for inlet air is shown, more detail about this flowmeter will be covered in the next subsection. In the red rectangle, a heating-chamber is shown. This chamber can be heated to a constant temperature by supplying power to the black plug to the right. This will permit simulation of elevated inlet temperatures.

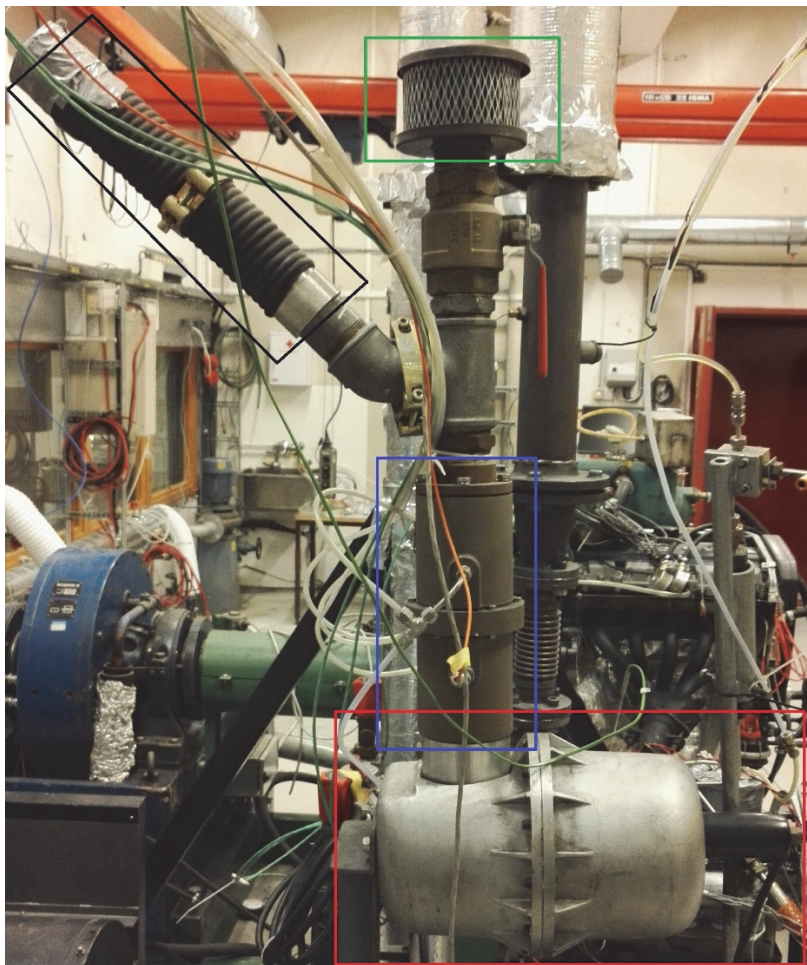


Figure 1 Picture of air inlet. Red rectangle - Air heater, Blue rectangle - Air flowmeter, Green rectangle – Air filter, Black rectangle - Compressed air inlet

The outlet from the air heater is the black pipe that goes into the inlet manifold shown in Figure 2. The inlet manifold is a standard inlet manifold for an Audi A4 2.5-liter diesel engine, with two of three ports plugged.

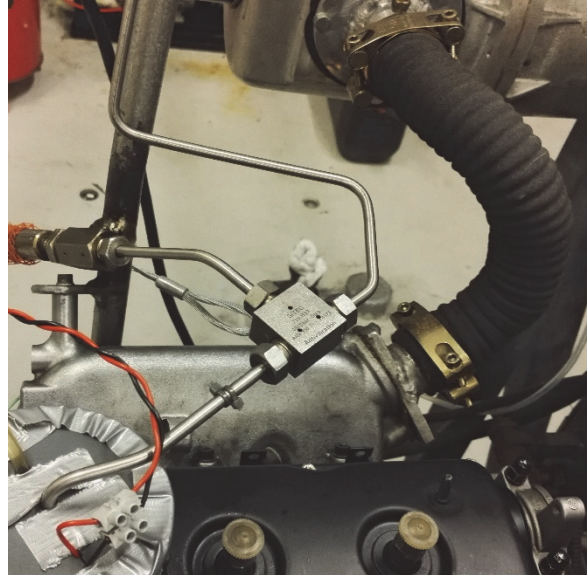


Figure 2 Inlet Manifold

1.2 Air Flow Meter

The air flow meter is of the differential pressure type. Utilizing Bernoulli's law, which states that the pressure drop across a restriction is proportional to the square of the fluid flow velocity. As can be seen from Figure 4 four sensors are connected to the flow meter. The two sensors to the right are differential pressure sensors, taking measurements on both sides of the mesh shown in Figure 3. The two sensors to the left is an absolute pressure sensor (top one) and a temperature sensor (bottom one).

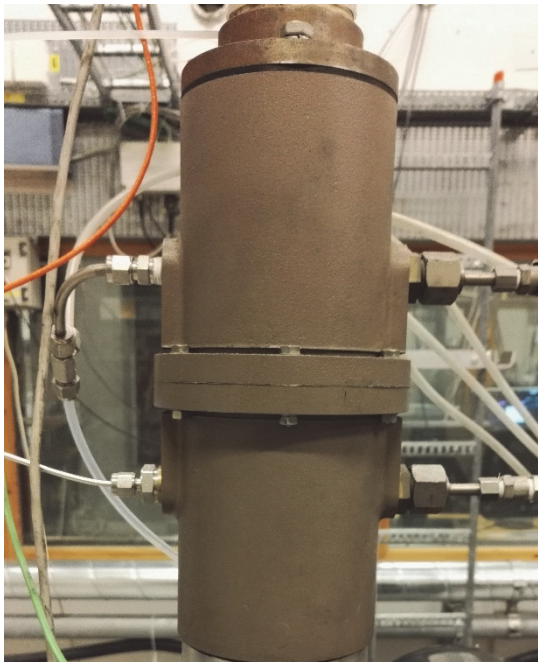


Figure 4 Air flow meter seen from front of Hydra Engine

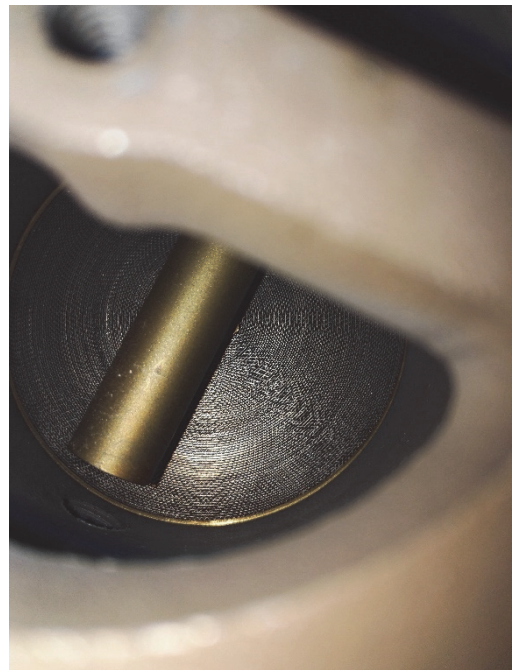


Figure 3 Laminar flow mesh, inside view

APPENDIX H – FUEL PROPERTIES

The next pages contain the data sheet for the MGO used in the experiments in this thesis.



Statoil Marine Gassolje LS

Anvendelse

Statoil Marine Gassolje LS anvendes som drivstoff i skipsdieselmotorer.

Fordeler

Statoil Marine Gassolje LS oppfyller de til enhver tid gjeldende norske lovkravene som stilles til marine gassoljer, samt kravene satt i den internasjonale standarden for marine gassoljer, ISO 8217:2012 klasse DMA. Det lave svovelinnholdet i Statoil Marine Gassolje LS gjør at utslippet av SO₂ er, ved forbrenning av dette produktet, lavere enn ved bruk av Marine Gassolje Normalsvovlig.

Egenskaper

Statoil Marine Gassolje LS tilfredsstiller Norsk Bransjestandard for Oljeprodukter. Dette produktet er et mellomdestillat som er farget grønt. Produktet har en karakteristisk lukt, og er tungt fordampelig. Produktet er uløselig i vann og løselig i organiske løsemidler.

HMS-fakta

For hver liter produkt som forbrennes dannes ca. 2.6 kg CO₂. Ved ufullstendig forbrenning utvikles røyk og farlige gasser, bl.a. CO som er giftig og meget brannfarlig. Produktet trenger ned i jord og forurensrer grunnvannet. Produktet brytes vanskelig ned i naturen. Basert på tilgjengelig informasjon forventes det ikke at dette produktet gir skadelige helsemessige virkninger når det brukes til det tiltenkte formålet og i henhold til anbefalinger som er gitt i Sikkerhetsdatabladet. Dette produktet må ikke brukes til andre formål enn det er tiltenkt. Unngå oppvarming, gnist og åpen ild. Unngå søl, hud og øyenkontakt. Unngå innånding av damper. Vask straks hud som har litt tilsølt. Ved svelging må ikke brekninger fremkalles-kontakt lege. Oppbevares utilgjengelig for barn. Apparaturl og røropplegg må jordes.

Typiske Analyser

EGENSKAPER	TYPISK VERDI	ENHET	ANALYSE METODE
Densitet	855	Kg/m ³	EN ISO 3675
Destillasjonsområde	170 - 370	°C	ASTM D 86
Flammepunkt	65	°C	EN ISO 2719
Viskositet ved 40 °C	3,0	mm ² /s	EN ISO 3104
Svovel-innhold	maks. 0,05	%-vekt	EN ISO 20847
Cloud Point (tåkepunkt)	0	°C	EN 23015
CFPP (blokkeringspunkt)	-11	°C	EN 116
Nedre brennverdi	42,8	MJ/kg	
Farge	grønn		